การหาค่าปริมาณรังสีของผู้ป่วยในการถ่ายภาพรังสีเต้านมระบบดิจิทัล

นางสาวธัญรัตน์ ชูศิลป์

วิทยานิพนธ์นี้เป็นส่วนหนึ่งของการศึกษาตามหลักสูตรปริญญาวิทยาศาสตรมหาบัณฑิต
สาขาวิชาฉายาเวชศาสตร์ ภาควิชารังสีวิทยา
คณะแพทยศาสตร์ จุฬาลงกรณ์มหาวิทยาลัย
ปีการศึกษา 2550

THE DETERMINATION OF PATIENT DOSE IN FULL FIELD DIGITAL MAMMOGRAPHY

Miss Thunyarat Chusin

A Thesis Submitted in Partial Fulfillment of the Requirements
for the Degree of Master of Science Program in Medical Imaging
Department of Radiology
Faculty of Medicine
Chulalongkorn University
Academic Year 2007

Thesis Title	THE DETERMINATION OF PATIENT DOSE IN FULL FIELD DIGITAL MAMMOGRAPHY
By	Miss Thunyarat Chusin
Field of Study	Medical Imaging
Thesis Advisor	Associate Professor Anchali Krisanachinda, Ph.D.

Accepted by the Faculty of Medicine, Chulalongkorn University in Partial Fulfillment of the Requirements for the Master's Degree

.....Dean of the Faculty of Medicine
(Associate Professor Adisorn Patradul, M.D.)

THESIS COMMITTEE

.....Chairman
(Associate Professor Somjai Wangsuphachart, M.D., M.Sc.)

.....Thesis Advisor
(Associate Professor Anchali Krisanachinda, Ph.D.)

.....External Member
(Professor Franco Milano, Ph.D.)

.....Member
(Associate Professor Sukalaya Lerdlum, M.D., M.Sc.)

.....Member
(Associate Professor Somrat Lertmaharit, M.Sc., M.Med.Stat.)

ธัญรัตน์ ชูศิลป์ : การหาค่าปริมาณรังสีของผู้ป่วยในการถ่ายภาพรังสีเต้านมระบบดิจิทัล. (THE DETERMINATION OF PATIENT DOSE IN FULL FIELD DIGITAL MAMMOGRAPHY) อ.ที่ปรึกษา: รศ.ดร. อัญชลี กฤษณจินดา, 89 หน้า.

การถ่ายภาพรังสีเต้านมระบบดิจิทัลเป็นเทคโนโลยีการสร้างภาพทางการแพทย์แบบใหม่ที่ใช้ในการตรวจวินิจฉัยรอยโรคของเต้านม เทคโนโลยีนี้จำเป็นต้องเน้นความสามารถที่จะลดปริมาณรังสีแก่ผู้ป่วยเพื่อลดความเสี่ยงจากการเกิดโรคมะเร็งขณะที่ได้ภาพซึ่งมีคุณภาพสูง เพราะเต้านมเป็นอวัยวะที่มีความไวต่อรังสีสูงและมีนัยสำคัญกับการเกิดมะเร็งเต้านม

วัตถุประสงค์ของงานวิจัยนี้เพื่อหาค่าปริมาณรังสีดูดกลืนของเต้านมในผู้ป่วยหญิงไทยที่มารับการตรวจวินิจฉัยด้วยการถ่ายภาพรังสีเต้านมระบบดิจิทัลและหาปัจจัยต่างๆที่มีผลต่อปริมาณรังสีที่ผู้ป่วยได้รับ งานวิจัยนี้ทำการเก็บข้อมูลในกลุ่มตัวอย่างจำนวน 749 คน เป็นผู้ป่วยที่มารับการถ่ายภาพรังสีเต้านม ด้วยเครื่องเอกซเรย์เต้านมระบบดิจิทัล ผลิตภัณฑ์โฮโลจิค โลแรด รุ่น ซีลีเนีย ระหว่างเดือนกุมภาพันธ์ 2549 ถึง เดือนกุมภาพันธ์ 2550 เครื่องมือติดตั้งอยู่ที่ สาขารังสีวิทยาวินิจฉัย โรงพยาบาลจุฬาลงกรณ์ สำหรับการควบคุมคุณภาพของเครื่องมือมีการปฏิบัติเป็นงานประจำโดยใช้มาตรฐานสากล ส่วนข้อมูลของกลุ่มตัวอย่างได้มาโดยเรียกดูข้อมูลย้อนหลังจากแฟ้มข้อมูลผู้ป่วยซึ่งเก็บเป็นข้อมูลภาพและรายละเอียดผ่านระบบเครือข่ายภายในโรงพยาบาลจุฬาลงกรณ์ โดยปริมาณรังสีดูดกลืนของเต้านมและค่าเทคนิคในการถ่ายภาพต่างๆ ปรากฏอยู่บนโปรแกรมดูภาพที่ใช้ในคอมพิวเตอร์ของงานรังสีวิทยา การวิเคราะห์หาความสัมพันธ์ระหว่างปัจจัยค่าเทคนิคต่างๆกับปริมาณรังสีของผู้ป่วยใช้สถิติการหาความสัมพันธ์แบบตัวแปรอิสระหลายตัว ผลของงานวิจัยนี้ได้ค่าเฉลี่ยอายุของผู้ป่วย 51.3 ปี มีความหนาของเต้านมเฉลี่ยสำหรับการจัดท่า ซีซีและ เอ็มเอลโอ เท่ากับ 6.2 และ 6.1 เซนติเมตร ตามลำดับ ส่วนค่าเฉลี่ยปริมาณรังสีที่ผิวเต้านมสำหรับการจัดท่า ซีซีและ เอ็มเอลโอ เท่ากับ 11.89 และ 11.84 มิลลิเกรย์ ตามลำดับ สำหรับค่าปริมาณรังสีดูดกลืนของเต้านมเมื่อใช้กริดสำหรับการจัดท่า ซีซีและ เอ็มเอลโอ เท่ากับ 1.80 และ 1.81 มิลลิเกรย์ ตามลำดับ โดยค่าเฉลี่ยของการตรวจของเต้านมทั้ง 2 ท่าเท่ากับ 3.62 มิลลิเกรย์ ส่วนผลของปริมาณรังสีอ้างอิงที่กำหนดขึ้นสำหรับโรงพยาบาลจุฬาลงกรณ์ คือ 2.0 มิลลิเกรย์ต่อภาพ โดยสรุปค่าปริมาณรังสีดูดกลืนของเต้านมสำหรับการจัดท่า ซีซี และ เอ็มเอลโอ คิดเป็น 91.2 เปอร์เซนต์ น้อยกว่า 3 มิลลิเกรย์ โดยอ้างอิงกับ วิทยาลัยรังสีวิทยาแห่งสหรัฐอเมริกา ผลการวิเคราะห์หาความสัมพันธ์ระหว่างปัจจัยค่าเทคนิคต่างๆกับปริมาณรังสีที่ผู้ป่วย พบว่า ค่าเอ็มเอเอส(กระแส-วินาที) มีนัยสำคัญทางสถิติกับปริมาณรังสีที่ผู้ป่วยได้รับ ปัจจัยสำคัญอีกประการหนึ่งคือการควบคุมคุณภาพและการสอบเทียบเครื่องมือสร้างภาพที่ใช้อยู่เป็นประจำซึ่งส่งผลต่อปริมาณรังสีที่ผู้ป่วยได้รับโดยตรง

ภาควิชา รังสีวิทยา ลายมือชื่อนิสิต ธัญรัตน์ ชูศิลป์

สาขาวิชา ฉายาเวชศาสตร์ ลายมือชื่ออาจารย์ที่ปรึกษา

ปีการศึกษา 2550

4974728430: MAJOR MEDICAL IMAGING
KEYWORDS: AVERAGE GLANDULAR DOSE (AGD) / FULL FIELD DIGITAL MAMMOGRAPHY/ PATIENT DOSE.

THUNYARAT CHUSIN: THE DETERMINATION OF PATIENT DOSE IN FULL FIELD DIGITAL MAMMOGRAPHY.THESIS ADVISOR: ASSOC. PROF. ANCHALI KRISANACHINDA, Ph.D., 89 pp.

Full field digital mammography (FFDM) is the new technology of digital imaging for clinical use. It is an application where an emphasis on patient dose management and risk reduction are required. Nevertheless, the breast tissue has a relatively high sensitivity to some adverse effects of radiation and significant risk of radiation induced carcinogenesis associated with the radiation absorbed dose to the breast.

The objective of this study is to determine the average glandular dose (AGD) for Thai female undergoing FFDM system and to identify the factors affecting it. This study involves 749 women underwent mammography examinations using the FFDM system, Hologic Lorad Model Selenia during the period from February 2006 to February 2007. The system was installed at the Department of Radiology, King Chulalongkorn Memorial Hospital. The quality control of FFDM system is routinely performed. AGD displayed on the monitor is verified by dosimetry and calculation methods. The information has been extracted from the digital mammographic image in DICOM header. The AGD, entrance skin exposure (ESE) and technique factors were displayed on the monitor of FFDM system. The factors affecting AGD per woman were studied using a multivariable analysis. Mean (±SD) value for patient age was 51.3 (±8.6) years and mean compressed breast thickness (CBT) for craniocaudal (CC) and mediolateral oblique (MLO) views were 6.2 cm and 6.1 cm, respectively. The mean ESE per image was 11.89 mGy for CC and 11.84 mGy for MLO views. The mean AGD per image (with grid) was 1.80 mGy for CC and 1.81 mGy for MLO views. The mean AGD per woman was 3.62 mGy therefore, a new dose reference level (DRL) of 2.0 mGy (third quartile) per image is proposed. The mAs is directly affected AGD by stepwise regression (p-value < 0.001). The result could not represent the FFDM examination in Thailand because it is a localized survey at one department. In addition, the quality control of the system and the calibration of the flat panel detectors play an important role in the patient dose achieved. The mean AGD per image obtained for both CC and MLO views was 91.2% lower than the reference level of 3.0 mGy as recommended by the American College of Radiology (ACR).

Department Radiology Student's signature Thunyarat Chusin
Field of study Medical Imaging Advisor's signature Anchali Kr
Academic 2007

ACKNOWLEDGEMENTS

I would like to greatly thank Associate Professor Anchali Krisanachinda, Division of Nuclear Medicine, Department of Radiology, Faculty of Medicine, Chulalongkorn University, my advisor for her support, instruction, care and polish my English language in this research.

I would like to greatly thank Associate Professor Sivalee Suriyapee, Division of Radiation Oncology, Department of Radiology, Faculty of Medicine, Chulalongkorn University, my teacher for her advice and comments in the research.

My sincere thanks to Professor Franco Milano, who is the external examiner of the thesis, for his help in the experiment, kind suggestion, constructive comments in the experiments and English language improvement in this research.

I would like to deeply thank Associate Professor Somjai Wangsuphachart, Chief of Department of Radiology, Faculty of Medicine, Chulalongkorn University for her advice and comments in the research.

I would like to deeply thank Associate Professor Somrat Lertmaharit, Department of Preventive and Social Medicine, Faculty of Medicine, Chulalongkorn University for her advice and comments in the research.

I would like to thank the staff at Breast Imaging Centre, Department of Radiology, King Chulalongkorn Memorial Hospital for their helps in data collection.

I am thankful for all teachers, lecturers and staff in the Master of Science Program in Medical Imaging, Faculty of Medicine, Chulalongkorn University for their unlimited teaching of knowledge in Medical Imaging.

My thanks include Chief of Department of Radiology, Faculty of Medicine, Thammasat University for the full support to this graduate study in Medical Imaging.

Finally, this thesis is dedicated to my father and mother, Tongdaeng and Sunya Chusin for the moral and spiritual compass instilled in me.

CONTENTS

Page

Page

LIST OF TABLES

Table **Page**

LIST OF FIGURES

Figure **Page**

Figure **Page**

LIST OF ABBREVIATIONS

Abbreviation	Terms
AAPM	American Association of Physicists in Medicine
ACR	American College of Radiology
AEC	Automatic Exposure Control
AGD	Average Glandular Dose
ALARA	As Low As Reasonably Achievable
Al	Aluminum
a-Se	Amorphous selenium
a-Si	Amorphous silicon
Be	Beryllium
BRCA	Breast cancer
Ca 15.3	Carbohydrate antigen 15.3
CBT	Compressed Breast Thickness
CC	Cranio Caudal
CF	Compression Force
cm	Centimeter
CsI	Cesium Iodide
CsI(Tl)	Cesium Iodide with Thallium doping
CT	Computed Tomography
CV	Coefficients of Variation
DES	Diethylstilbestrol
DICOM	Digital Imaging and Communications in Medicine

Abbreviation	Terms
DNA	Deoxyribonucleic acid
DQE	Detective Quantum Efficiency
ESAK	Entrance Surface Air Kerma
ESD	Entrance Skin Dose
ESE	Entrance Skin Exposure
FDA	Food and Drug Administration
FFDM	Full Field Digital Mammography
Gd_2O_2S	Gadolinium Oxysulfide
Gd_2O_2S: Tb	Gadolinium Oxysulfide activated Terbium
HVL	Half-Value Layer
ICRU	International Commission on Radiation Units and Measurements
Ka	Air kerma
kVp	Kilo-volt peak
LCIS	Lobular carcinoma in situ
mAs	Milliampere seconds
MGD	Mean Glandular Dose
mGy	Milligray
MLO	Mediolateral Oblique
mm	Millimeter
Mo	Molybdenum
MQSA	Mammography Quality Standards Act
mR	Milliroentgen
mrad	Millirad

Abbreviation	Terms
MRI	Magnetic Resonance Imaging
MTF	Modulation Transfer Function
NCI	National Cancer Institute
N	Newton
p	p-value
PET	Positron Emission Tomography
PMMA	Polymethylmethacrylate
QA	Quality Assurance
QC	Quality Control
R	Roentgen
r	Correlation coefficient
Rh	Rhodium
R^2	The coefficient of determination
s	Second
SD	Standard Deviation
SFM	Screen Film Mammography
SID	Source to Image Distance
SPSS	Statistical Package for the Social Sciences
TEC	Tissue Exposure Control
TLD	Thermoluminescent Dosemeter
W	Tungsten

CHAPTER 1

INTRODUCTION

1.1 Background and rationale

Breast cancer remains a leading cause of cancer death among women in many parts of the world. In Thailand, the estimated incidence rate of breast cancer is 17.2 per 100,000 and the number of 12,000 new cases per year expected in 2008 [1]. Early detection of breast cancer is the key to successful long-term control of the disease and good prognosis. Mammography is the most effective method to produce a high photographic sensitivity image, based on x-ray attenuated through the image receptor and absorbed as a latent image on the recording devices. Most standard mammography includes two views per breast, the craniocaudal (CC) and mediolateral oblique (MLO) views. Mammography requires the highest quality of imaging techniques and fine detail over a wide spectrum of object contrasts in order to successful identify cancerous growths in their earliest stages of development.

Screen-film image receptors have been the standard detector used in conventional mammography. Disadvantages with screen-film mammography are the radiation and that the sensitivity for detecting breast cancer is diminished in radiographically dense breasts, which limits its usefulness in high-risk younger women. New developments in detector technology and computers are altering the landscape of mammography imaging. Full Field Digital Mammography (FFDM) offers the promise of revolutionizing the practice of mammography through its superior dose and contrast performance. For clinical use it is a highly effective imaging method for detecting, diagnosing, and managing a variety of breast diseases, especially cancer. It is an application where an emphasis on patient dose management and risk reduction is required [2]. The important of digital imaging devices provide a dose index to give an indication of the exposure received by the detector. Nevertheless, the breast tissue has a relatively high sensitivity to some adverse effects of radiation and significant risk of radiation induced carcinogenesis associated with the radiation absorbed dose to the breast. Law et al. [3] estimated that for a UK population aged 50-54 years, lifetime cancer induction rate is 13 per 10^6 per mGy. Although breast imaging techniques have been developed to minimize the radiation dose in full field digital mammography, there is still the largest single non-occupational source of radiation exposure to the breast.

The estimation of the absorbed dose to the breast is an important part of the quality control of the mammographic examination. Knowledge of breast dose is essential for the design and performance assessment of mammographic imaging systems. Minimizing radiation risk is important in general as manifested by the as low as reasonably achievable (ALARA) principle. Radiation risk is a factor in the benefit-risk ratio of mammography [3]. To quantify the risk from radiation in mammography, the average glandular dose (AGD) is used. AGD is currently accepted as an estimation of the patient dose in mammography. The Food and Drug Administration (FDA), American College of Radiology (ACR) and Mammography Quality Standards Act (MQSA) have established limits of 3.0 mGy for AGD in order to minimize the risk to the glandular tissue [4]. A number of researches on AGD determination (Gennaro et al., 2006; Chevalier et al., 2005; Hermann et al., 2002) were conducted in European females underwent FFDM. However, no research has studied the

determination of AGD and the factors affecting used in FFDM, and reports the distribution of doses in Thai female.

1.2 Research objectives

1.2.1 To determine the AGD and the distribution of doses in Thai female.

1.2.2 To determine the correlation between the AGD and mAs, kVp,CBT, compression force, target/filter and half-value layer (HVL).

CHAPTER 2

LITERATURE REVIEW

2.1 Theory

2.1.1 The breasts [5].

The breasts sit on the chest muscles that cover the ribs. Each breast is made of 15 to 20 lobes, which contain many smaller lobules. Lobules contain groups of tiny glands that can produce milk. Milk flows from the lobules through thin tubes called ducts to the nipple. The nipple is in the center of a dark area of skin called the areola. Fat fills the spaces between the lobules and ducts as shown in Figure 2.1.

The breasts also contain lymph vessels lead to small, round organs called lymph nodes. Groups of lymph nodes are near the breast in the axilla, above the collarbone, in the chest behind the breastbone, and in many other parts of the body. The lymph nodes trap bacteria, cancer cells, or other harmful substances.

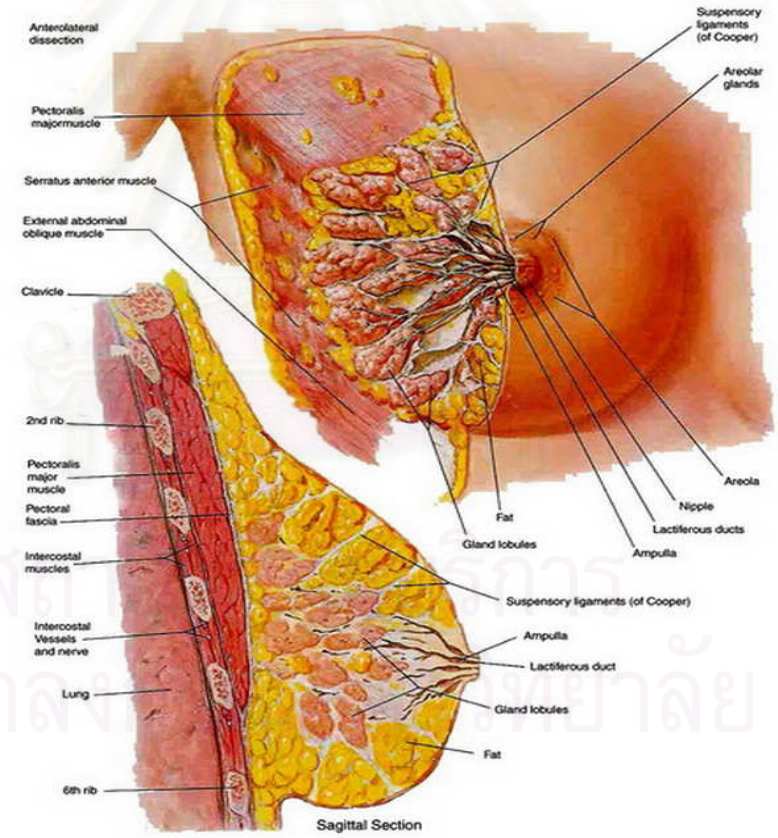

Figure 2.1 The female breasts structure

2.1.2 Breast cancer [5].

Breast cancer is a malignant (cancerous) tumor that starts from cells of the breast. The disease occurs mostly in women, but men can get breast cancer too. Most breast cancers begin in the cells that line the ducts (ductal cancer), some begin in the lobules (lobular cancer), and the rest in other tissues as shown in Figure 2.2.

If the breast cancer cells reach the underarm lymph nodes and continue to grow, they cause the nodes swell. Once cancer cells have reached these nodes they are more likely spreading to other organs of the body such as the bones, liver, lungs, and brain.

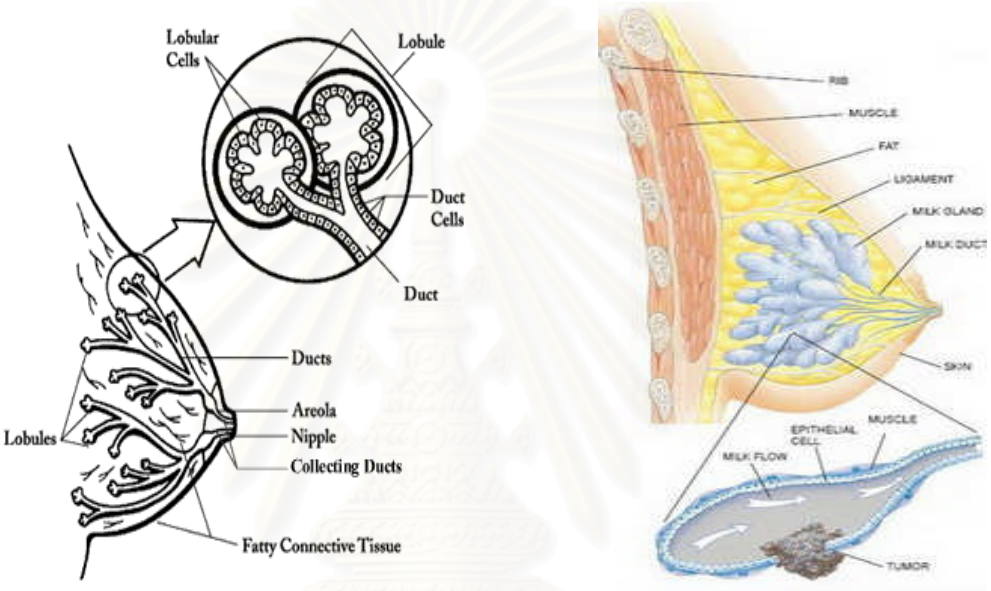

Figure 2.2 The breast structures showing cancer starting from cells of the breast

2.1.2.1 Risk factors

No one knows the exact causes of breast cancer. Today, breast cancer, like other forms of cancer, is considered to be a result of damage to DNA. This mechanism may occur from several known or hypothesized factors such as exposure to ionizing radiation, or viral mutagenesis. Some factors lead to an increased rate of mutation (exposure to estrogens) and decreased repair genes.

Research has shown that women with certain risk factors are most likely developing breast cancer. A risk factor is something that may increase the chance of developing a disease.

Previous studies showed the following risk factors causing breast cancer:

1. Age: The chance of getting breast cancer goes up as a woman gets older. Most cases of breast cancer occur in women over 60. This disease is not common before menopause.
2. Personal history of breast cancer: A woman who had breast cancer in one breast has an increased risk of getting cancer in her other breast.

3. Family history: The risk of breast cancer in woman is higher if her mother, sister, or daughter had breast cancer. The risk is higher if her family member got breast cancer before the age of 40. Having other relatives with breast cancer (in either her mother's or father's family) may also increase a woman's risk.
4. Certain breast changes: Some women have cells in the breast that look abnormal under a microscope. Having certain types of abnormal cells (atypical hyperplasia and lobular carcinoma in situ [LCIS]) increases the risk of breast cancer.
5. Gene changes: Changes in certain genes increase the risk of breast cancer. These genes include BRCA1, BRCA2, and others. Tests can sometimes show the presence of specific gene changes in families with many women who have had breast cancer. Health care providers may suggest ways to reduce the risk of breast cancer, or to improve the detection of this disease in women who have these changes in their genes. National cancer institute (NCI) offers publications on gene testing.
6. Reproductive and menstrual history:
    a. The older a woman having her first child, the greater her chance of breast cancer.
    b. Women who had their first menstrual period before the age of 12 are at an increased risk of breast cancer.
    c. Women who went through menopause after the age of 55 are at an increased risk of breast cancer.
    d. Women who never had children are at an increased risk of breast cancer.
    e. Women who take menopausal hormone therapy with estrogen plus progestin after menopause also appear to have an increased risk of breast cancer.

    Large, well designed studies have shown no link between abortion or miscarriage and breast cancer.
7. Race: Breast cancer is diagnosed more often in white women than Latin American, Asian, or African American women.
8. Radiation therapy to the chest: Women who had radiation therapy to the chest (including breasts) before the age of 30 are at an increased risk of breast cancer. This includes women treated with radiation for Hodgkin's lymphoma. Studies show that the younger a woman who received radiation treatment, the higher the risk of breast cancer appear later in her life.
9. Breast density: Breast tissue may be dense or fatty. Older women whose mammograms show more dense tissue are at increased risk of breast cancer.
10. Taking diethylstilbestrol (DES): DES was given to some pregnant women in the United States between about 1940 and 1971. (It is no longer given to pregnant women.) Women who took DES during pregnancy may have a slightly increased risk of breast cancer. The possible effects on their daughters are under study.
11. Being overweight or obese after menopause: The chance of getting breast cancer after menopause is higher in women who are overweight or obese.
12. Lack of physical activity: Women who are physically inactive throughout life may have an increased risk of breast cancer. Being active may help reduce risk by preventing weight gain and obesity.

13. Drinking alcohol: Studies suggest that the more alcohol a woman drinks, the greater her risk of breast cancer.
14. Other possible risk factors are under study. Researchers are in progress for the effect of diet, physical activity, and genetics on breast cancer risk. They are also studying whether certain substances in the environment can increase the risk of breast cancer.
15. Many risk factors can be avoided except the family history. Women can help protect themselves by staying away from known risk factors whenever possible.
16. It is not confirmed that most women who have known risk factors showed get breast cancer. Also, most women with breast cancer are not necessary have a family history of the disease. In fact, except for growing older, most women with breast cancer have no clear risk factors.

2.1.2.2 Symptoms

Early breast cancer can in some cases be painful. Usually breast cancer is discovered before any symptoms are present, either on mammography or by feeling a breast lump. A lump under the arm or above the collarbone that does not go away may be present. Other possible symptoms include breast discharge, nipple inversion and changes in the skin overlying the breast.

2.1.2.3 Screening

Due to the high incidence of breast cancer among the older women, screening is now recommended in many countries, the same also applies to men. Screening methods suggested include breast self-examination and mammography. Mammography has been shown to reduce breast cancer-related mortality by 20-30%. Routine (annual) mammography of women older than 40 is encouraged as a screening method to diagnose early breast cancer and has demonstrated a protective effect in multiple clinical trials.

2.1.2.4 Diagnosis

The diagnosis of breast cancer is established by the pathological examination of removed breast tissue. Such tissue is generally obtained at the time of surgical treatment. A number of procedures have been devised to obtain tissue or cells prior to the treatment for histological or cytological examination. Such procedures include fine-needle aspiration, nipples aspirates, ductal lavage, core needle biopsy, and local surgical biopsy. Most of these diagnostic steps, however, have some limitations as they may not yield enough tissue or miss the cancer, while the surgical biopsy already becomes an invasive procedure. Imaging tests are used to detect metastasis and include chest x-ray, bone scan, CT, MRI, and PET scanning. Carbohydrate antigen 15.3, Ca 15.3 epithelial mucin is a tumor marker determined in blood test which can be used to follow up disease activity.

2.1.2.5 Treatment

The mainstay of breast cancer treatment is surgery when the tumor is localized, with possible adjuvant hormonal therapy (with tamoxifen or an aromatase inhibitor), chemotherapy, and/or radiotherapy. At present, the treatment recommendations after surgery (adjuvant therapy) follow a pattern, which may be adapted as every two years a worldwide conference takes place in St.Gallen, Switzerland to discuss the actual results of worldwide multi center studies. Depending on clinical criteria, age, type of cancer, size, metastasis, the patients are roughly divided according to the high risk and the low risk cases which follow different rules for therapy. Treatment possibilities include Radiation Therapy, Chemotherapy, Hormone Therapy, and Immune Therapy.

2.1.3 Breast dosimetry

2.1.3. 1 Average glandular dose (AGD) [6].

AGD is a universal term used in the field of diagnostic breast imaging that provides a means of characterizing the carcinogenic risk associated with diagnostic mammograms. This term represents the average absorbed radiation dose to the most radiosensitive tissues (glandular tissues) of the female breast. The AGD to the female breast from diagnostic mammograms is contingent on properties and qualities of both the x-ray beam and the breast tissue itself. The two most important characteristics of the breast tissue are the thickness of the breast and the tissue composition of the breast. Glandular breast tissues are more susceptible to radiation induced carcinogenesis than adipose and skin tissues. Additionally, it takes more x-ray exposure to penetrate denser (glandular) breast tissue than fatty (adipose) breast tissue and more exposure to penetrate a thicker breast than a thinner breast. The characteristics of the x-ray beam also influence the absorbed dose to breast tissue. The x-ray beam characteristics that are of particular importance to AGD determination are the beam quality (HVL) and the target materials (anode) of the x-ray tube. The HVL is the indirect measure of the energies of the photons from the x-ray beam and is determined by the amount of material required to reduce the x-ray beam intensity by 50%. Both of these properties are important in the determination of AGD, because both influence the energy spectrum of the phtons in the mammography beam.

The estimation of the absorbed dose to the breast is an important part of the quality control of the mammographic examination. Knowledge of breast dose is essential for the design and performance assessment of mammographic imaging systems. The approved ACR methodology for AGD determination entails a direct measurement of collisional air Kerma (Ka) and its conversion to absorbed dose through the use of calculated conversion factors. This methodology is the standard used for AGD determination and is based upon the conventional screen-film image receptor used in mammography. Digital mammography uses a solid-state detector (amorphous selenium with Cesium Iodide (CsI)) as its image receptor. This difference in image receptor could result in differences in radiation backscatter and ultimately AGD measurements. In order to verify the applicability of the ACR's AGD methodology to digital mammography, AGD measurements were performed using thermoluminescent dosimeter (TLD) and ionization chamber measurements.

2.1.3.2 Calculation and determination of AGD [7].

The traditional and approved methods of determining AGD is the measurement of the entrance skin exposure (ESE) and converting it to AGD. The ESE measurements are performed using an ionization chamber placed next to a 4.2 cm 50% adipose 50% glandular phantom. These measurements require off central axis free in air measurements of ESE and use of conversion tables developed by Wu, et al [9]. The conversion tables in the ACR's mammography quality standards act (MQSA) manual include the following factors: the x-ray tube voltage in kVp, target and filter combination and the HVL of the beam. The table values convert the air exposure measured in Roentgens (R) to absorbed dose in units of millirad (mrad) and is expressed in equation 2.1 [8].

$$D_g = D_{gN} \times X_{ESE} \qquad (2.1)$$

The term D_g represents the AGD, D_{gN} is the normalized average glandular dose per ESE (conversion factors) and X_{ESE} is the measured ESE. The conversion factors (D_{gN}) are based on Monte Carlo calculations of the predominant photon-tissue interactions in mammography [9]. The specific photon-tissue interactions of interest in mammography are the photoelectric effect, incoherent scattering and coherent scattering. This calculated AGD represents the average dose to the most radiosensitive breast tissues (glandular tissue) and describes the carcinogenic risk associated with ionizing radiation exposure from mammography.

2.1.4 Screen-film and digital mammography systems [2].

Mammography units are special radiographic x-ray machines that are specifically designed to image the female breast. The units consist of the standard components as in a general radiographic x-ray machine with some selective changes that are necessary to image the softer tissues in the female breast. The important differences between the general radiographic machines and mammography units involve the target (anode) material and filters used. The most common target materials in use in mammography units are molybdenum (Mo), with the availability to change target material to rhodium (Rh) and tungsten (W). The typical x-ray beam filtration in mammographic machines include some form of inherent filtration such as beryllium (Be) and the capability to select additional filtration materials such as Mo and Rh. The versatility of mammography machines to be adjusted to select target, filtration combinations and tube voltages (kVp) allows for optimized image quality. However, the most important aspects of the mammography unit involve the image receptor used to record the image. The most common type of image receptor used is screen-film mammography. The screen-film units use single emulsion film with a special cassette. These cassettes contain a low attenuation carbon fiber with a Terbium-activated Gadolinium Oxysulfide (Gd_2O_2S: Tb) phosphor screen. The cassette and film combination are designed to ensure the best spatial resolution of the image. This is accomplished by placing the film on top of the phosphor screen, which allows the x-rays passing through the top of the cassette and film before interacting with the phosphor screen.

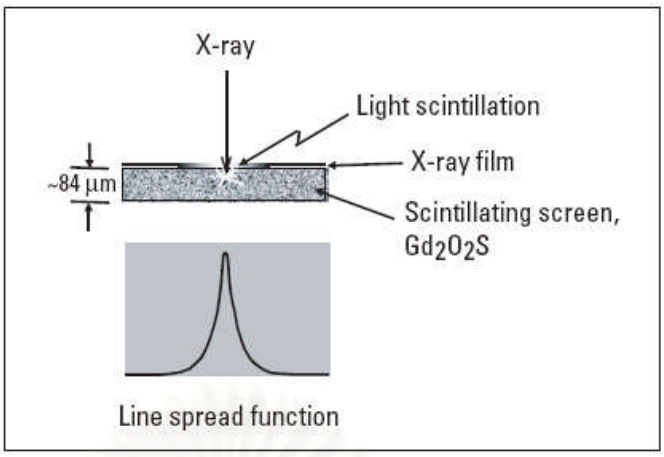

Figure 2.3 Diagram showing screen-film systems using a scintillating screen to absorb the x-rays and generate light photons, captured by the film

Digital mammography units employ a completely different type of image receptor from screen-film units. The image receptor is amorphous selenium as the photoconductor, a thickness of 250 microns is adequate to stop more than 95 percent of the x-rays in the mammographic energy range, as shown in Figure 2.3. Standard screens used in film mammography only have about 50 to 70 percent quantum efficiency, a photoconductor absorbs the x-rays more than 95 percent and directly generates the signal (direct conversion). Under the influence of an external electric field, holes or electrons, drift towards a pixel electrode and are collected on a pixel capacitor. Because the electrons and holes travel along the direction of the electric field lines, they move without lateral charge spreading. This results in an exceptionally narrow point spread response, of about 1 micron. Digital detectors require an array of pixels that collect electronic signals. The signals on these pixels are transferred to a computer during a readout sequence. This is known as direct readout, a function of all digital systems, which are different from direct conversion digital detection as shown in Figure 2.4.

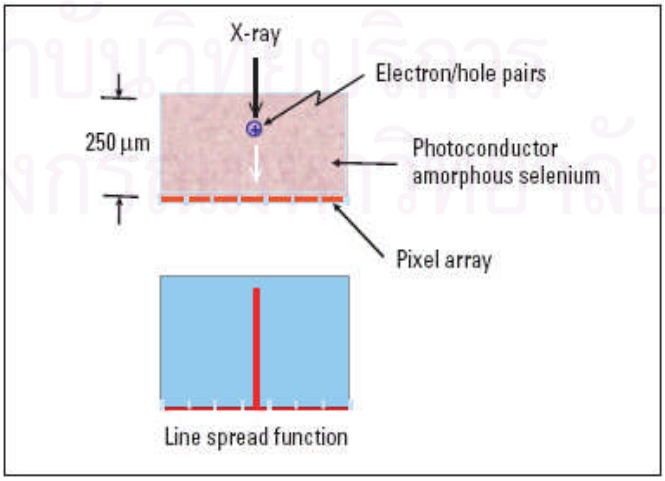

Figure 2.4 Diagram showing direct conversion detectors using a photoconductor to absorb the x-rays and directly generate the signal

2.2 Literature review

Gennaro et al. [10] compared between doses delivered by a FFDM system and a SFM unit, both using the same type of X-ray tube. Exposure parameters and breast thickness were collected for 300 screen/films (GE Senographe DMR) and 296 digital mammograms (GE Senographe 2000D). The entrance surface air kerma (ESAK) was calculated from anode/filter combination, kVp, mAs values and breast thickness, by simulating spectra through a program based on the experimental x-ray spectra. The AGD was computed which the result was 1.92 mGy for SFM and 1.40 mGy for FFDM. An overall reduction of average glandular dose by 27% of digital over SFM. The dose saving was about 15% for thin and thick breasts, while it was between 30% and 40% for intermediate thicknesses. FFDM dose reduction is allowed by wider dynamic range and higher efficiency of digital detector, which can be exposed at higher energy spectra than SFM, and by the separation between acquisition and displaying processes.

Hermann et al. [11] determined the average glandular dose with a FFDM system using a flat-panel X-ray detector based on amorphous silicon technology for a large group of patients. The patient group includes women who were examined in a 4 month period with the digital mammographic system Senographe 2000D. The number of women was 591 and the number of exposures was 1,116, only CC projection was considered. Various quantities, including entrance surface air kerma, tube loading, and compressed breast thickness (CBT), were determined during mammography. The AGD was determined using conversion factors g for standard breast composition. The results showed the mean AGD of 1.51 mGy (0.66 - 4.05 mGy) for a single view. The mean CBT was 55.7 mm. The mean age of patients was 55 years (34 - 81 years). The results demonstrated that FFDM with a flat-panel detector based on amorphous silicon offer about 25 % less dose in comparison with SFM.

Bouzariomehri et al. [12] determined the mean glandular dose (MGD) resulting from mammography examinations in Yazd, southeastern Iran and to identify the factors affecting it. The clinical data were collected from 946 mammograms taken from 246 women who were referred to four mammography centers during May to December 2005. The mammography instruments in these centers were four film-screen systems with a molybdenum anode and either molybdenum or rhodium filter. The exposure conditions of each mammogram were recorded. The breast glandular content of each mammogram was estimated by a radiologist. The MGD was calculated based on measuring the normalized entrance skin dose (ESD) in air, HVL, kVp, mAs, breast thickness and glandular content. HVL, kVp and ESD were measured by a solid-state detector. The mean±SD CBT for CC and MLO views were 47.6±12.5 and 56.7±13.3 mm, respectively. The analytical method of Sobol et al. was used for calculation of MGD. The mean±SD MGD per film was 1.2±0.6 mGy for CC and 1.63±0.9 mGy for MLO views. The mean±SD MGD per woman was 5.57±3.1 mGy. A positive correlation was found between the beam HVL with MGD (r=0.38) and the breast thickness with MGD (r=0.5).

Jamal et al. [13] determined the MGD during diagnostic mammography in Malaysia and evaluated the factors affecting MGD. A survey of standard MGD was performed based upon quality control records for the period of October 1999 to August 2001. This covered 30 screen-film mammography units from 9 manufacturers. MGD was also measured for a series of patients attending mammography examinations at three other mammography units. MGD per film was estimated from recorded radiographic factors, the CBT and X-ray unit calibration data. MGD per

woman was calculated by summing the MGDs for all films, and averaging it over both breasts. 300 women drawn equally from three major ethnic groups, namely Malay, Chinese and Indian, took part in the study. The difference of MGD per woman between ethnic groups was tested for significance using non-parametric Kruskal–Wallis and median tests. The factors affecting MGD per woman were tested for significance using a multivariate analysis of variance. The MGD for the phantom was 1.23 mGy (range 0.22– 2.39 mGy) while the mean patient based MGD per film was 1.54 mGy and 1.82 mGy for the CC and MLO views, respectively. The mean MGD per woman was 3.37 mGy. The multivariate test two factors, namely half value layer of the x-ray beam ($p<0.001$) and CBT ($p=0.045$), had a direct correlation on MGD per woman. No significant relationships were seen between MGD per woman with respect to ethnicity, body mass index or age.

CHAPTER 3

RESEARCH METHODOLOGY

3.1 Research design

This study is a retrospective descriptive research.

3.2 Research questions

3.2.1 Primary research question

What is the AGD and mean breast thickness in Thai female undergoing full field digital mammography at King Chulalongkorn Memorial Hospital?

3.2.2 Secondary research question

Which factor (s) (kVp, mAs, CBT, compression force, target/filter) affect(s) the patient dose?

3.3 Research design model

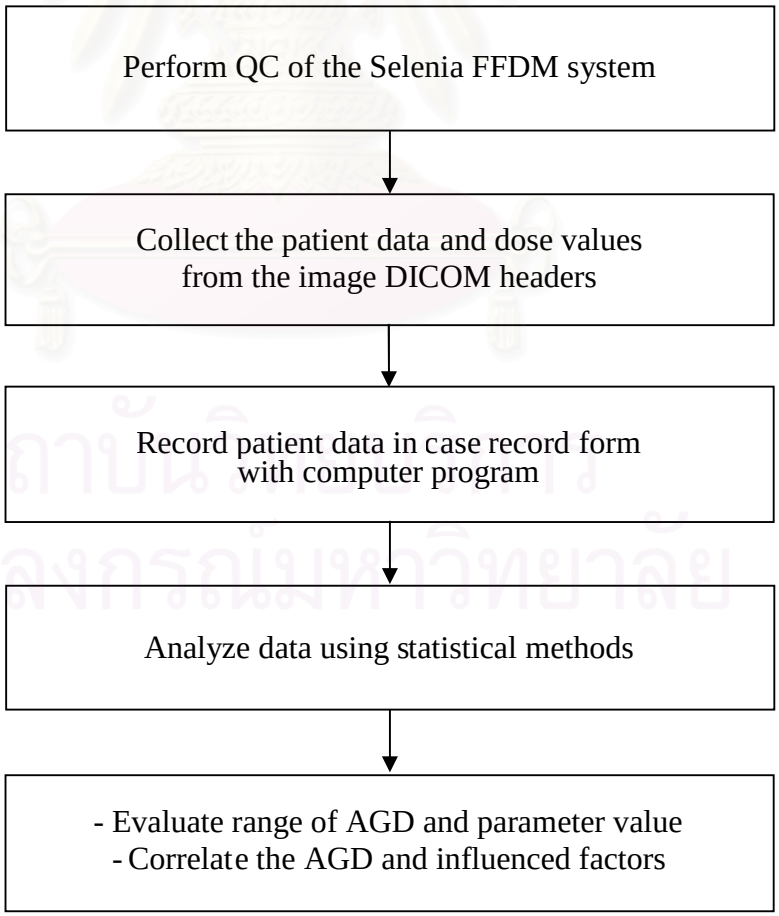

3.4 Conceptual framework

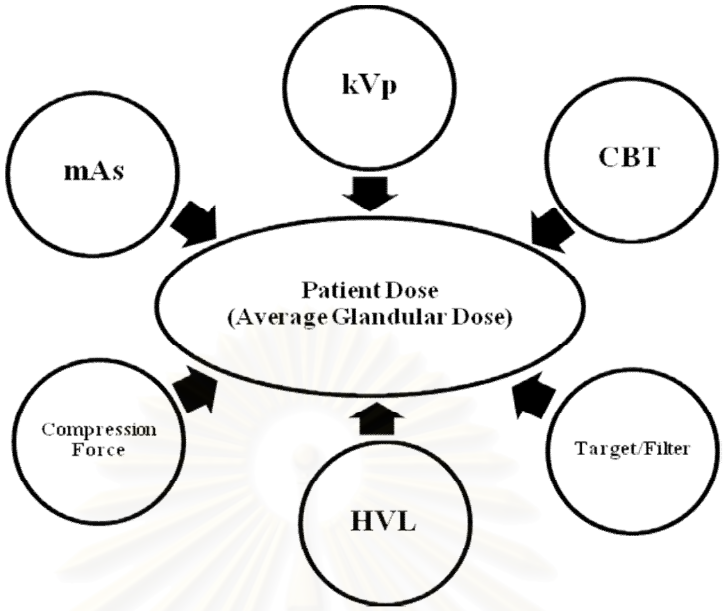

3.5 The Sample

3.5.1 Target population

The Thai female undergoing FFDM at King Chulalongkorn Memorial Hospital.

Inclusion criteria : Thai female, screening and diagnostic mammography.

Exclusion criteria : Implant breast , breast conservation surgery, non Automatic Exposure Control(AEC) cases.

3.5.2 Sample population

The number of Thai female undergoing FFDM at King Chulalongkorn Memorial Hospital during the period February 2006 to February 2007.

3.5.3 Sample

The sample of 749 Thai female, who meet the criteria, without sampling technique.

3.6 Materials

3.6.1 Full field digital mammography

The Hologic (LORAD) model Selenia FFDM consists of an image acquisition system with a digital image receptor. This receptor, which covers an area of 24 cm × 29 cm, is direct conversion detector using amorphous selenium (a-Se) photoconductor to absorb the x-rays and directly generate the signal. The x-ray tube consists of a Molybdenum (Mo) anode material, Mo and Rhodium (Rh) filtration materials. The two focal spot sizes are 0.3 mm for large nominal and 0.1 mm for small nominal. The

source to image distance (SID) is 66 cm. The three modes selective performances are AEC mode, Tissue Exposure Control (TEC) mode and manual mode. For AEC mode, one of three modes: auto kV, auto time, or auto filter could be selected. During AEC, the kVp is calculated by the set AEC table as a function of compression thickness (Appendix A). The pre-exposure (50 milliseconds) is used to calculate the mAs, the mA setting as a function of kV. During the pre-exposure, the resulting pixel value is evaluated and the appropriate mAs that will produce a targeted pixel value are determined. The CBT is estimated from the digital compression paddle height readout. The dose detection is a measure of the percentage of x-rays absorbed by the detector. The FFDM system is shown in Figure 3.1.

Figure 3.1 The LORAD Selenia FFDM system showing an image acquisition system and the x-ray system with direct detector

3.6.2 Radiation dosemeter

The Victoreen model 4000M+ sizes 8 cm height, 22 cm width, 23 cm depth using parallel plate ionization chamber of 36 cm^3 volume is shown in Figure 3.2. In a single exposure, it simultaneously displays various parameters of:

- kVp
- Exposure or Air Kerma
- Exposure Rate or Air Kerma Rate
- Time

The model 4000M+ could be used to measure the output from the radiographic, fluoroscopic, mammography and dental x-ray systems. In addition, it is calibrated for both tungsten anode (W) and Mo anode, making it suitable for screen film mammography applications. Its automatic waveform phase determination and extensive diagnostics minimize the potential for error. The external ion chamber port accepts a variety of accessory ionization chambers for various applications, including mammography, photo-timer calibration, and input phosphor image intensifier

measurements. A separate internal ionization chamber measures tube output. Time is measured with crystal quartz accuracy. The specifications of measured quantities:

Kilovoltage:

- Measured during the first 300 ms of exposure: kVp average, kVp effective, kVp maximum
- Accuracy: not available
- Range: W/Al: 27 to 155 kVp, calibrated to a tungsten anode tube with 4.5 mm Al total filtration; Mo/Mo: 21-50 kVp, calibrated to a molybdenum anode tube with 0.03 mm Mo total filtration; Accuracy: 1 kV Mo/Mo (22 to 35 kVp)

Time:

- Measured during entire exposure; referenced to 90% rise/fall kV time.
- Accuracy: Within2% or 2 ms
- Range: 1 ms to 10 sec

Exposure:

- Measured during entire exposure, kVp corrected
- Accuracy: ±10%
- Range: 10 mR to 10 R

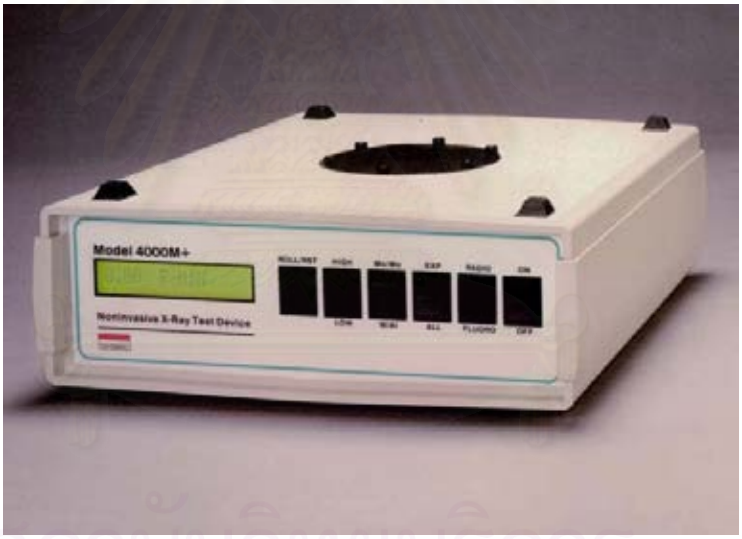

Figure 3.2 Ionization chamber manufacturer Victoreen model 4000M+

3.6.3 Breast phantom

The GAMMEX/RMI mammographic accreditation phantom RMI 156 is made of a wax block as shown in Figure 3.3. The technical data are 0.55 kg weight and 4.5 cm x 10.2 cm x 10.8 cm sizes (H x W x L). This phantom was designed to attenuate the x-ray beam in the same way as a human breast of 50% adipose and 50% glandular tissue compressed to a thickness of 4.5 cm.

The test objects that represent malignancies or small breast structures are embedded as an insert in an acrylic base. It contains 6 fibrils, 5 speck groups of simulated microcalcifications and 5 masses. The phantom includes appropriate details that range from visible to invisible on a standard mammographic film image.

The fibers with diameters of 1.56, 1.12, 0.89, 0.75, 0.54 and 0.40 mm; specks with diameters of 0.54, 0.40, 0.32, 0.24 and 0.16 mm; and masses with decreasing diameters of 2.00, 1.00, 0.75, 0.50 and 0.25 mm are shown in Figure 3.4.

Figure 3.3 ACR Breast phantom model RMI 156

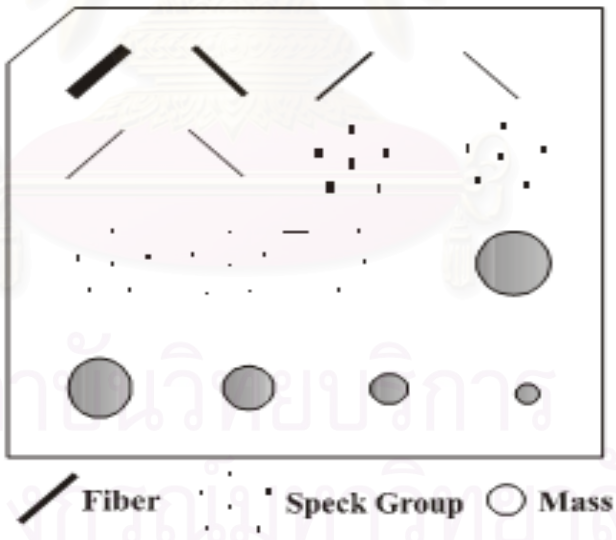

Figure 3.4 Location of the test objects in the RMI 156 breast phantom

3.6.4 Case record form

Clinical data are collected for mammographic examination (Appendix B).

3.6.5 EBM DICOM viewer (UniSight version 4.1e) software

The FFDM system is connected to two PACS namely AGFA (IMPAX Enterprise 4.5) and EBM technologies. UniSight is the viewer for the EBM PACS system. It consists of features and functions provide to read and perform diagnosis, navigate through images, and receive relevant patient information.

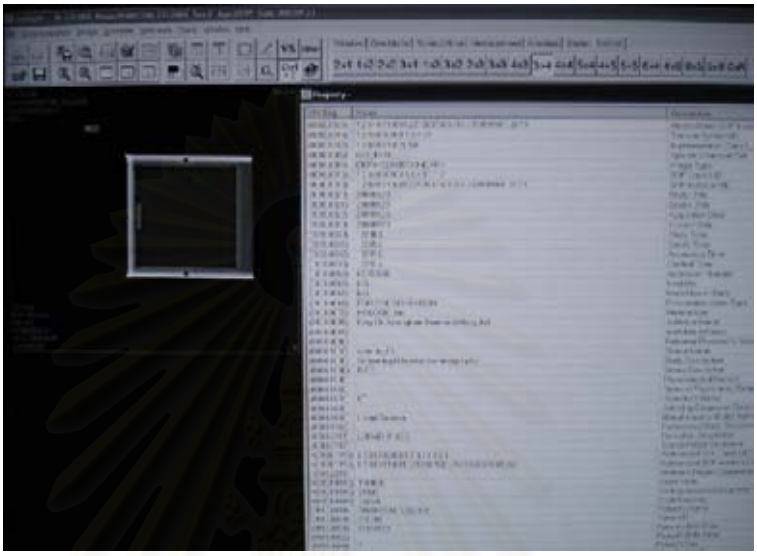

Figure 3.5 EBM DICOM viewers using for displayed images and patient information

3.6.6 Patient

This research involved 749 women underwent mammography examinations using the FFDM system.

3.7 Methods

3.7.1 Quality control

The quality control of FFDM system is performed during the period of data collection using quality control manual recommended by Lorad which include measurement frequency and methodology [19].

3.7.2 HVL and breast entrance skin exposure (X_{ESE}) measurement

The HVL and X_{ESE} measurement were designed according to the mammography quality control tests in the medical physicists section of the ACR manual [7].

The kVp, mAs and target/filter combination technique involved the identification and matching of the HVL and X_{ESE} measurement for digital mammography, which is provided in Table 3.1.

Table 3.1 The technique factors of the HVL and X_{ESE} measurement

Type of Measurement	kVp	mAs	Targrt/Filter
HVL	26,28,30,32	30	Mo/Mo
	28,30,32,34	30	Mo/Rh
X_{ESE}*	26,28,30,32	120	Mo/Mo
	28,30,32,34	120	Mo/Rh

* The X_{ESE} measurement was repeated 3 times for each kVp value and both Mo/Mo and Mo/Rh targrt/filter combinations

Victoreen system model 4000M+ used in the HVL and X_{ESE} measurement is shown in Figure 3.7.

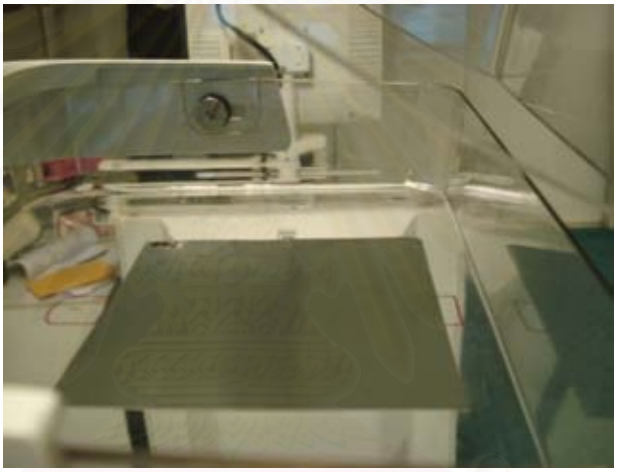

Figure 3.6 Aluminum addition for HVL measured of Mo/Mo and Mo/Rh target/filter combinations

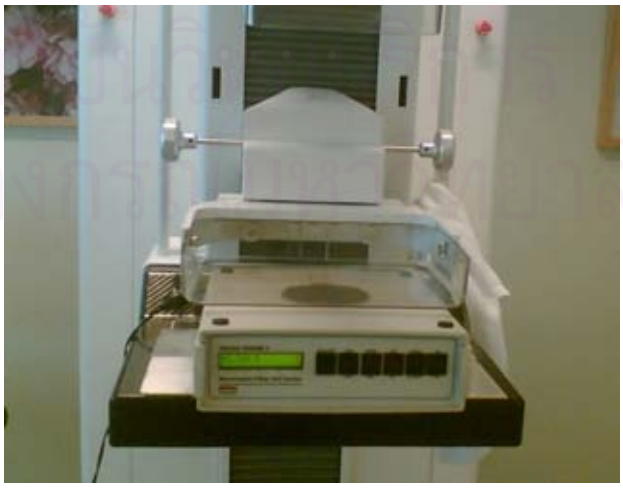

Figure 3.7 The X_{ESE} measured of Mo/Mo and Mo/Rh target/filter combinations

3.7.3 AGD verification

The traditional and approved method of determining AGD is by measuring the X_{ESE} and converting it to AGD. These measurements require off central axis free in air measurements of X_{ESE} and use of conversion factor; (D_{gN}). The conversion factor tables in the ACR manual include the following factors: the x-ray tube voltage in kVp, target and filter combination and the HVL of the beam (Appendix C). The table values convert the air exposure measured in Roentgens (R) to absorbed dose in units of millirad (mrad) and is expressed in equation 3.1[9].

$$D_g = D_{gN} \times X_{ESE} \tag{3.1}$$

Where D_g is the AGD unit in grays (Gy) and D_{gN} is the normalized average glandular dose per ESE (conversion factors) and X_{ESE} is the measured ESE. Used the D_{gN} table from the 1999 ACR mammography quality control manual, breast entrance exposure, AEC reproducibility, average glandular dose, and radiation output rate section to determine the exposure to glandular dose conversion factor for the kVp and target/filter combination used and measured HVL[7]. The X_{ESE} was correct exposure with an inverse square correction factor to obtain the exposure at surface of Victoreen system as an entrance level.

Breast phantom was also used to determine the glandular dose, as the percentage of x-rays absorbed by the detector related to the attenuation characteristics of the breast phantom. The kVp, mAs and target/filter combination technique use as in Table 3.2. The glandular dose is displayed on the acquisition workstation as shown in Figure 3.9.

Table 3.2 The technique factors based on manual mode used to determine the glandular dose

Type of Measurement	kVp	mAs	Targrt/Filter
AGD*	26,28,30,32	120	Mo/Mo
	28,30,32,34	120	Mo/Rh

* The AGD measurement was repeated 3 times for each kVp value and both Mo/Mo and Mo/Rh target/filter combinations

HVL and AGD are verified by measurements method (set as the standard method) and calculated method by determine percent of variation according to

$$Variation\ (\%) = \frac{(Calculated - Measured)}{Measured} \times 100 \tag{3.2}$$

Figure 3.8 The AGD determination using ACR breast phantom

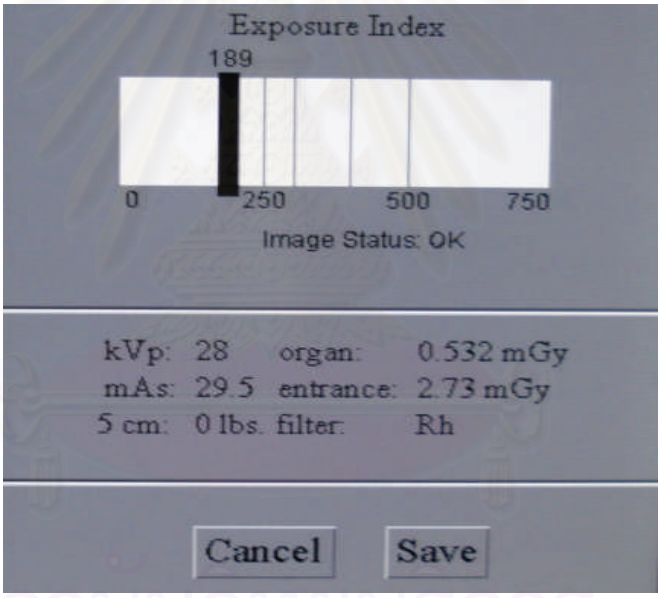

Figure 3.9 Display of calculated AGD displayed on acquisition workstation

3.8 Data collection

In this study, the information of the mammographic examinations were delivered from EBM PACS through the local data network and automatically sent to the workstation. The computer program reads the DICOM file, extracts patients data and dose values from the header, and recorded in excel program. The study involved 749 Thai female underwent mammography examinations using the FFDM system, operated by AEC mode based on auto filter mode routinely (kVp and filter automatically selected by system) during the period from February 2006 to February 2007. The inclusion criteria for population were Thai female, screening and diagnostic mammography and the exclusion criteria were implant breast, breast conservation surgery and the study with non AEC mode. The routine technique of the mammography examination is two views namely CC and MLO views. The number of images per examination is 4.

3.9 Data analysis

3.9.1 The quality control data was analyzed with excel program developed by the American Association of Physicists in Medicine (AAPM).

3.9.2 The paired samples test was used to compare the differences in the AGD determination between the measured and calculated method.

3.9.3 Patient data such as, patient age, exposure factors, CBT, compression force and patient dose were analyzed to obtain, the mean, median, ranges and standard deviation (SD) by the SPSS statistical program.

3.9.4 Compare and correlate of the data from dependent variables and independent variables. Multiple regression analysis was used determine the correlation of AGD with variables.

3.9.5 Data presentation, the table, chart, histogram, whisk box-plot and scatter plot were presented.

3.10 Outcome

3.10.1 The AGD and the distribution of doses in Thai female.

3.10.2 The distribution (mean, median, ranges value) of technique factors for patient study in FFDM system, such as mAs, kVp, CBT, compression force, target/filter combination.

3.10.3 The AGD determination among the external dosimetry method and internal dosimetry method.

3.10.4 Correlate AGD and influence factors.

3.11 Expected benefits and application

3.11.1 The guidance level of AGD for a group of Thai female performed mammography at King Chulalongkorn Memorial Hospital.

3.11.2 The range of parameters such as mAs, kVp, CBT, compression force, target/filter combination in this study.

3.11.3 The factors influenced AGD for the awareness of the radiologists and technologist in the examinations performed with FFDM system.

3.12 Ethical considerations

This research was covering the determination of patient dose and factors affecting in full field digital mammography. The patient data collection during the period of February 2006 to February 2007 had been extracted from the image DICOM headers. However, the research proposal was approved by the Ethical Committee of Faculty of Medicine, Chulalongkorn University.

CHAPTER 4

RESULTS

4.1. Quality control

The quality control of FFDM system for medical physicist and radiologic technologist shows the results are within acceptable range as recommended in the performance criteria of MQSA, which provide in Appendix D.

The results of the HVL measurements for Mo/Mo and Mo/Rh target/filter combination obtained by different methods are shown in Table 4.1 and 4.2

Table 4.1 The measured and calculated HVL for Mo/Mo target/filter combination

kVp	Measured HVL (mm Al)	Calculated HVL (mm Al)	Difference HVL value (mm Al)	Variation (%)
26	0.325	0.315	0.010	3.17
28	0.347	0.337	0.010	2.88
30	0.364	0.355	0.009	2.47
32	0.371	0.370	0.001	0.27

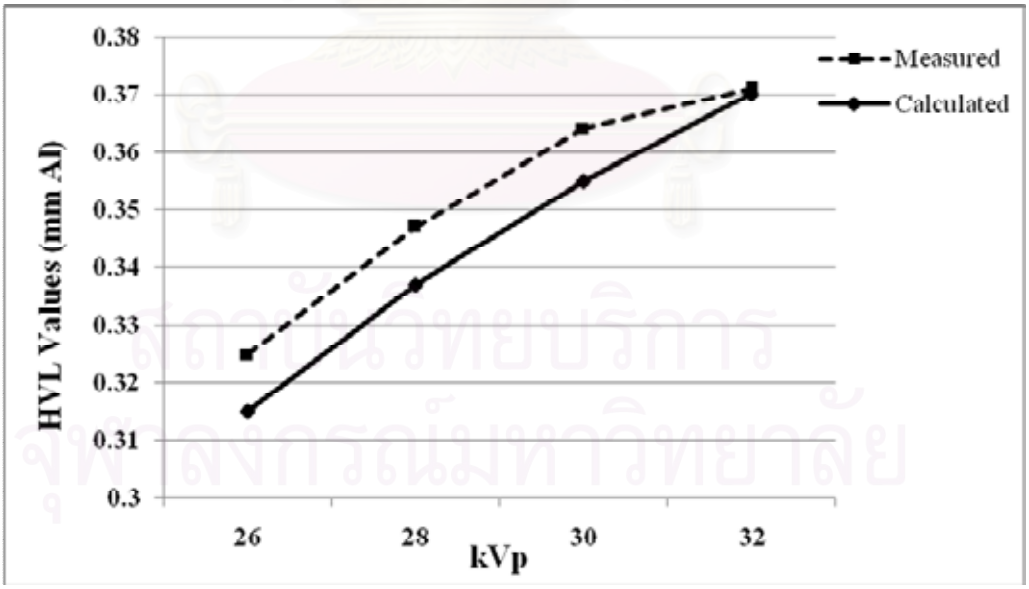

Figure 4.1 The relationship between the measured and calculated HVL for Mo/Mo target/filter combination

Table 4.2 The measured and calculated HVL for Mo/ Rh target/filter combination

kVp	Measured HVL (mm Al)	Calculated HVL (mm Al)	Difference HVL value (mm Al)	Variation (%)
28	0.395	0.424	0.029	6.84
30	0.416	0.437	0.021	4.81
32	0.439	0.449	0.010	2.23
34	0.447	0.459	0.012	2.61

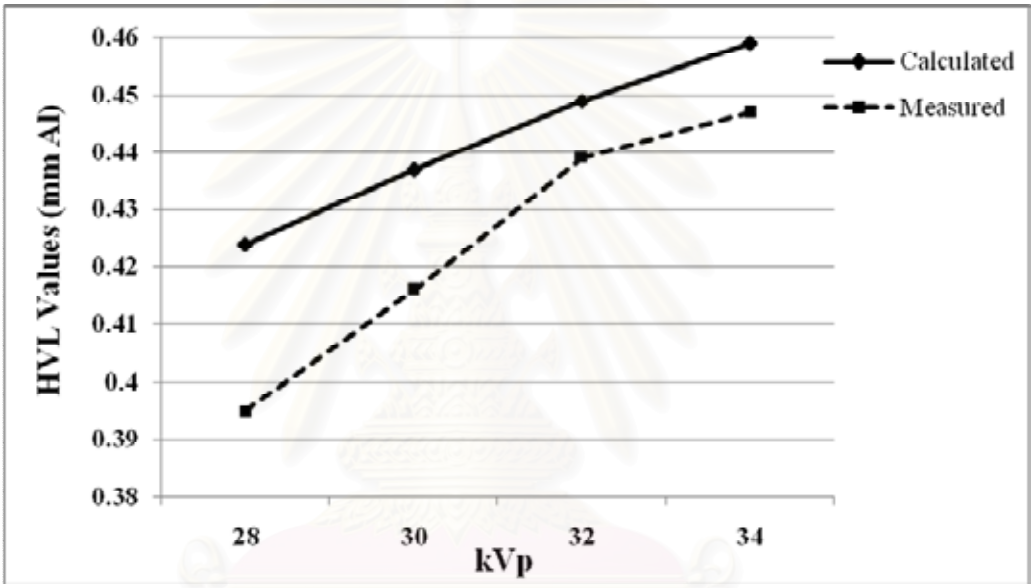

Figure 4.2 The relationship between the measured and calculated HVL for Mo/Rh target/filter combination

Table 4.3 to 4.6 show the result of measured and calculated glandular dose for each kVp, target/filter combination.

Table 4.7 and 4.8 show the verification of AGD for each kVp and target/filter combination.

Figure 4.3 and 4.4 show the relation between the measured and calculated glandular dose.

Table 4.3 The measured entrance exposure for Mo/Mo target/filter combination using Victoreen dosemeter system and converted to AGD by conversion factor

kVp	mAs	Mean entrance exposure (R)	Inverse square law conversion factor	Corrected exposure (R)	ACR conversion factor (mrad/R)	AGD (mrad)	AGD (mGy)
26	120	1.4990	0.7327	1.0983	168	184.51	1.85
28	120	1.9110	0.7327	1.4002	178	249.24	2.49
30	120	2.3586	0.7327	1.7281	185	319.70	3.20
32	120	2.8320	0.7327	2.0750	191	396.33	3.96

Table 4.4 The measured entrance exposure for Mo/ Rh target/filter combination using Victoreen dosemeter system and converted to AGD by conversion factor

kVp	mAs	Mean entrance exposure (R)	Inverse square law conversion factor	Corrected exposure (R)	ACR conversion factor (mrad/R)	AGD (mrad)	AGD (mGy)
28	120	1.2257	0.7327	0.8981	204	183.21	1.83
30	120	1.5343	0.7327	1.1242	213	239.45	2.39
32	120	1.8687	0.7327	1.3692	223	305.33	3.05
34	120	2.2230	0.7327	1.6288	228	371.37	3.71

Table 4.5 The AGD automatically calculated for images acquired of FFDM system for Mo/Mo target/filter combination

kVp	mAs	CBT (cm)	SID (cm)	ACR Phantom	AGD (mGy)
26	120	5	66	RMI156	1.99
28	120	5	66	RMI156	2.71
30	120	5	66	RMI156	3.52
32	120	5	66	RMI156	4.43

Table 4.6 The AGD automatically calculated for images acquired of FFDM system for Mo/Rh target/filter combination

kVp	mAs	CBT (cm)	SID (cm)	ACR Phantom	AGD (mGy)
28	120	5	66	RMI156	2.16
30	120	5	66	RMI156	2.81
32	120	5	66	RMI156	3.51
34	120	5	66	RMI156	4.26

Table 4.7 The AGD verification between the measured and calculated glandular dose for Mo/Mo target/filter combination in terms of the percent variation

kVp	mAs	Measured AGD (mGy)	Calculated AGD (mGy)	Difference dose value (mGy)	Variation (%)
26	120	1.85	1.99	0.14	7.57
28	120	2.49	2.71	0.22	8.84
30	120	3.20	3.52	0.32	10.00
32	120	3.96	4.43	0.47	11.87

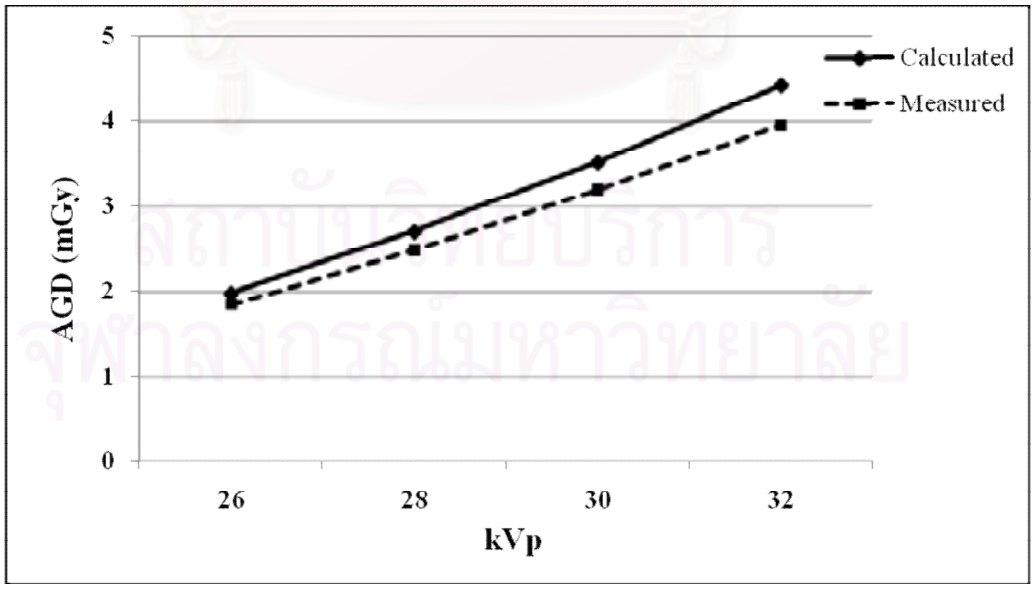

Figure 4.3 The relationship between the measured and calculated glandular dose for Mo/Mo target/filter combination

Table 4.8 The AGD verification between the measured and calculated glandular dose for Mo/Rh target/filter combination in terms of the percent variation

kVp	mAs	Measured AGD (mGy)	Calculated AGD (mGy)	Difference dose value (mGy)	Variation (%)
28	120	1.83	2.16	0.33	18.03
30	120	2.39	2.81	0.42	17.57
32	120	3.05	3.51	0.46	15.08
34	120	3.71	4.26	0.55	14.82

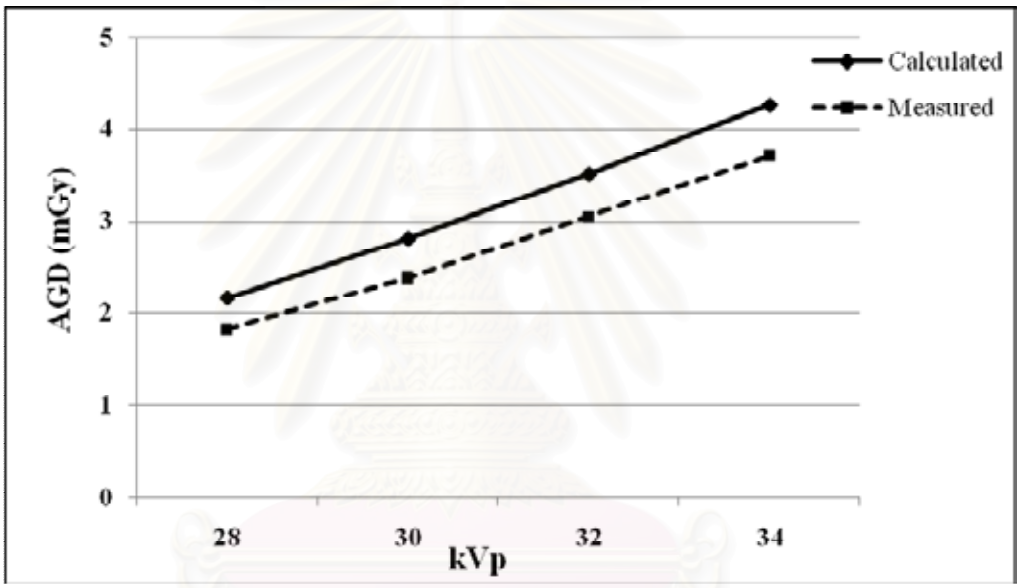

Figure 4.4 The relationship between the measured and calculated glandular dose for Mo/Rh target/filter combination

4.2 Patient information and technique factor

The patient age ranged from 29 to 81 years, with the mean of 51.3(SD±8.6) years, median of 51 years and mode of 47 years. The distribution of patient age is shown in Figure 4.5,

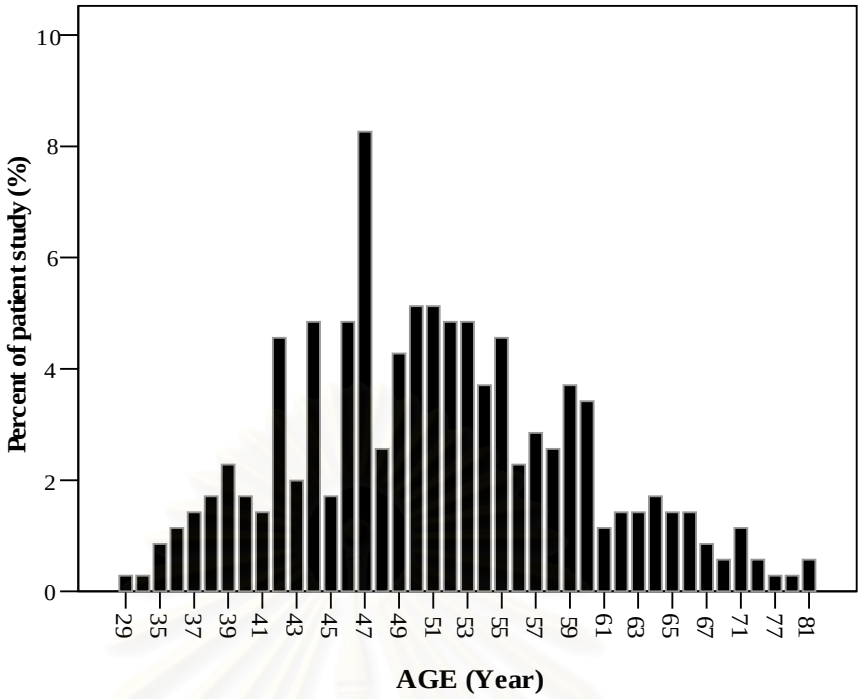

Figure 4.5 Distribution of age with percentage of patient study

The CBT ranged from 2.9 to 10.0 cm, with mean CBT for CC and MLO views were 6.2 cm and 6.1 cm respectively. The CBT is summarized in Table 4.10 and 4.11, the distributions is shown in Figure 4.6.

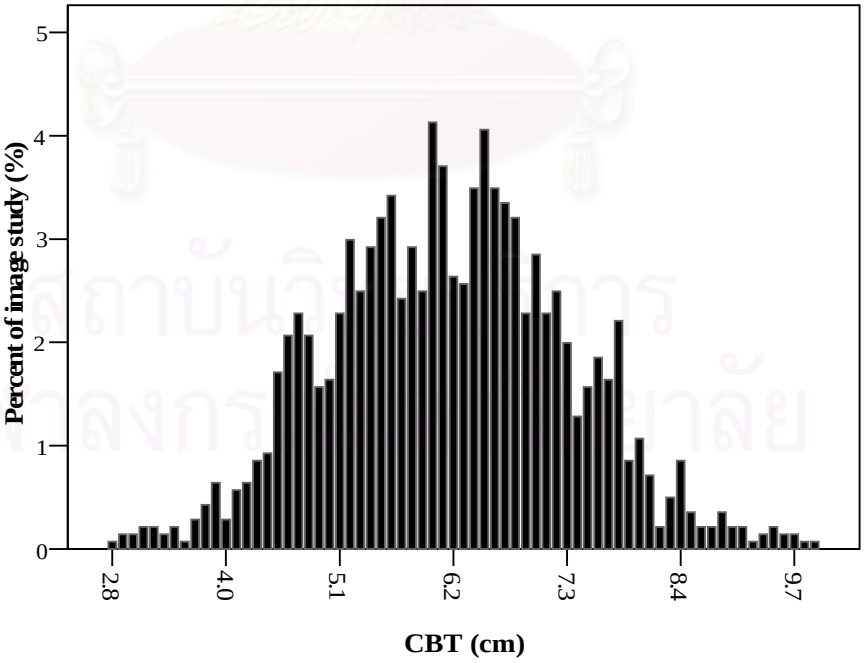

Figure 4.6 Distribution of the CBT for CC and MLO views with percentage of patient study

The patient age is not a good indicator of glandularity and there is also significant variation within and between populations and with breast size. Geise and Palchevsky[18] estimated breast glandularities and showing the effective glandular content was 16% in breasts of at least 7 cm thick when compressed; 26%, more than 5 to up to 7 cm thick; 42%, more than 3 to up to 5 cm thick, and 68% in breasts at most 3 cm thick. Similar results have been obtained by Klein et al. [24]. In this study, the CBT as classified by glandular content groups according to above studies review, the most frequency of CBT was 5-7 cm, 56.27% and 61.40% of image study for CC and MLO views as shown in Figure 4.7.

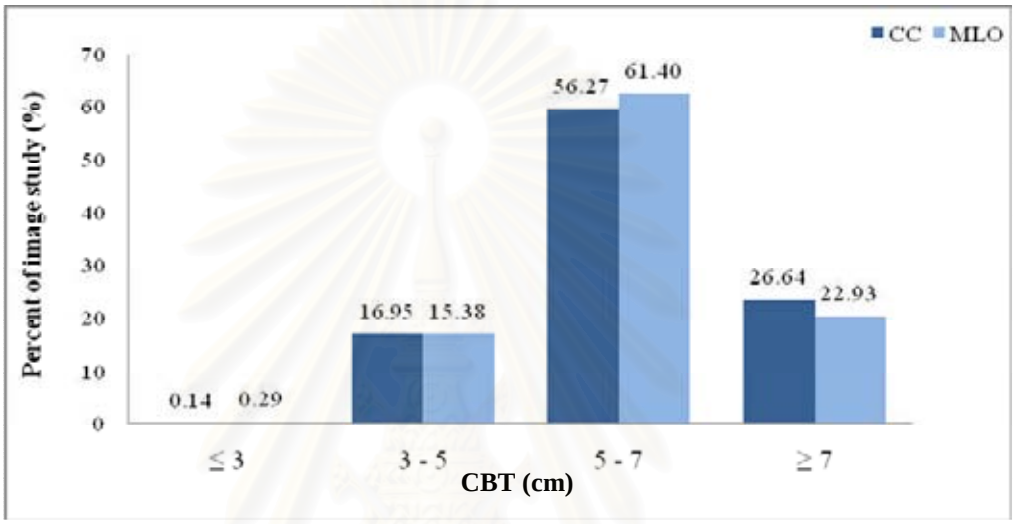

Figure 4.7 CBT distribution of the patient study according to various compressed breast thickness

The mean age of 5-7 cm CBT were 52 years for CC view and 51.8 years for MLO view as shown in Figure 4.8.

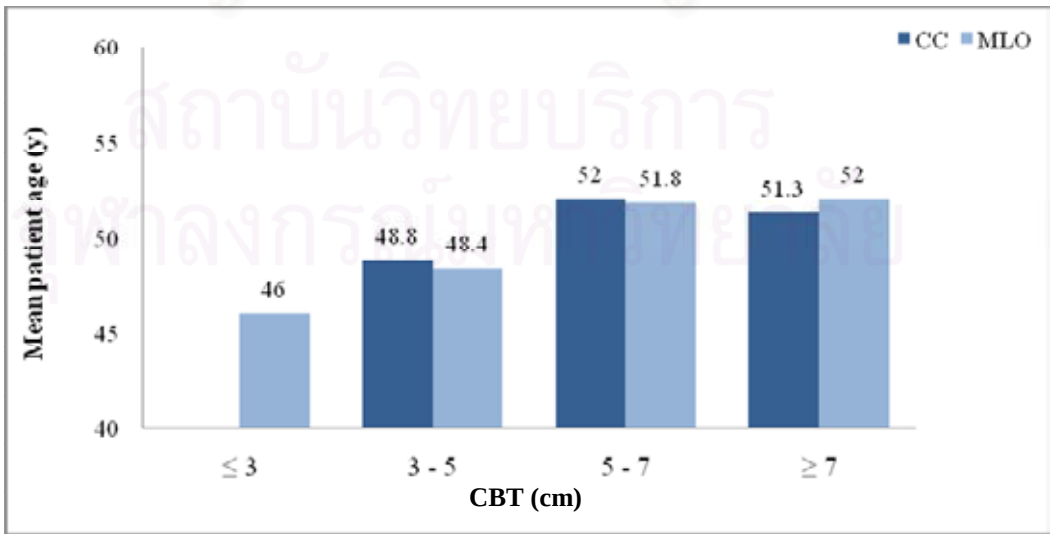

Figure 4.8 Mean age distribution of the patient study according to various compressed breast thickness

In auto filter mode, the system automatically selects all the technique factors such as the kVp using the lookup table (Appendix A) based on the CBT. If the kVp goes over 32 kVp, the system moves the Rhodium filter in place. A final kVp, post mAs value, and filter selection displays after the exposure at acquisition workstation.

The x-ray tube voltage increases from 24 to 35 kVp with breast thickness. The HVL related to the kVp value ranged from 0.295 mm Al (24 kVp) to 0.471 mm Al (35 kVp). The mAs ranged from 10.1 to 188 and the nominal values of the compression force ranged from 44.5 to 209.1 newtons (N). Descriptive statistics include mean, median, ranges value of technique factors for patient study in FFDM system, such as mAs, kVp, compression force and HVL. Those are summarized in Table 4.10 and 4.11.

The percentage of number of images acquired with each target/filter combination, median and range of kVp values are summarized in Table 4.9. Those are shown in Figure 4.9 and 4.10.

Table 4.9 The percentage of number of images acquired with each target/filter combination, median and range kVp values for CC and MLO views

CC View				MLO View			
Target/Filter	Percent selected	kVp median	kVp range	Target/Filter	Percent selected	kVp median	kVp range
Mo/Mo	40.7	29	24-30	Mo/Mo	43.9	30	24-30
Mo/Rh	59.3	32	31-35	Mo/Rh	56.1	32	31-34

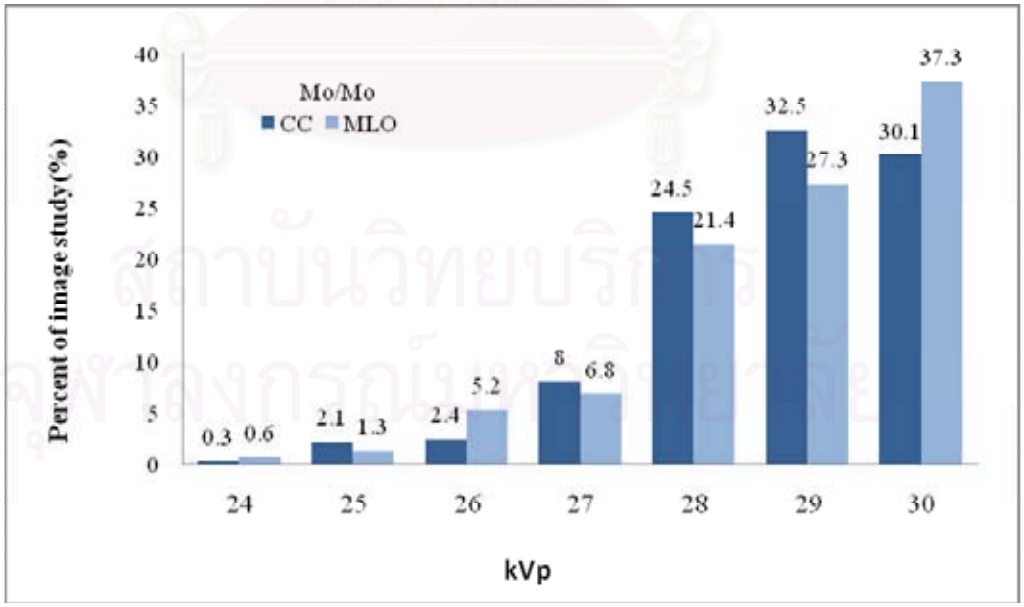

Figure 4.9 The percentage of kVp settings according to Mo/Mo target/filter combination automatically selected for image acquisition

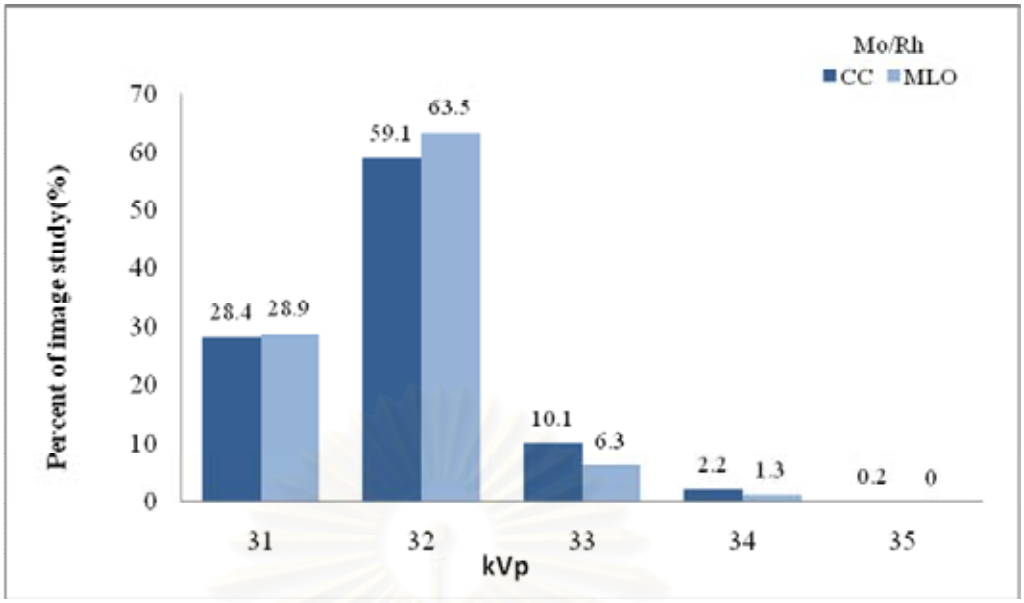

Figure 4.10 The percentage of kVp settings according to Mo/Rh target/filter combination automatically selected for image acquisition

The percentage of image study used target/filter combination for the CBT as classified by glandular content groups as shown in Figure 4.11, with 5-7 cm CBT were 25.14 for Mo/Mo and 35.75 for Mo/Rh target/filter combination.

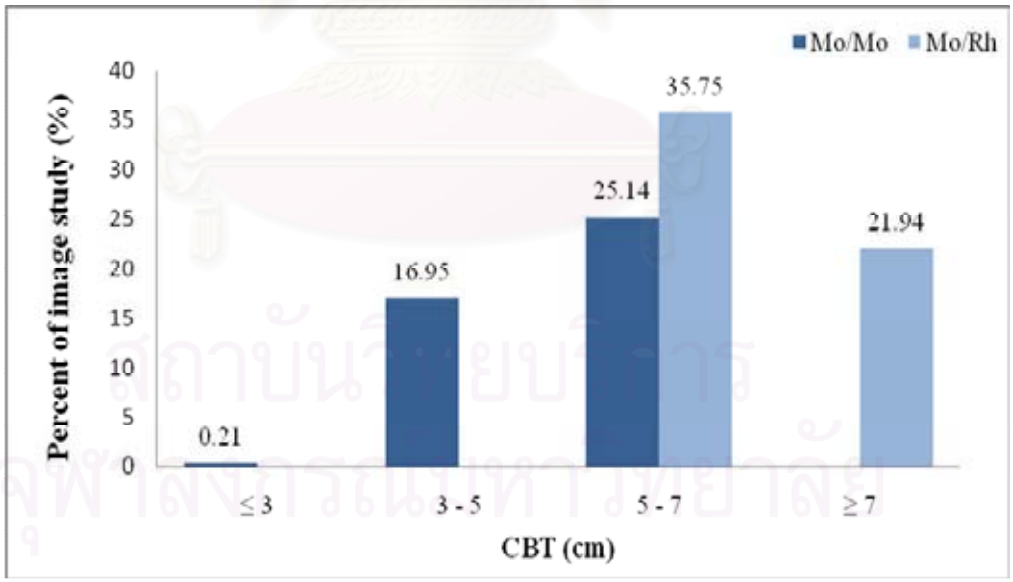

Figure 4.11 The percentage of target/filter combination settings according to various compressed breast thickness for patient study

The histogram showing the percentage of image study as a function of the compression force for CC and MLO views are shown in Figure 4.12 and 4.13.

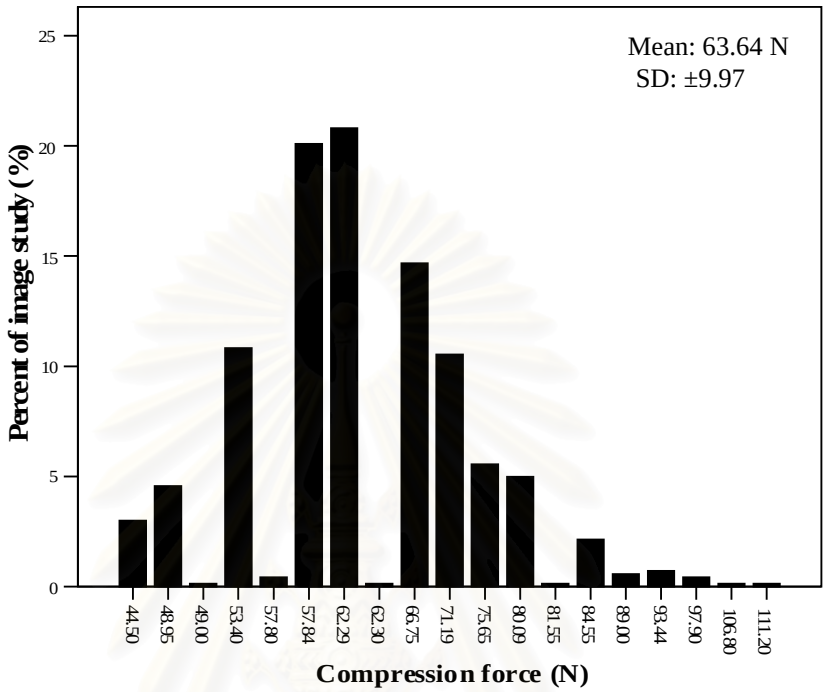

Figure 4.12 Distribution of compression force of CC view for image study

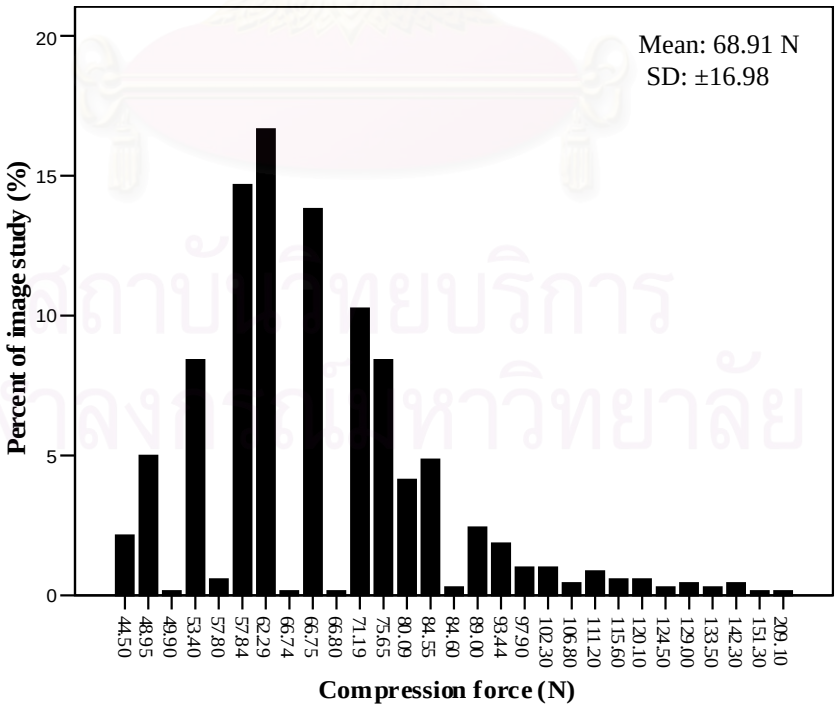

Figure 4.13 Distribution of compression force of MLO view for image study

The median compression force were 57.84, 62.29, 66.75 and 71.19 N for CC and MLO views as shown in Figure 4.14.

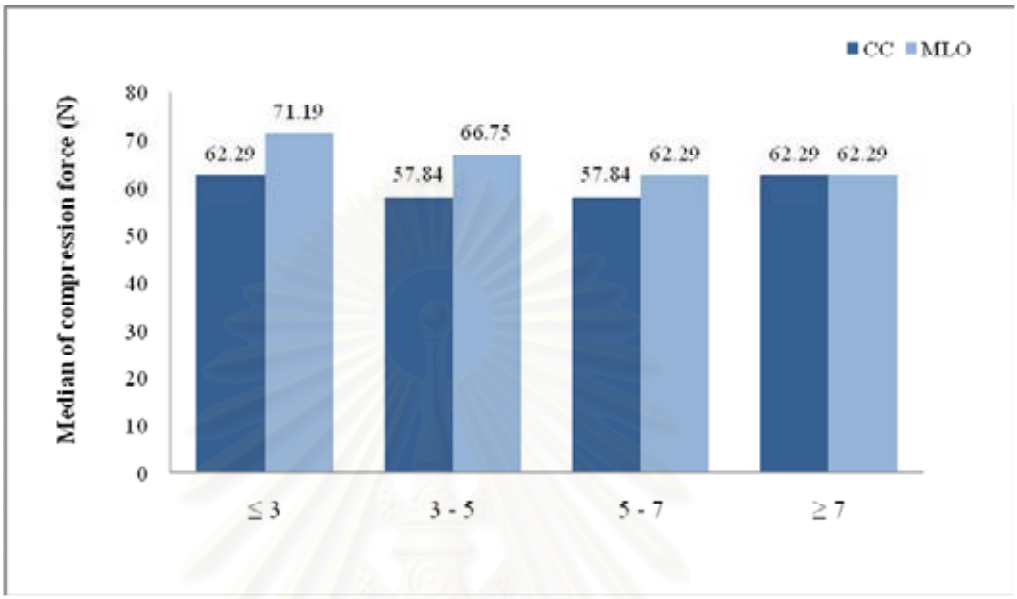

Figure 4.14 The median of compression force according to various compressed breast thickness for patient study

The histogram showing the percentage of image study as a function of the mAs values for CC and MLO views are shown in Figure 4.15 and 4.16.

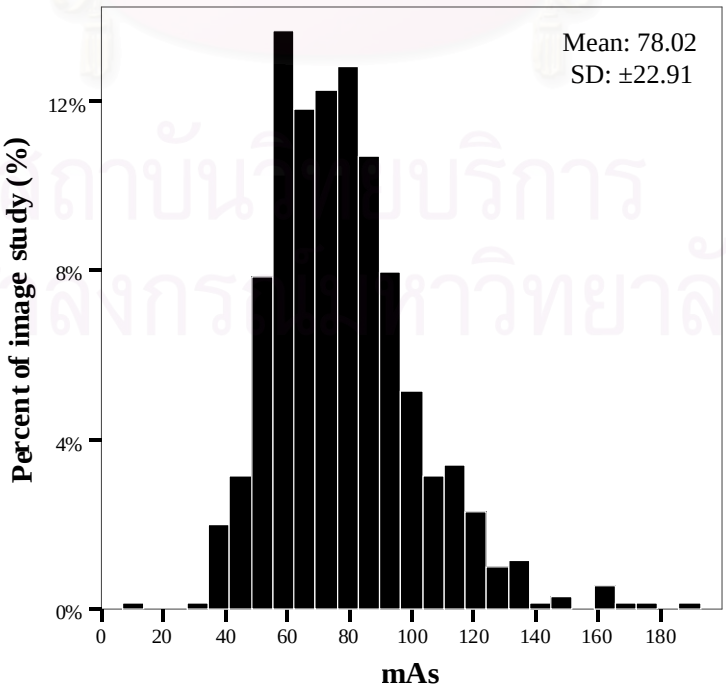

Figure 4.15 Distribution of mAs of CC view for image study

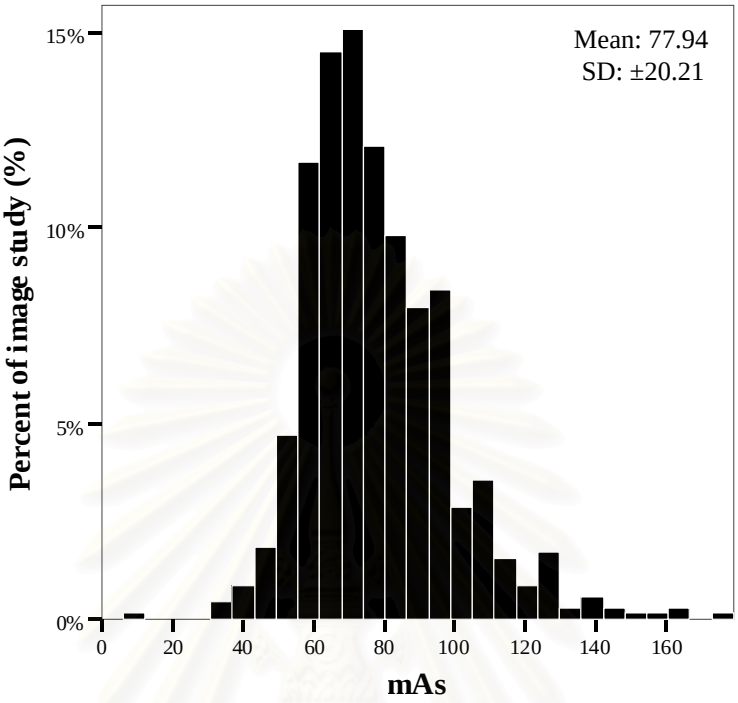

Figure 4.16 Distribution of mAs of MLO view for image study

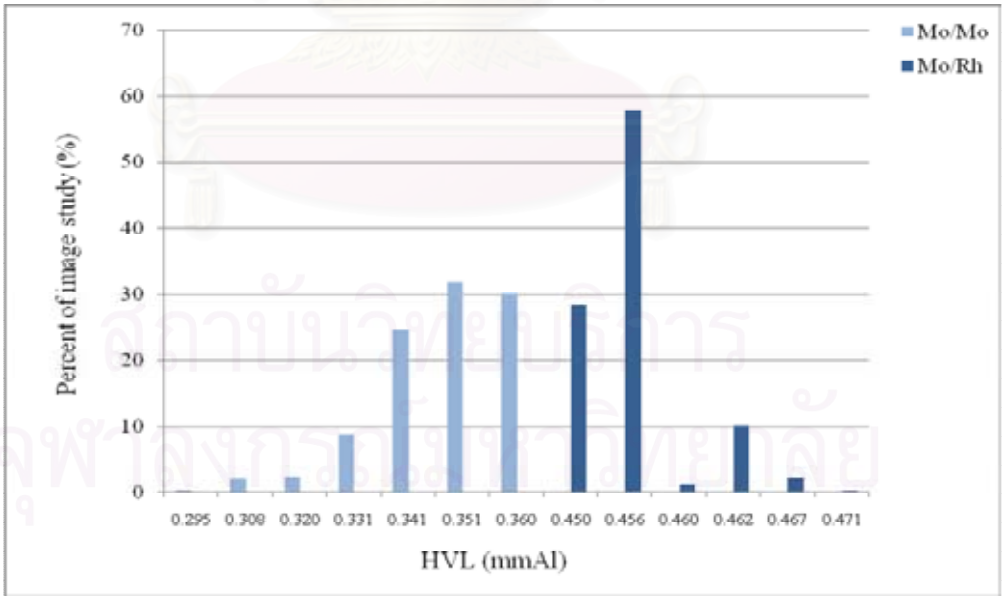

Figure 4.17 The percentage of HVL setting for Mo/Mo and Mo/Rh target/filter combinations for CC view

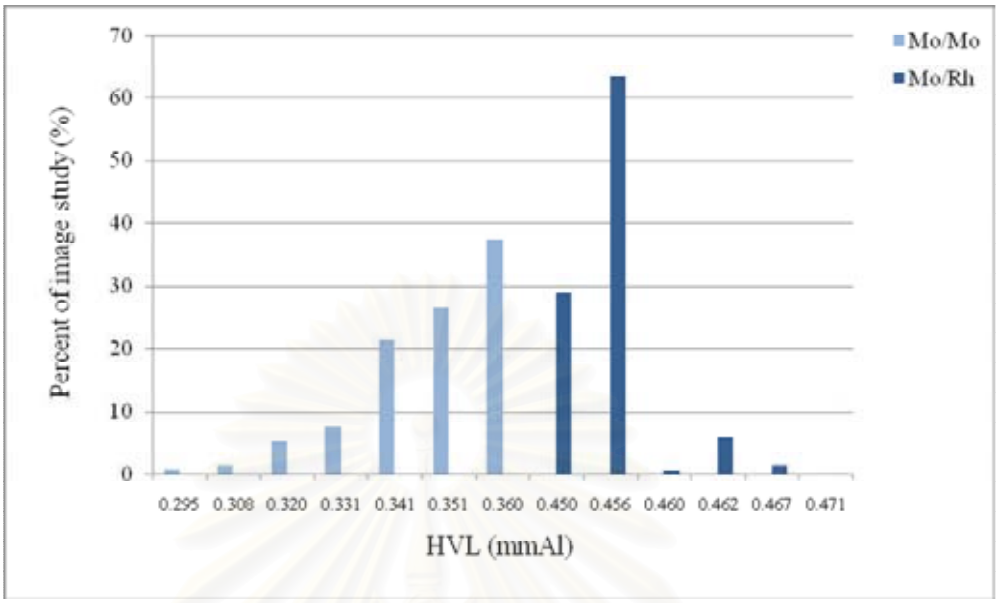

Figure 4.18 The percentage of HVL setting for Mo/Mo and Mo/Rh target/filter combinations for MLO view

4.3 Mean doses and dose distributions

The result of AGD from patient study is summarized in Table 4.12 and 4.13. The histogram showing the percentage of image study as a function of the AGD per image and woman for CC and MLO views are shown in Figure 4.19 to 4.22.

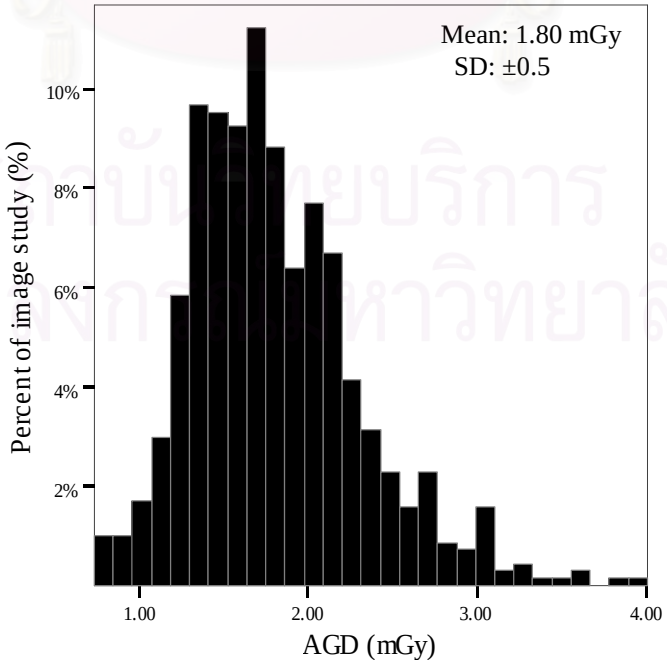

Figure 4.19 Distribution of AGD per image of CC view for image study

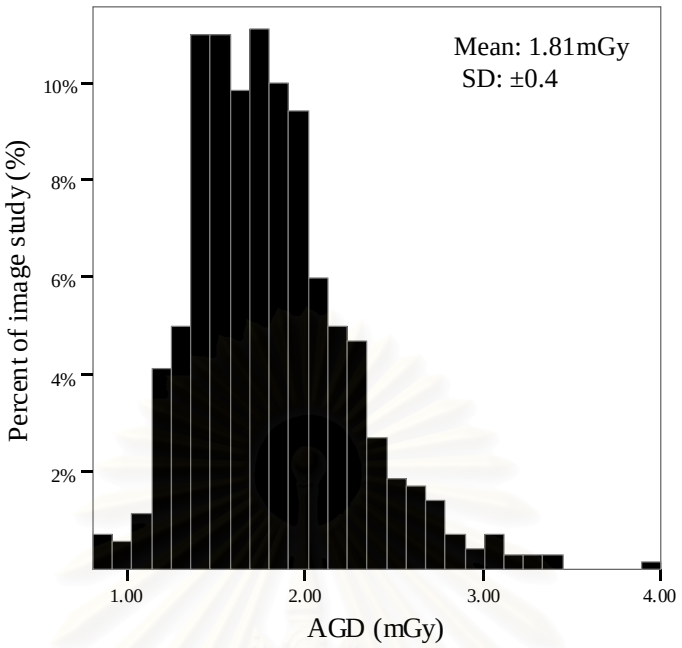

Figure 4.20 Distribution of AGD per image of MLO view for image study

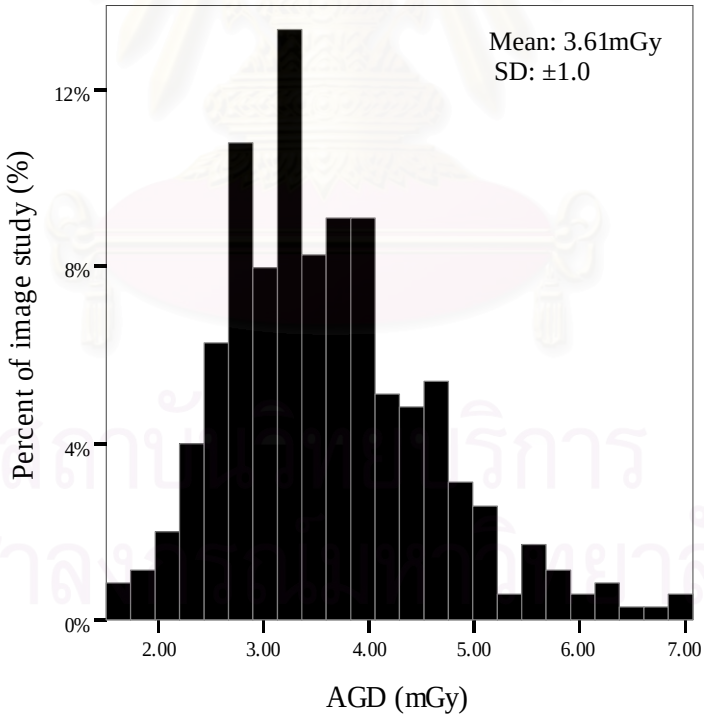

Figure 4.21 Distribution of AGD per woman of CC view for image study

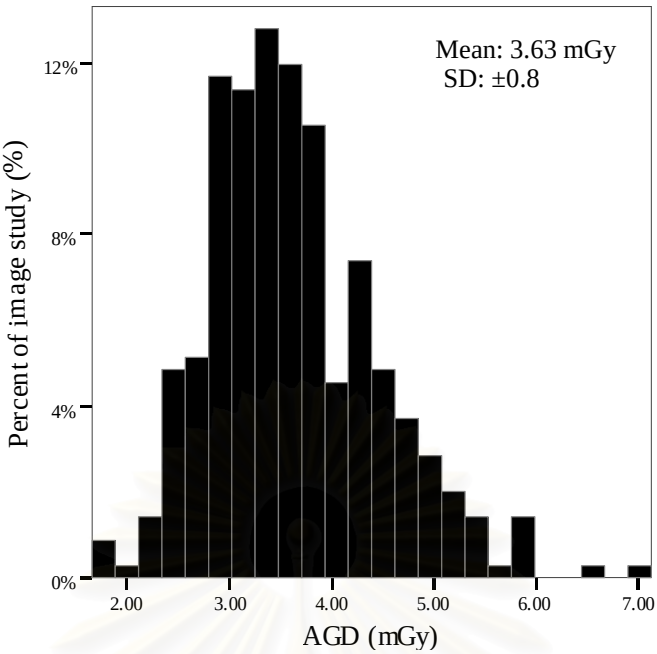

Figure 4.22 Distribution of AGD per woman of MLO view for image study

The result of ESE from patient study is summarized in Table 4.10 and 4.11. The histogram showing the ESE distributions corresponding to the AGD distributions are shown in Figure 4.23 to 4.26.

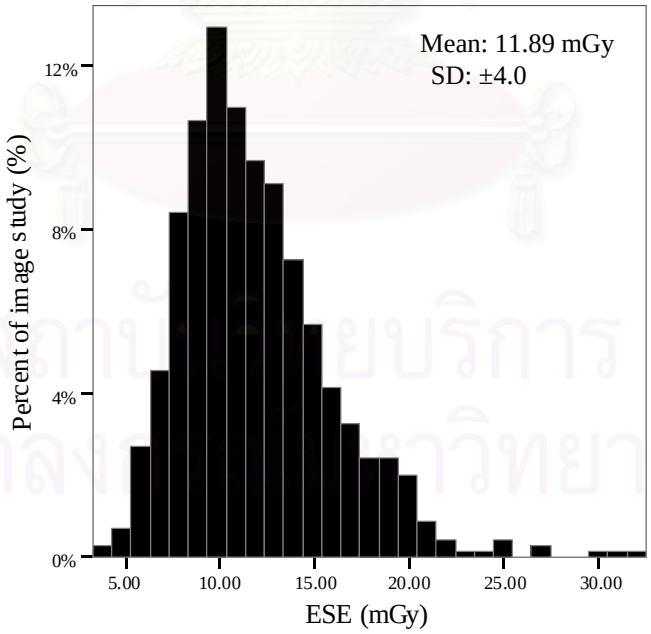

Figure 4.23 Distribution of ESE per image of CC view for image study

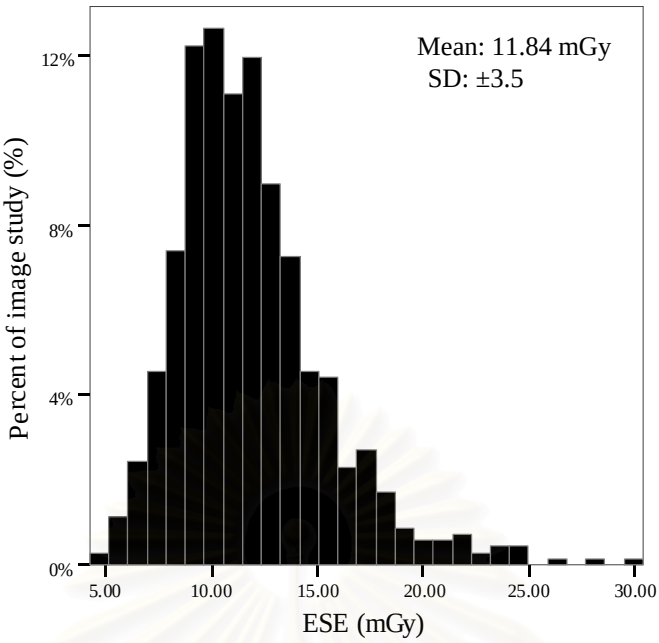

Figure 4.24 Distribution of ESE per image of MLO view for image study

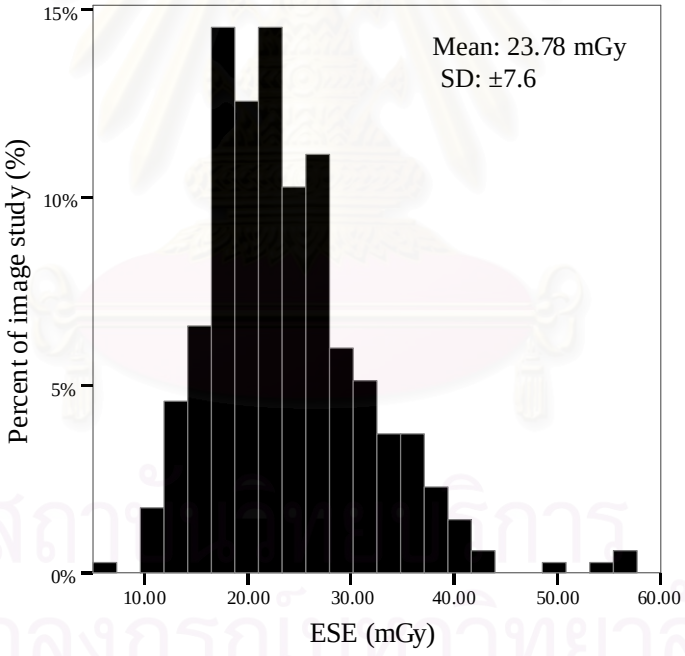

Figure 4.25 Distribution of ESE per woman of CC view for image study

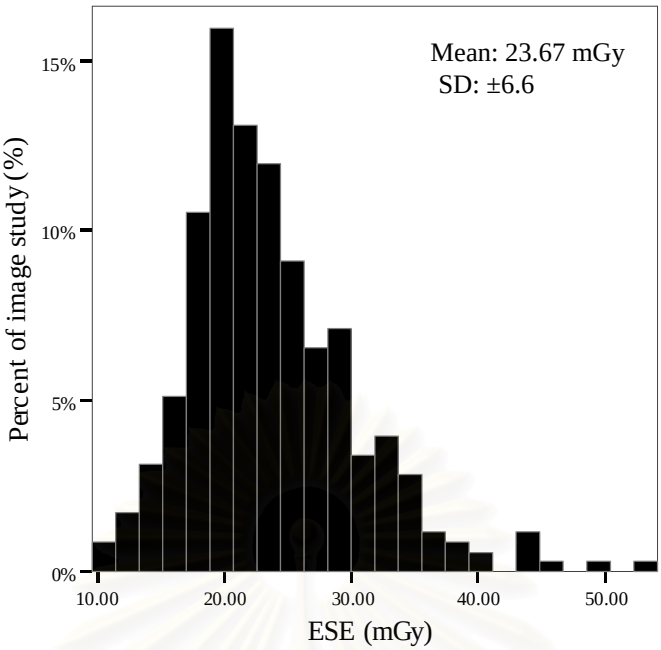

Figure 4.26 Distribution of ESE per woman of MLO view for image study

A bar graph showing the mean of AGD per image for difference of the CBT as classified by glandular content groups for CC and MLO views is shown in Figure 4.27.

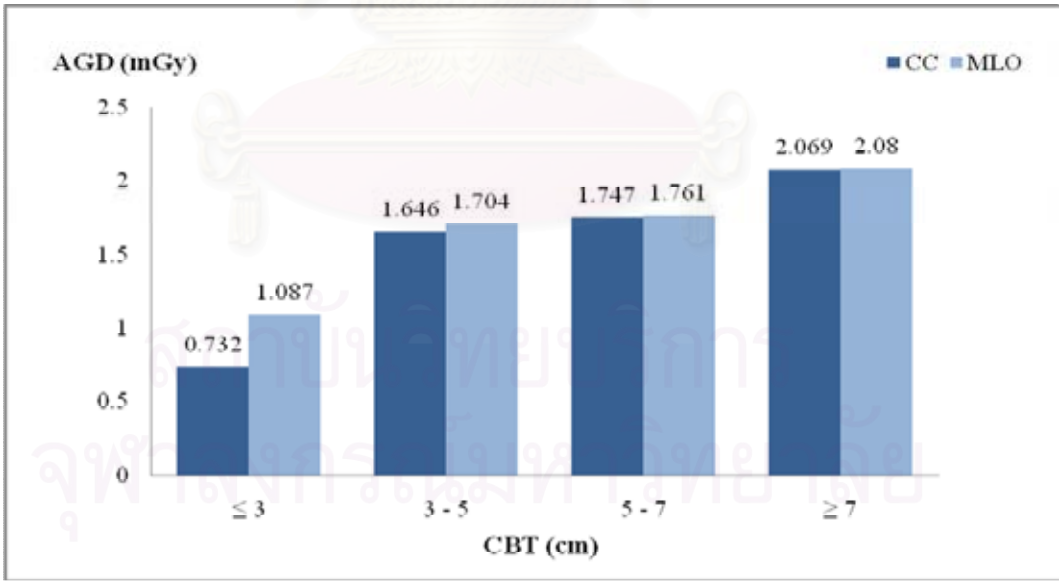

Figure 4.27 The mean AGD per image according to various compressed breast thickness for patient study

Whisk box-plot of AGD per woman for different age band. The 25th and 75th percentile mark the box and whiskers extend to the range outliers exclude. The median is marked in the box. The median is not at the central represents the study population, not normally distributed. The open circles (o) are outliers that represent cases that have values of more than 1.5 box-lengths from the 75th percentile.

The AGD per woman as a function of age and the CBT as classified by glandular content groups as shown in Figure 4.28 and 4.29.

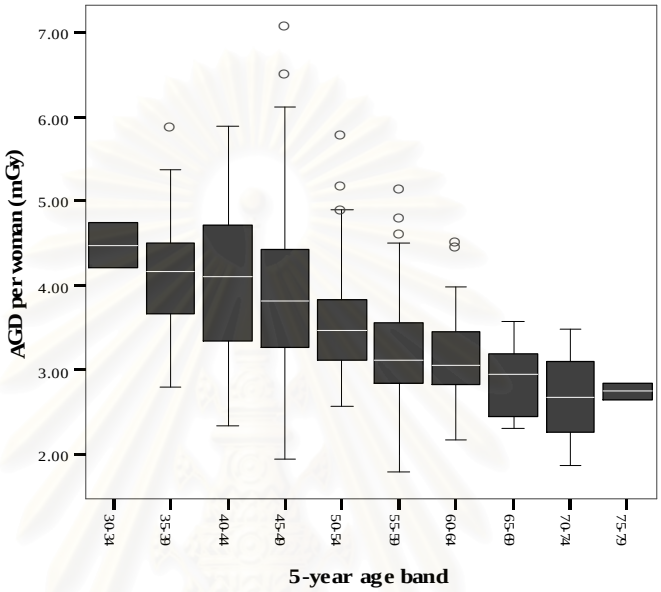

Figure 4.28 Whisk box-plot showing variations of AGD per woman as a function of age

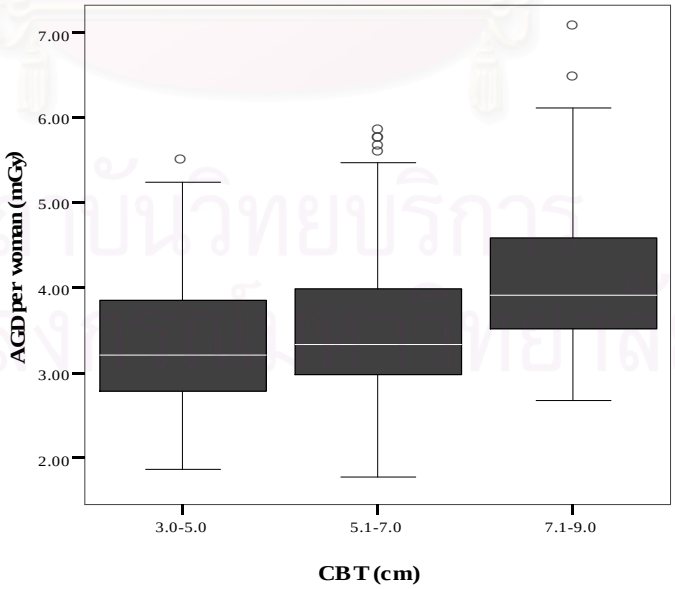

Figure 4.29 Whisk box-plot showing variations of AGD per woman as a function of the CBT as classified by glandular content groups

The percentage of image study for CC and MLO views of both breasts with the AGD per image higher than the limit of 3.0 mGy as recommended by ACR is shown in Figure 4.30.

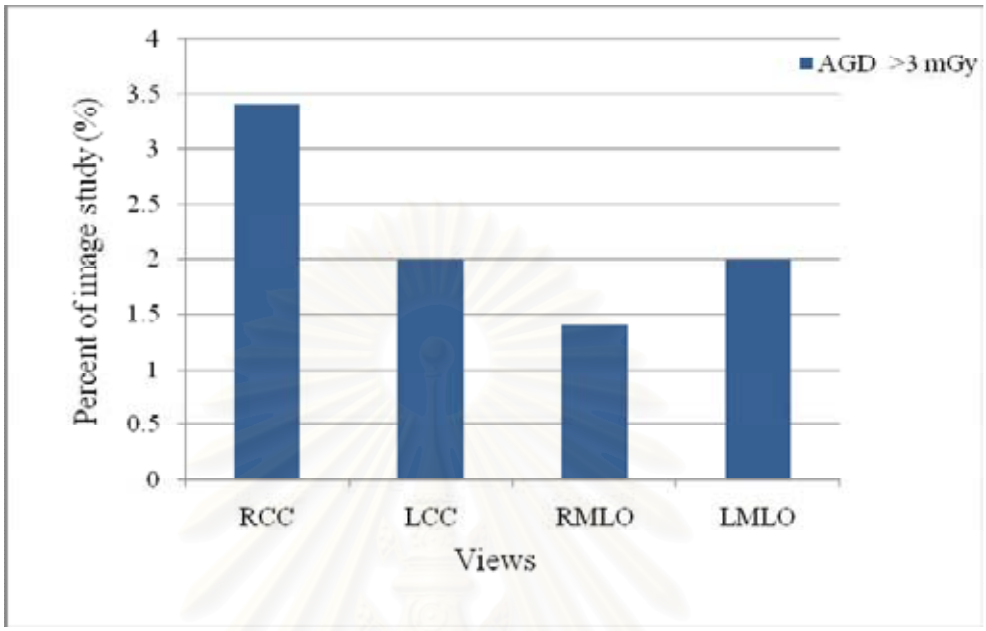

Figure 4.30 The percentage of AGD of more than 3 mGy for RCC, LCC, RMLO, LMLO views

4.4 The factors influenced AGD

This study involves the relationship between the AGD and affecting factors, such as a dependent variables (AGD) and several independent variables (kVp, mAs, CBT, compression force, HVL). Multiple regressions are statistics test for a dependent variable and several independent variables, this analyzed using SPSS program.

Factors affecting the AGD such as kVp, mAs, CBT, compression force, and HVL are shown in Table 4.15. The results show the mAs has a good correlation with the AGD per women($r=0.945$, $p<0.001$). In addition, the influence factors show the correlations between the kVp and CBT($r=0.948$), HVL and kVp ($r=0.921$), HVL and CBT ($r=0.862$).

Figure 4.31 to 4.35 show the correlations between AGD and affecting factors as a scatter plot.

Table 4.10 The pearson correlation of the multiple regressions test between the AGD and affecting factors

		AGD	kVp	mAs	CBT	CF	HVL
Pearson Correlation (r)	AGD	1.000	0.183	0.945	0.263	0.134	0.081
	kVp	0.183	1.000	0.275	0.948	-0.010	0.921
	mAs	0.945	0.275	1.000	0.389	0.122	0.245
	CBT	0.263	0.948	0.389	1.000	-0.015	0.862
	CF	0.134	-0.010	0.122	-0.015	1.000	-0.020
	HVL	0.081	0.921	0.245	0.862	-0.020	1.000

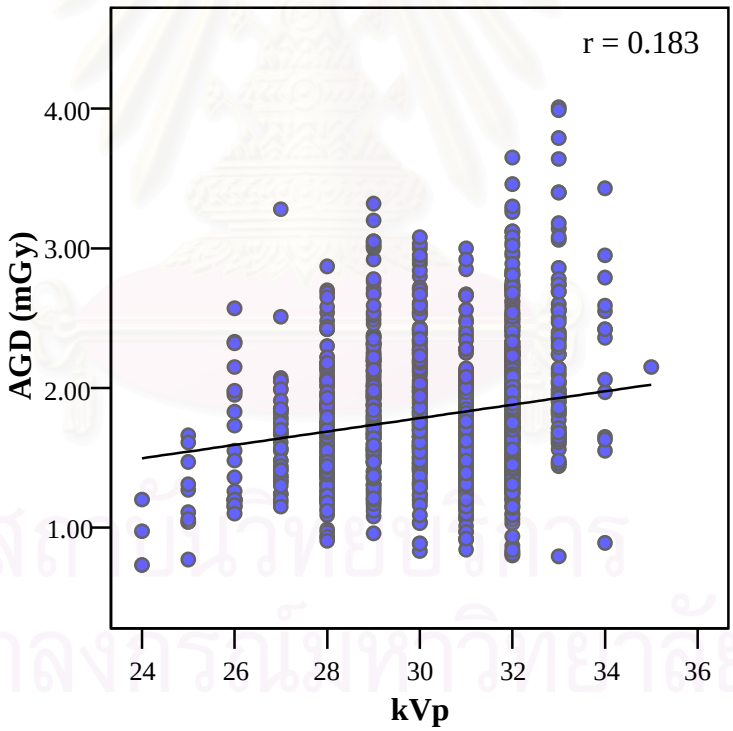

Figure 4.31 The scatter plot showing the poor correlation between the AGD and kVp (r =0.183)

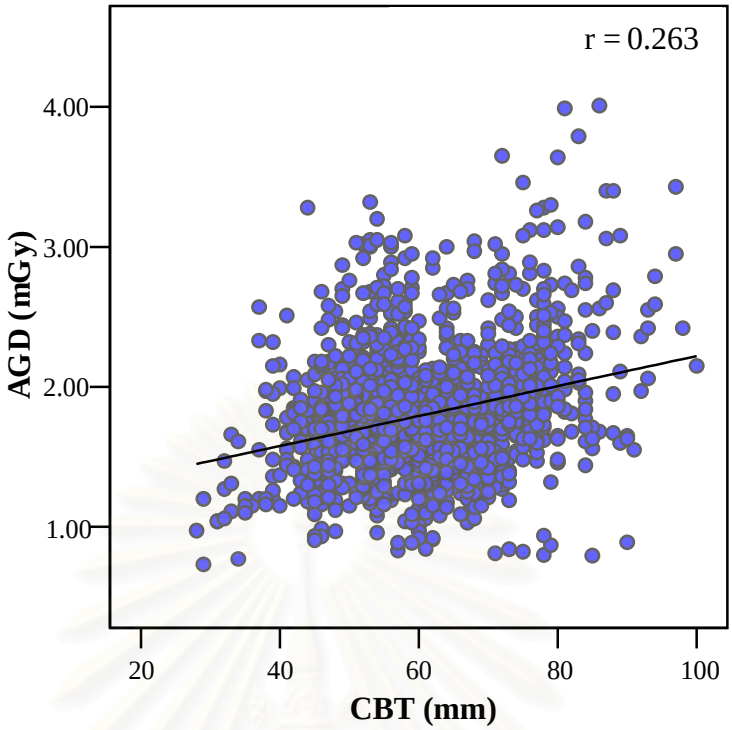

Figure 4.32 The scatter plot showing the poor correlation between the AGD and CBT (r =0.263)

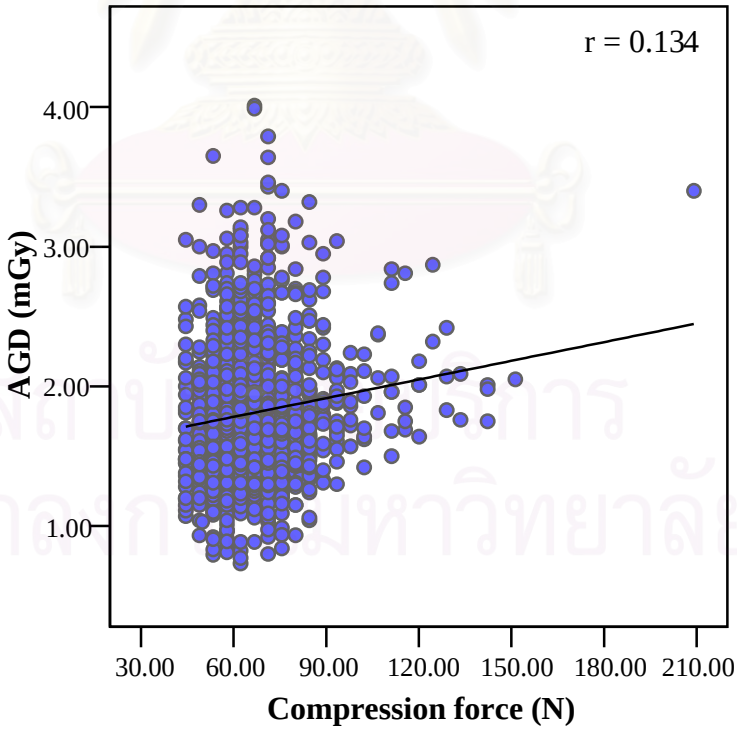

Figure 4.33 The scatter plot showing the poor correlation between the AGD and compression force (r =0.134)

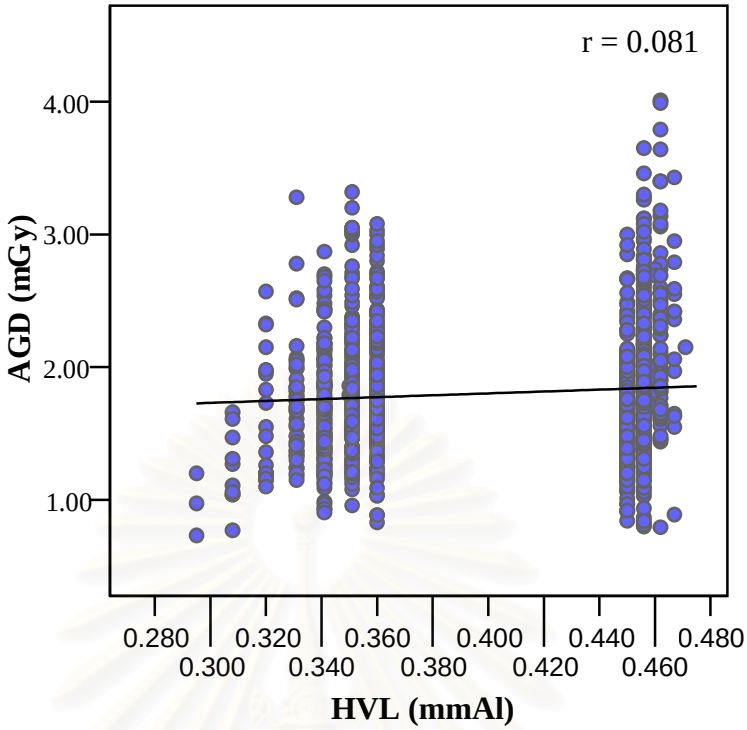

Figure 4.34 The scatter plot showing the poor correlation between the AGD and HVL (r =0.081)

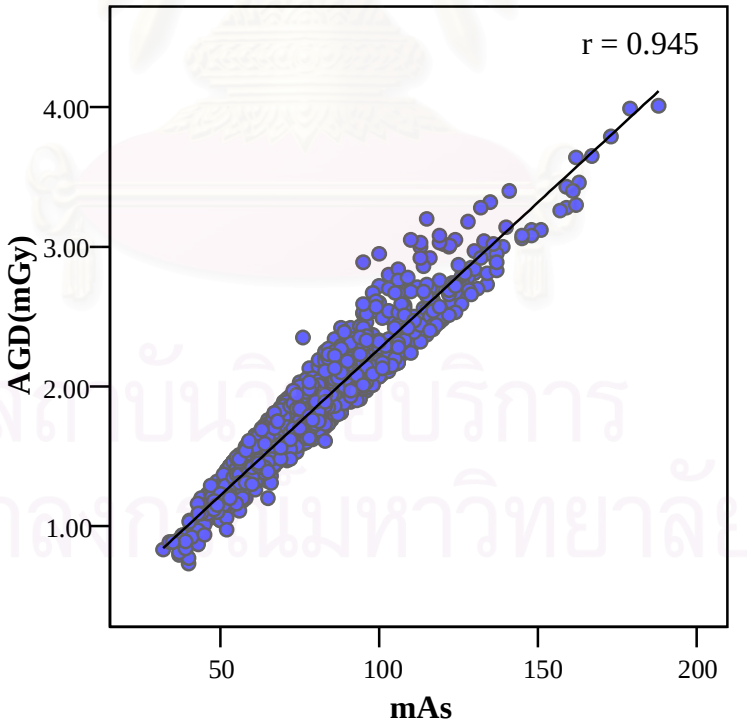

Figure 4.35 The scatter plot showing a strong correlation between the AGD and mAs (r =0.945)

Table 4.11 The factor variables of the two views, CC and MLO from the patient study

View (image)	Target/Filter Combination (% Frequency)	Compress Breast Thickness (cm)	Compression Force (N)	kVp	mAs	HVL (mm Al)
		Mean(Range) ±SD	Mean(Range) ±SD	Mean(Range) ±SD	Mean(Range) ±SD	Mean(Range) ±SD
CC+MLO (2,996)	Mo/Mo (42.3) Mo/Rh (57.7)	6.16 (2.8-10.0) ±11.6	66.27(44.5-209.1) ±14.2	30.53(24-35) ±1.8	77.98(10.10-188) ±21.6	0.41(0.29-0.47) ±0.1
CC (1,498)	Mo/Mo (40.7) Mo/Rh (59.3)	6.22 (2.9-10.0) ±11. 97	63.64(44.5-111.2) ±9.97	30.59(24-35) ±1.81	78.02(10.3-188) ±22.91	0.41(0.29-0.47) ±0.05
MLO (1,498)	Mo/Mo (43.9) Mo/Rh (56.1)	6.11(2.8-9.4) ±11.17	68.91(44.5-209.1) ±16.98	30.48(24-34) ±1.78	77.94(10.10-179) ±20.21	0.40 (0.29-0.46) ±0.05

Table 4.12 The factor variables of RCC, LCC, RMLO and LMLO views from the patient study

View (image)	Target/Filter Combination (% Frequency)	Compress Breast Thickness (cm)	Compression Force (N)	kVp	mAs	HVL (mm Al)
		Mean(Range) ±SD	Mean(Range) ±SD	Mean(Range) ±SD	Mean(Range) ±SD	Mean(Range) ±SD
RCC (749)	Mo/Mo (39.6) Mo/Rh (60.4)	6.24 (2.9-9.8) ±12.1	64.79(44.5-106.8) ±10.6	30.61(24-34) ±1.8	80.12(38-188) ±24.0	0.41(0.29-0.46) ±0.1
LCC (749)	Mo/Mo (41.9) Mo/Rh (58.1)	6.19 (3.1-10.0) ±11.9	62.49(44.5-111.2) ±9.2	30.56(25-35) ±1.8	75.91(10.3-173) ±21.6	0.41(0.30-0.47) ± 0.1
RMLO (749)	Mo/Mo (43.9) Mo/Rh (56.1)	6.09 (2.9-9.4) ±11.0	69.28(44.5-209.1) ±18.0	30.45(24-34) ±1.8	77.94(34-161) ±19.8	0.41(0.29-0.46) ±0.1
LMLO (749)	Mo/Mo (43.9) Mo/Rh (56.1)	6.13(2.8-9.3) ±11.4	68.53(44.5-151.3) ±15.9	30.50(24-34) ±1.8	77.95(10.1-179) ±20.7	0.41(0.29-0.46) ±0.1

Table 4.13 Variable characteristics of ESE and AGD of the two views, CC and MLO from the patient study

View (image)	AGD per woman (mGy)	Third Quartile	ESE per woman (mGy)	Third Quartile	AGD per image (mGy)	Third Quartile	ESE per image (mGy)	Third Quartile
	Mean(Range)±SD		Mean(Range)±SD		Mean(Range)±SD		Mean(Range)±SD	
CC+MLO (2,996)	3.62(1.5-7.13) ±0.9	4.11	23.73(7.04-57.70))±7.1	27.6	1.81(0.73-4.01) ±0.5	2.06	11.86(3.27-32.5) ±3.8	13.9
CC (1,498)	3.61(1.50-7.07)±1.0	4.09	23.78(7.04-57.70)±7.6	27.8	1.80(0.73-4.01) ±0.5	2.08	11.89(3.27-32.5) ±4.0	14.1
MLO (1,498)	3.63(1.65-7.13)±0.8	4.14	23.67(9.57-54.10) ±6.6	27.1	1.81(0.81-3.99) ±0.4	2.05	11.84(4.23-30.4) ±3.5	13.6

Table 4.14 Variable characteristics of ESE and AGD of RCC, LCC, RMLO and LMLO views from the patient study

View (image)	ESE per image (mGy) Mean(Range)±SD	Third Quartile	AGD per image (mGy) Mean(Range) ±SD	Third Quartile
RCC (749)	12.15(3.27-32.5) ±4.1	14.3	1.84(0.73-4.01) ±0.5	2.10
LCC (749)	11.63(3.77-29.6) ±3.8	13.6	1.77(0.77-3.79) ±0.5	2.05
RMLO (749)	11.78(4.91-27.9) ±3.5	13.4	1.81(0.81-3.40) ±0.4	2.05
LMLO (749)	11.90(4.23-30.4) ±3.6	13.8	1.82(0.84-3.99) ±0.4	2.05

Table 4.15 Characteristics of the technique factors of RCC, LCC, RMLO, LMLO views from the patient study with the AGD greater than 3 mGy

View (image)	Mean Age(y)	Target/Filter Combination (% Frequency)	Compress Breast Thickness (cm)	Compression Force (N)	kVp	mAs	HVL (mm Al)
			Mean(Range)	Mean(Range)	Mean(Range)	Mean(Range)	Mean(Range)
RCC (14)	46.3	Mo/Mo (41.7) Mo/Rh (58.3)	6.77(4.4-9.7)	71.19(53.4-93.4)	30.91(27-34)	148.8(124-188)	0.41 (0.33-0.46)
LCC (24)	44.7	Mo/Mo (57.1) Mo/Rh (42.9)	6.57(5.1-8.7)	65.47(44.5-84.5)	30.7(29-33)	132.9(110-173)	0.39 (0.35-0.46)
RMLO (10)	46.4	Mo/Mo (0.0) Mo/Rh (100.0)	8.20(7.7-8.8)	95.21(57.8-209.1)	32.6(32-33)	150.0(140-161)	0.45 (0.45-0.46)
LMLO (14)	45.4	Mo/Mo (14.3) Mo/Rh (85.7)	7.67(5.8-8.9)	66.74(48.9-80.1)	32.14(30-33)	145.3(119-179)	0.44 (0.36-0.46)

CHAPTER 5

DISCUSSION AND CONCLUSION

5.1 Discussions

5.1.1 Quality control

The measured HVL for Mo/Mo target/filter combination is higher than calculated one, the maximum variation is 3.17% at 26 kVp. For the Mo/Rh target/filter combination, the measured HVL is lower than the calculated one, the maximum variation of 6.84% at 28 kVp. The mean variation is 2.2% and 4.12% for Mo/Mo and Mo/Rh respectively, it decreases with increasing tube voltage.

For the verification of AGD at each kVp and target/filter combination, the measured is lower than the calculated one. For Mo/Mo target/filter combination, the maximum different value is 0.47 mGy at 32 kVp and the maximum variation is 11.87% at 32 kVp, it increases with increasing kVp. For Mo/Rh target/filter combination, the maximum different value is 0.55 mGy at 34 kVp and the maximum variation is 18.03% at 28 kVp, it decreases with increasing tube voltage. The mean variation is 9.57% and 16.38% for Mo/Mo and Mo/Rh respectively.

The variation of both HVL and AGD values for different method are higher in Mo/Rh target/filter combination.

The AGD was determined using the measured and calculated method. The data obtained from each method of AGD determination were compared statistically using paired t-test. The data for the AGD determination was tested for normality performed on the Mo/Mo (26,28,30,32 kVp) and Mo/Rh (28,30,32,34 kVp) combination technique. The results indicate the mean output data for these were normally distributed, based on Shapiro-Wilk (p values >0.05), as using for the sample unit is less than 50 as shown in Table 5.1.

Table 5.1 Tests of normality for the output data of the AGD determination

Target/Filter		Shapiro-Wilk		
		Statistics	df	Sig.
Mo/Mo	Measured	0.991	4	0.962
Mo/Mo	Calculated	0.990	4	0.960
Mo/Rh	Measured	0.989	4	0.951
Mo/Rh	Calculated	0.992	4	0.967

Table 5.2 Paired samples test of the AGD determination

	Paired Differences							
				95% Confidence Interval of the Difference				
	Mean	Std. Deviation	Std. Error Mean	Lower	Upper	t	df	Sig. (2-tailed)
Mo/Mo(Target/Filter) Measured - Calculated	-0.287	0.142	0.071	-0.513	-0.061	-4.043	3	0.027
Mo/Rh(Target/Filter) Measured - Calculated	-0.440	0.091	0.045	-0.585	-0.294	-9.640	3	0.002

The results of the paired t-tests performed on the AGD determination are shown in Table 5.2. There is significantly different between the measured and calculated methods (all p values <0.05).

The discrepancy between the measured and the calculated AGD is from the different geometry in radiation dosemeters and calibration factors. Victoreen 4000M^{+} calibration factors can produce the variation in output measurement. The uncertainties associated with the AGD estimates (measured) in this research include several factors, such as the HVL measurement and the conversion factors. It must be considered that conversion factors published by Wu et al [9] are approximately 10% higher than the corresponding factors published by Dance [14]. These are the reasons why the output measurement is less than output calculation in FFDM system. It is small at low kVp and become large at high kVp and also at different filters.

5.1.2 Patient information

The age of the patient ranges from 29 to 81years, with the mean of 51.3 years (SD±8.6), the median of 51 years and the mode of 47 years. The number of patient is 749 and the number of exposure is 2,996.

5.1.3 Compress breast thickness (CBT)

The accuracy, maximum deviation, for the CBT is ± 0.3 cm as the results in QC of FFDM system (Appendix D). The mean CBT of CC view is 6.22 cm and the MLO view is 6.11 cm, which is higher than those reported by Chevalier et.al [17] of 4.9 and 5.4 cm. The compression force reported by Chevalier et.al [17] was between 190 and 210 N, while our study was between 57.84 and 62.29 N. The compression force decreases for digital image acquisition, which could be perhaps justified by image processing. In fact, the post-processing algorithm applied to digital mammography, called tissue equalization algorithm, together with the wide dynamic range of the digital detector could compensate the lack of contrast due to the lower compression force [10]. However, radiologic technologist must be aware of the effect of the compression force. This is the reason of the mean CBT is high for both CC and MLO views, which results in increasing glandular dose of the patients.

The frequency for the 5-7 cm CBT as classified by glandular content groups was 56.27% and 61.40 % of image study for CC and MLO views. CBT is more than 5 cm in Thai female as presented in this research. The relation between CBT and the patient age is the CBT increases with increasing age (mean), it is similar in 5-7 and ≥7 cm CBT. In fact, the older woman had fatty breast [18]. The pair t-test is significantly different of the CBT between CC and MLO views ($p<0.05$), as shown in Table 5.3.

Table 5.3 Paired samples test of the CBT between CC and MLO views

		Paired Differences						
					95% Confidence Interval of the Difference			
		Mean	Std. Deviation	Std. Error Mean	Lower	Upper	t	Sig. (2-tailed)
CBT	CC- MLO	1.072	1.155	0.043	0.987	1.158	24.604	0.000

5.1.4 Technique factors

The accuracy, maximum deviation, of the x-ray tube voltage accuracy, is ±1.1 kilovolts for the range between 25 and 30 kVp as in the results QC of FFDM system (Appendix D). The target/filter combination and kVp is automatically selected by system according to CBT. For CC view, 40.7% of Mo/Mo target/filter is selected with kVp median value of 29, while 43.9% has been selected for MLO view of Mo/Mo target/filter with kVp median value of 30. The kVp setting ranged from 24 to 30 kVp for Mo/Mo target/filter combination related to the HVL value from 0.29 mm Al(24 kVp) to 0.36 mm Al (30 kVp). For Mo/Rh target/filter combination of 59.3% and 56.1% are the most selection with median kVp setting of 32 for both CC and MLO views respectively. The kVp setting range from 31 to 35 kVp for Mo/Rh target/filter combination related to the HVL value range from 0.45 mm Al(31 kVp) to 0.47 mm Al (35 kVp). The tube voltage and HVL are increases with increasing breast thickness and with increasing glandularity content [17]. The higher rate of Mo/Rh target/filter combination with median kVp setting of 32 with AEC system employed, indicates that a dose reduction due to the beam energy increases [15]. In the future, the optimal dose and image quality should be obtained by using the different mode such as, AEC (auto kV, auto time), TEC and manual.

The accuracy, maximum deviation for compression force is ± 2.2 N as presented in QC of FFDM system (Appendix D). The compression force range from 44.5 to 209.1 N, the most using for compression force is 62.29 N for both CC and MLO views. In our study, the compression force is lower than the results reported by Chevalier et.al [17] of 190 and 210 N. This is the reason for the AGD increases with increasing CBT.

5.1.5 Mean doses and dose distributions

AEC is calibrated to give a set dose for standard breast (ACR standard phantom) default at 1.6 mGy for AEC Table 0 and 1.9 mGy for AEC Table 1(Appendix A) [19]. In our study, the dose for the ACR standard phantom is 1.34 mGy, base on auto filter mode of AEC system (Mo/Mo and 30 kVp). It is within criteria of AEC table.

The mean AGD per image is 1.80 mGy for CC view and 1.81 mGy for MLO view, those values are closely as reported by Chevalier et.al [17] of 1.79 mGy for CC view and 1.91 mGy for MLO view. Gennaro et.al [15], calculated the mean AGD of both CC and MLO views of 1.4 mGy, which were different from reported by Chevalier et.al 25%. The dose calculations in these two studies used conversion factor according to Dance et.al [14] based on assuming breasts of two glandularity content groups. They found the dose calculations made by assuming all breasts were 50% glandularity content decreased the mean AGD by 6%. This finding was similar to the results reported by Heggie [23] and Klein et.al [24] of 5.2% and 15% respectively.

Table 5.4 Paired samples test of the AGD between CC and MLO views

		Paired Differences						
					95% Confidence Interval of the Difference			
		Mean	Std. Deviation	Std. Error Mean	Lower	Upper	t	Sig. (2-tailed)
AGD per image	CC- MLO	-0.000	0.273	0.010	-0.020	0.019	-0.055	0.956

The pair t-test is no significantly different of the AGD per image between CC and MLO views ($p>0.05$) as shown in Table 5.4. The smaller difference of the mean AGD, 0.5% between CC and MLO views related to the difference of mean CBT, 1.8% with the same reason of the trend for the compression force was decreased during digital image acquisition. It is clearly reported that the mean AGD for CC view is lower than those for MLO view while the mean CBT for CC view was higher than those for MLO view.

For the different breast side, the right(R) and left (L) breast dose, the AGD per image is significantly different of RCC and LCC views ($p<0.05$) and no significantly different of RMLO and LMLO views ($p>0.05$). Those are shown in Table 5.5.

The statistical Oneway ANOVA test is significantly different of the AGD per image for the CBT as classified by glandular content groups ($p<0.001$) as shown in Table 5.6. The AGD per image is significantly different between the 3-5 CBT and 7-9 CBT, 5-7 CBT and 7-9 CBT, no significantly different between 3-5 CBT and 5-7 CBT. Those are shown in Table 5.7. This could be explained by the fact that the breast glandularity content decreases by age, which affected the AGD in patient study.

Table 5.5 Paired samples test of the AGD per image for different breast side

		Paired Differences						
					95% Confidence Interval of the Difference			
		Mean	Std. Deviation	Std. Error Mean	Lower	Upper	t	Sig. (2-tailed)
AGD per image	RCC - LCC	0.074	0.259	0.013	0.047	0.101	5.367	0.000
	RMLO - LMLO	-0.008	0.268	0.014	-0.036	0.020	-0.564	0.573

Table 5.6 The statistical Oneway ANOVA test of the AGD per image for the CBT as classified by glandular content groups for patient study

Dependent Variable: AGD	Sum of Squares	df	Mean Square	F	Sig.
Between Groups	20.587	2	10.294	15.001	0.000
Within Groups	238.800	2992	0.686		
Total	259.387	2994			

Table 5.7 The post hoc tests (Bonferroni) of the statistical Oneway ANOVA test of the AGD for the CBT as classified by glandular content groups by analyzing comparisons of variance estimates, the dependent variable of the AGD per image

(I) CBT	(J) CBT	Mean Difference (I-J)	Std. Error	Sig.	95% Confidence Interval	
					Lower Bound	Upper Bound
3-5	5-7	-0.145	0.127	0.761	-.452	0.160
	7-9	-0.705*	0.150	0.000	-1.067	-0.342
5-7	3-5	0.145	0.127	0.761	-0.160	0.452
	7-9	-0.559*	0.112	0.000	-0.828	-0.289
7-9	3-5	0.705*	0.150	0.000	0.342	1.067
	5-7	0.559*	0.112	0.000	0.289	0.828

* The mean difference is significant at the 0.05 level.

The mean AGD per woman based on a simple assumption of a two view examinations is 3.62 mGy. This finding is lower than the results reported by Chevalier et.al [17] of 3.8 mGy. For the woman at the age of less than 50 years, the AGD is 3.96 mGy which is higher than AGD of patient at the age over 50 years (3.29 mGy) of 16.9%. Young et.al [20] reported the AGD of 9% higher for the young group, Chevalier et.al [17] had opposite result of 3% lower for the young group. This could be explained by the uncertainty of several factors associated with the individual AGD estimated as 14%, which 5% error was the glandular content. In present research, the trend for the AGD per woman decreases with increasing age, as illustrated in Figure 4.28. This trend is similar to Beckett and Kotre [21]. The trend for the AGD per woman is associated with the glandular content. It should be kept in mind that most of the older women with large thickness breast had fatty breasts. In addition, the potentially FFDM systems could provide a more accurate estimation of the individual breast glandularity because the whole acquired image can be analyzed.

The mean AGD per image obtained from this research for both CC and MLO views was 91.2% lower than the reference level of 3.0 mGy as recommended by ACR. About 8.8% of all study, the AGD is higher than the reference level of 3.0 mGy, which the mean age is 47.35 years and the mean CBT is 7.16 cm. The mean CBT of 7.16 cm, include the range of 7-9 CBT that the present research have the high AGD (maximum and mean) per women, as illustrated in Figure 4.30.

5.1.6 The factors influenced AGD

There is a strong correlation between the AGD per woman and mAs with $r=0.945$, $R^2=0.913$, as illustrated in Figure 4.35. The mAs is significant affect the AGD ($p<0.001$). This result could be explained by the digital mammography system related to auto filter mode of AEC system in mammographic examinations, which adjust the radiation dose, as defined by the mAs product, based on the patient breast thickness.

The AEC of area detector systems use a low-dose pre-exposure to optimize exposure parameters and find the densest region. A scanning system must use a different approach to find the densest region. AEC design has been described for scanning digital mammography in which the emission current was determined based on the transmission of the densest region found in a low-dose pre-scan. While the AEC of area detector systems can control the exposure of a pixel by changing either the emission current or the exposure length, a scanning system controls the exposure by changing the emission current or the scan time. To minimize the scan time, the digital mammography system uses the maximal emission current and changes the scan time.

5.2 Conclusions

The determination of patient dose in FFDM at King Chulalongkorn Memorial Hospital in 2006 revealed that the mean AGD(±SD) per image is 1.80±0.5 mGy for CC view and 1.81±0.4 mGy for MLO view with no significant differences of the AGD from CC and MLO views ($p > 0.05$). Overall, 97.3 % of CC view and 98.3% of MLO view were lower than the reference level of 3.0 mGy as recommended by ACR. The AGD per image is significantly different between the CBT as classified by glandular content groups ($p<0.001$). It increases with increasing CBT, while decreases with increasing age. The mean AGD per woman is 3.62 mGy. The results represent the FFDM examination at one department is capable of achieving acceptable dose levels for patient safety. In this research, the image quality assessment was judged to be clinically acceptable. Digital mammography detectors have a much wider dynamic range. Thus, the contrast can be modified before the image is displayed on a monitor or printed on a film [6]. The quality control of the system and the calibration of the detectors play an important role in the patient dose.

The statistics shows the significantly different between the measured and calculated methods for AGD (p values <0.05). The uncertainties associated with the AGD estimate (measured) is 13% on average in this research included several factors, such as the HVL measurement of 3.2% of average and the conversion factors. In addition, the discrepancy between the measured and the calculated AGD is according to the output measurement of the FFDM in air while the calculated one, using the phantom. It is small at low kVp and become large at high kVp and also at different filters.

The measured and the calculated AGD are smaller than third quartile which could be set as the guidance level of AGD at King Chulalongkorn Memorial Hospital. The local AGD per image (with grid) for Thai female undergoing FFDM system, is 1.80 and 1.81 mGy for CC and MLO views respectively. A new dose reference level (DRL) for the AGD at this hospital is 2.0 mGy (third quartile) per image.

The mAs is significantly affect on the AGD ($p<0.001$). The AGD in the digital mammography system is related to auto filter mode of AEC system, which adjust the radiation dose, as defined by the mAs product, based on the patient thickness. These are useful for the patients that the risk of cancer induction can be considered. It is an important for radiologists and radiologic technologists to increase the awareness in the study for the patient especially the adult one.

5.3 Limitations

This research involves both limitation on the radiation dosemeter geometrical parameters and calibration factor. Victoreen 4000M^{+} calibration factors can produce the variation in output measurement. The uncertainties associated with the AGD estimates (measured) in this research include several factors, such as the HVL measurement and the conversion factors. The differences between the measured and calculated AGD, are difficult to analyses due to the lack of information regarding the methodology followed by the FFDM system for estimating AGD values. The digital systems have the advantage of storing the complete set of data related to each individual exposure. Data related to the exposure factors, breast characteristics, detector properties, image processing software could be extracted from the DICOM header. To manipulate this information, it is necessary to understand the origin or method of calculation of the data stored in the DICOM file, which, in some case, requires manufacturer support. It would be very useful for the DICOM conformance statement from the manufacturer to include definitions for the parameters or methods used to calculate some of the quantities.

REFERENCES

[1] Sriplung, H., et al. Cancer incidence in Thailand 1995-1997. Asian Pacific J Cancer Prev 6 (2005): 276-281.

[2] Andrew, PS. Fundamentals of digital mammography: physics, technology and practical considerations[Online]. Hologic Inc (Distributor), 2005. Available from: http://www.hologic.com/oem/pdf/R-BI-016_FundDig%20Mammo.pdf [2007, Apr 17]

[3] Law, J. Risk and benefit associated with radiation dose in breast screening programmes an update. Br J Radiol 68 (1995): 870-876.

[4] American College of Radiology. ACR practice guideline for the performance of whole breast digital mammography. ACR, 2006.

[5] U.S National Institutes of Health. Breast cancer[Online]. National Cancer Institute (Distributor), 2005. Available from: http://www.cancer.gov/cancertopics/wyntk /breast/[2007, Apr 17]

[6] John, JT. Digital mammography breast dosimetry using copper-doped lithium fluoride (LiF:MCP) thermoluminescent dosimeters (TLDs). Master's Thesis. Uniformed Services University of the Health Sciences, 2003.

[7] American College of Radiology. Mammography quality control manual, medical physicist section. Reston,VA: ACR,1999.

[8] Ng, KH., Aus, RJ., DeWerd, LA., and Vetter, JR. Entrance skin exposure and mean glandular dose: effect of scatter and field gradient at mammography, Radiol 205 (1997): 395-398.

[9] Wu, X., Barnes, GT., and Tucker, DM. Spectral dependence of glandular tissue dose in screen-film mammography. Radiol 179 (1991): 143-148.

[10] Gennaro, G., and di Maggio, C. Dose comparison between screen-film and full field digital mammography. Eur Radiol 16 (2006): 2559-2566.

[11] Hermann, KP., Obenauer, S., Marten, K., Kehbel, S., Fischer, U., and Grabbe, E. Average glandular dose with amorphous silicon full field digital mammography, clinical results. Rofo Fortschr Geb Rontgenstr Neuen Bildgeb Verfahr 174 (2002): 696-699.

[12] Bouzariomehri, F., Mostaar, A., and Ghasemi, A. The study of mean glandular dose in mammography in Yazd and the factors affecting it. Radiol 4 (2006): 29-35.

[13] Jamal, N., Ng, KH., and McLean, D. A study of mean glandular dose during diagnostic mammography in Malaysia and some of the factors affecting it. Br J Radiol 76 (2003): 238-245.

[14] Dance, DR., Skinner, CL., and Young, KC. Additional factors for the estimation of mean glandular dose using the UK mammography dosimetry protocol. Phys Med Biol 45 (2000): 3225-3240.

[15] Gennaro, G., Baldelli, P., and Taibi, A. Patient dose in full field digital mammography: an Italian survey. Eur Radiol 14 (2004): 645-652.

[16] International Commission on Radiological Units and Measurements. Review of monte carlo calculations for assessment of mean glandular dose in mammography. ICRU, 2005.

[17] Chevalier, M., Morán, P., and Ten, JI. A survey of patient dose and clinical factors in a full field digital mammography system. Radiat Prot Dosimet 114 (2005): 1-3.

[18] Dance, DR., Skinner, CL., and Carlsson, G. Breast dosimetry. Appl Radiat Isot 50 (1999): 185-203.

[19] Hologic Inc., and Lorad. Selenia full field digital mammography system quality control manual P/N 9-500-0285. United States of America: Hologic, 2003.
[20] Young, KC. Radiation dose in the UK trial of breast screening in women aged 40-48 years. Br J Radiol 75 (2002): 362-370.
[21] Beckett, JR., and Kotre, CJ. Doseimetric implications of age related glandular changes in screening mammography. Phys Med Biol 45 (2000): 801-813.
[22] Magnus, A. Digital mammography with a photon counting detector in a scanned multislit geometry. Master's Thesis. Department of Physics Royal Institute of Technology, 2007.
[23] Heggie, JCP. Survey of dose in screening mammography. Australas Phys Eng Sci Med 19 (1996): 207-216.
[24] Klein, R., Aichinger, H., Dierker, J., Jansen, JTM., Joit Barfub, S., and Sabel, M. Determination of average glandular dose with modern mammography units for two large groups of patient. Phys Med Biol 42 (1997): 651-671.

APPENDICES

APPENDIX A

BREAST COMPRESSION LOOKUP TABLES

In auto filter mode, the system automatically selects all the technique factors. The system automatically sets the kVp using the lookup table based on the compressed breast thickness. If the kVp goes over the site is default filter switch point, usually 32 kVp, the system moves the Rhodium filter into place. The breast compressed lookup table can be selected from AEC table. The clinical range of breast thickness is shown in Table A.1.The mA setting as a function of kVp is shown in Table A.2. A final kVp, post mAs value, and filter selection displays after the exposure.

Table I Breast Compression Lookup Table

Thickness	AEC Table 0*		AEC Table 1**	
(mm)	Filter	kVp	Filter	kVp
20	Mo	24	Mo	24
25	Mo	24	Mo	24
30	Mo	25	Mo	25
35	Mo	26	Mo	25
40	Mo	27	Mo	25
45	Mo	28	Mo	26
50	Mo	29	Mo	27
55	Mo	30	Mo	28
60	Mo	31	Mo	29
65	Rh	32	Mo	29
70	Rh	32	Mo	30
75	Rh	32	Mo	31
80	Rh	33	Rh	32

* Table 0 is configurable by field service to meet local standards (e.g, max 200 mrad) as required by a number of states in U.S, Canada, and other regions of the world.
** Table 1 is consistent with MQSA average glandular dose requirement not to exceed 300 mrad per exposure to an average (4.2 cm thick compressed) breast. This table is set by default for US sites.

Table II kVp/mA Range

Large Focal Spot		Small Focal Spot	
kVp	mA	kVp	mA
20	75 mA	20	20 mA
21	80 mA	21	22 mA
22	85 mA	22	24 mA
23	90 mA	23	26 mA
24	95 mA	24	28 mA
25-32	100 mA	25-32	30 mA
33	85 mA	33-34	28 mA
34-35	80 mA	35-37	26 mA
36-37	75 mA	38-39	24 mA
38-39	70 mA	-	-

APPENDIX B

CASE RECORD FORM

Clinical Data Collection for Mammography Examination										
Centre/room:					**Equipment:**					
Procedure										
Data Record										
PATIENT No.	AGE	VIEW	kVp	mAs	CBT (cm)	CPF (N)	AGD (mGy)	ESE (mGy)	HVL	FILTER
		RCC								
		LCC								
		RMLO								
		LMLO								

APPENDIX C

CONVERSION FACTOR TABLES

Mo/Mo Target-Filter Combination

HVL	X-Ray Tube Voltage (kVp)											
	23	**24**	25	26	27	28	29	30	31	**32**	**33**	**W/AL**
0.23	116											Target-Filter
0.24	121	124										Combination
0.25	126	129	131									
0.26	130	133	135	138								
0.27	135	138	140	142	143							
0.28	140	142	144	146	147	149						
0.29	144	146	148	150	151	153	154					
0.30	149	151	153	155	156	157	158	159				170
0.31	154	156	157	159	160	161	162	163	164			175
0.32	158	160	162	163	164	166	167	168	168	170	171	180
0.33	163	165	166	168	169	170	171	173	173	174	175	185
0.34	168	170	171	172	173	174	175	176	177	178	179	190
0.35		174	175	176	177	178	179	180	181	182	183	194
0.36			179	181	182	183	184	185	185	186	187	199
0.37				185	186	187	188	189	190	191	191	204
0.38					190	191	192	193	194	195	195	208
0.39						196	197	198	198	199	200	213
0.40							201	202	203	204	204	217
0.41								206	207	208	208	221
0.42									211	212	212	225
0.43										215	216	230
0.44											220	234
0.45												238

Mo/Rh Target-Filter Combination

HVL	X-ray Tube Voltage (kVp)										
	25	**26**	**27**	**28**	**29**	**30**	**31**	**32**	**33**	**34**	**35**
0.28	149	151	154								
0.29	154	156	158	159							
0.30	158	160	162	162	162	163					
0.31	163	164	166	166	166	167	167				
0.32	167	169	171	171	171	171	172	172			
0.33	171	173	175	176	176	176	176	177			
0.34	176	178	179	179	180	180	180	181	181		
0.35	180	181	183	183	184	185	185	186	187		
0.36	185	186	187	187	188	188	189	190	191	191	
0.37	189	190	191	191	192	193	193	194	195	195	
0.38	193	194	196	196	197	197	197	198	199	199	200
0.39	198	199	200	200	201	201	202	202	203	203	204
0.4	202	203	204	204	205	205	206	207	208	208	208
0.41	206	207	208	208	209	209	210	211	212	212	212
0.42	211	211	212	212	213	213	214	215	216	216	217
0.43	215	216	217	217	218	218	219	219	220	220	221
0.44	220	220	221	221	222	222	223	223	224	224	225
0.45	224	224	225	225	226	226	227	227	228	228	229
0.46		228	229	229	230	231	231	232	233	233	234
0.47			233	233	234	235	235	236	237	237	238
0.48			238	238	239	240	240	241	241	242	242
0.49				242	243	243	244	244	245	245	246
0.50					247	247	248	248	249	250	251
0.51						251	252	253	254	254	255
0.52							257	257	258	258	259
0.53							261	261	262	263	264
0.54								265	266	267	268
0.55								269	270	271	272
0.56									275	276	276
0.57									279	280	281
0.58										284	285
0.59										288	289
0.60											293

APPENDIX D

QUALITY CONTROL OF MAMMOGRAPHIC SYSTEM

1. Mammographic unit assembly evaluation

Objective

To ensure good and safe working condition of all interlocks, mechanical detents and safety switches and to ensure mechanical integrity of the x-ray tube and digital detector assembly. To study the variation in compressed breast thickness and the compression force

Regulatory action levels and corrective action

The Lorad Selenia FFDM System shall provide:

-An override of automatic decompression (if present) to allow maintenance of compression;

-A continuous display of the override status;

-A manual emergency compression release that can be activated in the event of power or automatic release failure.

-The compression thickness display test shall always be accurate to ±5 mm from the actual thickness.

- The compression force display test shall always be accurate to ±4.5 pounds (±20 N) from the actual force.

If the recommended performance criteria are not met, the source of the problem shall be identified and corrective action shall be taken within thirty days of the test date.

Results

Table I The mammographic unit assembly evaluated for the period 2006 to 2007

Pass/Fail/NA	
1.Free-standing unit is mechanically stable	Pass
2.All moving parts move smoothly, without obstruction to motion	Pass
3.All locks and detents work properly	Pass
4.Image receptor holder assembly is free from vibrations	Pass
5.Image receptor slides smoothly into holder assembly	Pass
6.Image receptor is held securely by assembly in any orientation	Pass
7.Compressed breast thickness scale accurate to +/-5 mm, reproducible +/-2 mm	Pass
8.Patient or operator is not exposed to sharp or rough edges, or other hazards	Pass
9.Operator technique control charts are posted	Pass
10.Operator protected during exposure by adequate radiation shielding	Pass
11.All indicator lights working properly	Pass
12.Auto decompression can be overridden to maintain compression(status displayed)	Pass
13.Manual emergency compression release can be activated in the event of power failure	Pass

Table II The compression thickness indicator test in 2006

Date	Phantom thickness (mm)	Compression force (pounds)	Indicated thickness value(mm)	Variation (mm)
5 June 2006	45	20	47	2
14 June 2006	45	20	48	3
19 June 2006	45	20	46	1
22 June 2006	45	20	45	0
26 June 2006	45	20	45	0
29 June 2006	45	20	45	0
3 July 2006	45	20	45	0
6 July 2006	45	20	45	0
13 July 2006	45	20	46	1

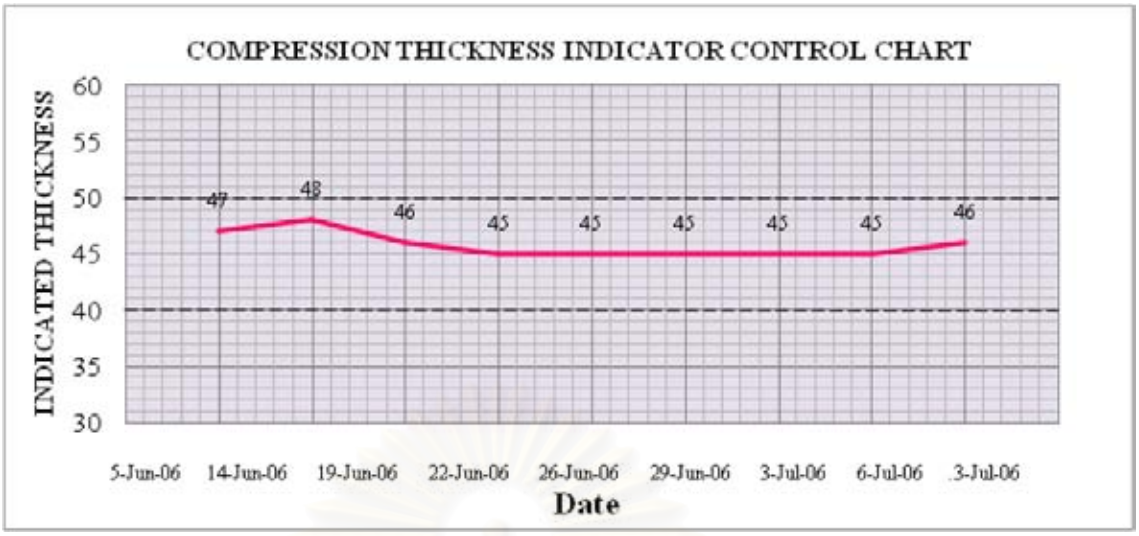

Figure I Graph showing the compress breast thickness scale in 2006

Table III The compression thickness indicator test in 2007

Date	Phantom thickness (mm)	Compression force (pounds)	Indicated thickness value(mm)	Variation (mm)
22 May 2007	45	20	46	1
30 May 2007	45	20	46	1
6 June 2007	45	20	45	0
13 June 2007	45	20	45	0
19 June 2007	45	20	45	0
4 July 2007	45	20	45	0
11 July 2007	45	20	45	0
18 July 2007	45	20	45	0

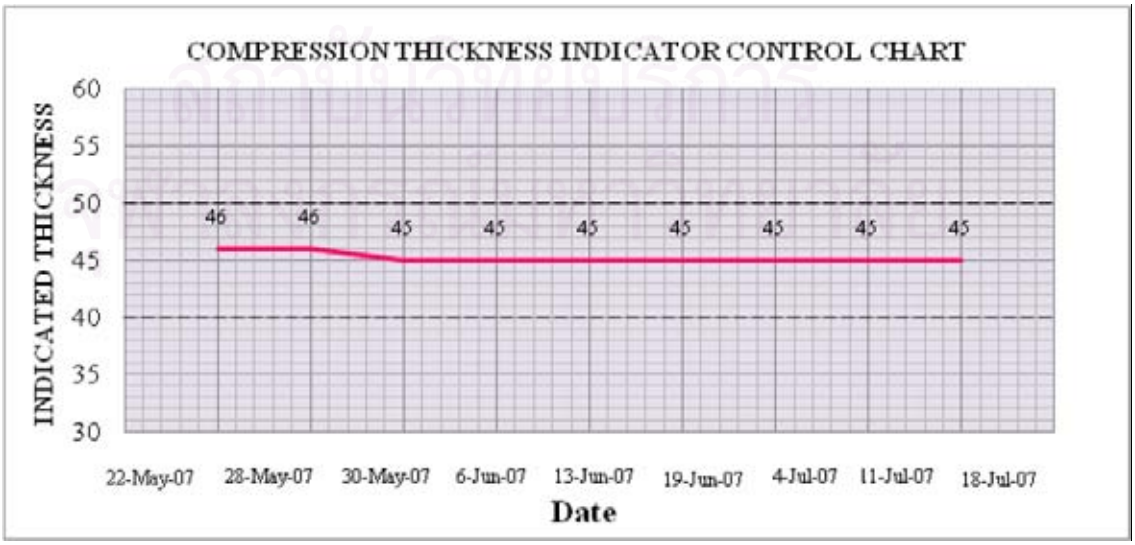

Figure II Graph showing the compress breast thickness scale in 2007

Table IV The compression force test in 2006

Date	Phantom thickness (mm)	Compression force (pounds)	Weighing meter read value	Variation (pounds)
6 June 2006	45	20	20	0

Table V The compression force test in 2007

Date	Phantom thickness (mm)	Compression force (pounds)	Weighing meter read value	Variation (pounds)
6 June 2007	45	20	19.5	0.5

Conclusion

All results of mammographic unit assembly evaluation are within recommended performance criteria. The result of compressed breast thickness scale and compression force are within the control limits.

2. Collimator assessment

Objective

To assure that the collimator assembly perform in the following way:
- The x-ray field coincides with the light field
- The x-ray field is aligned with the image receptor
- The compression paddle is aligned with the image receptor

Regulatory action levels and corrective action

X-ray field to light field coincidence

The total misalignment (sum of the misalignment on opposite sides) must be within 2% of SID.

X-ray field to image receptor alignment

The x-ray field should not extend by more than 2% of the SID at any of the four sides of the image receptor. The radiation field shall extend beyond the image receptor at the chest wall side of the detector.

Compression paddle to image receptor alignment

The anterior edge of the compression paddle should be aligned just beyond the chest wall edge of the image receptor so that it does not appear in the mammogram. In addition, the anterior edge of the compression paddle should not extend beyond the chest wall edge of the image receptor by more than 1% of the SID.

If the recommended performance criteria are not met, the source of the problem shall be identified and corrective action shall be taken within thirty days of the test date.

Result

Table VI The collimator assessment in 2007

Anode material	Mo/Mo	Mo/Mo
Collimator size (cm)	18×24	24×30
Deviation between x-ray field and light field:		
Sum of right and left edge deviations	0.55	-0.44
Sum as % of SID	0.83	-0.67
Sum of anterior & chest edge deviations	1.15	0.14
Sum as % of SID	1.74	0.21
Deviation between x-ray field & edges of the image receptor:		
Left edge deviation	0.64	0.03
% of SID (retain sign)	0.97	0.05
Right edge deviation	0	-0.47
% of SID (retain sign)	0	-0.71
Anterior edge deviation	0.5	0
% of SID (retain sign)	0.76	0.14
Chest edge deviation	0	0.14
% of SID (retain sign)	0	0.21
Alignment of chest wall edges of compression paddle and film:		
Difference between paddle edge and film	-0.1	-0.2
Difference as % of SID	-0.15	-0.3

Conclusion

The sum of the left plus right edge deviations and anterior plus chest edge deviations are within 2% of SID (1.32 cm). The x-ray field does not exceed image receptor at any side by less than 2% of SID (1.32 cm). The chest wall edge of compression paddle is within the image receptor.

3. Artifact evaluation

Objective

To assess the degree and source of artifacts visualized in the mammograms or phantom images. This procedure allows the source of artifacts to be isolated to x-ray equipment, laser printer, or film processor.

Regulatory action levels and corrective action

Artifacts that may interfere with image interpretation must be eliminated before performing clinical imaging.

Consult with a radiologist for assistance in evaluating whether artifacts may interfere with image interpretation. A qualified service engineer must eliminate any digital detector artifacts that may be clinically objectionable.

The acrylic attenuation block provided by the manufacturer and used for detector calibration replaced if it has permanent artifacts that may impact detector calibration.

The recommendations and corrective actions listed in the 1999 ACR Mammography Quality Control Manual should be followed for laser printer and film processor artifacts.

Result

Table VII The artifact evaluation in 2006

Target/ Filter	Mo/Mo	Mo/Rh
Image receptor size	18×24	18×24
Date	Digital Image Receptor	
24 July 2006	Artifact that appears on the digital image receptor at the right side on the top.	Artifact that appears on the digital image receptor at the right side on the top.
27 July 2006	Acceptable	Artifacts that appear on the mode filter Rh which is little line on the digital image receptor next the Chest wall about 3-5 cm length.

Conclusion

The artifact was found without significant artifacts visible. Detail of artifact is shown in Table VII, which was eliminated before clinical imaging by service engineer.

4. kVp Accuracy/Reproducibility

Objective

To assure that the selected kVp is accurate within limits and reproducible between exposures.

Regulatory action levels and corrective action

-The kVp shall be accurate within±5% of the indicated or selected kVp

-At 28 kVp, the coefficient of variation of the kVp shall be equal to or less than 0.02.

If the mean kVp differs from the nominal by more than ±5% of nominal kVp, or if the coefficient of variation exceeds 0.02, then seek service correction.

Result

Table VIII The kVp accuracy/reproducibility test in 2007

Nominal kVp setting	25	26	27	28	29	30
Nominal focal spot size	0.3	0.3	0.3	0.3	0.3	0.3
Target/ Filter	Mo/Mo	Mo/Mo	Mo/Mo	Mo/Mo	Mo/Mo	Mo/Mo
mAs setting	30	30	30	30	30	30
Measured kVp value:						
kVp 1	25.94	26.64	27.64	28.84	30.04	31.07
kVp 2	26.00	26.92	27.73	28.89	29.92	31.09
kVp 3	25.87	26.61	27.65	28.81	29.99	31.15
kVp 4	25.77	26.71	27.63	28.86	29.96	31.15
Mean kVp	25.90	26.72	27.66	28.85	29.98	31.12
Standard Deviation(SD)	0.09	0.12	0.04	0.03	0.04	0.04
Mean kVp - Nominal kVp	0.9	0.72	0.66	0.85	0.98	1.12
0.05 x Nominal kVp	1.25	1.30	1.35	1.40	1.45	1.50
% Error	3.6	2.77	2.44	3.04	3.38	3.73
kVp Coefficient of variation (SD/Mean kVp)	0.003	0.005	0.001	0.001	0.001	0.001

Conclusion

The kVp is accurate within limits and reproducible between exposures. The mean kVp differs from the nominal of various kVp of less than ±5% of nominal kVp. The kVp coefficient of variation is less than 0.02 for all kVp settings.

5. Beam quality assessment

Objective

To assure that the half-value layer (HVL) of the x-ray beam is adequate to minimize patient dose without being too excessive to compromise image contrast.

Regulatory action levels and corrective action

The measured HVL shall be less than (kVp/100)+C, where C=0.12 for Mo/Mo and C= 0.19 for Mo/Rh.

If the test results fall outside the control limits, the source of the problem shall be identified and corrective actions shall be taken within thirty days of the test date.

Result

Table IX HVL measurements for Mo/Mo target/filter combination in 2007

Nominal kVp setting	25	26	27	28	29	30
Nominal focal spot size	0.3	0.3	0.3	0.3	0.3	0.3
Target/ Filter	Mo/Mo	Mo/Mo	Mo/Mo	Mo/Mo	Mo/Mo	Mo/Mo
mAs setting	30	30	30	30	30	30
Exposure Measurements (mR):						
No Aluminum Filtration, E_0	308.7	358.9	406.6	454.7	506.1	559.2
0.2 mm of added Aluminum, E_2	197.8	229.9	262.9	298.2	335.7	375
0.3 mm of added Aluminum, E_3	160.6	187.4	215.8	245.9	277.9	311.5
0.4 mm of added Aluminum, E_4	132.5	155	180	206.4	233.1	261.9
Calculations:						
$E_{0/2}$ Value, $E_{1/2}$	154.35	179.45	203.3	227.35	253.05	279.6
Exposure greater than $E_{1/2}$: E_a	160.6	187.4	215.8	245.9	277.9	311.5
Al thickness at E_a: t_a	0.3	0.3	0.3	0.3	0.3	0.3
Exposure less than $E_{1/2}$: E_b	132.5	155	180	206.4	233.1	261.9
Al thickness at E_b: t_b	0.4	0.4	0.4	0.4	0.4	0.4
Calculated HVL(mm Al)	0.322	0.325	0.335	0.347	0.355	0.364

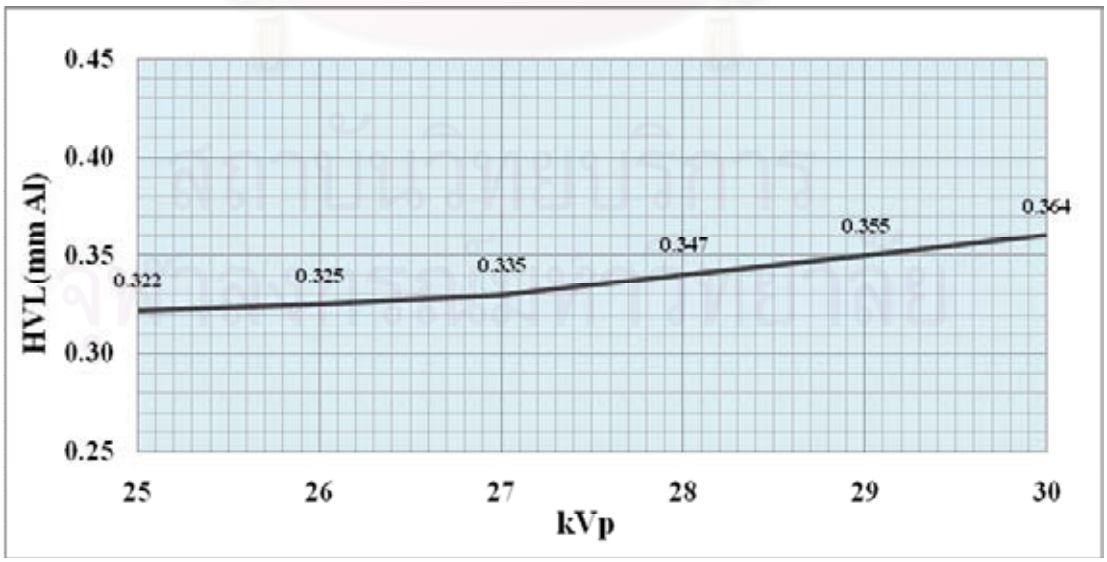

Figure III The relationship between kVp and HVL for Mo/Mo target/filter combination

Table X The HVL measurements for Mo/Rh target/filter combination in 2007

Nominal kVp setting	26	28	30	32	34
Nominal focal spot size	0.3	0.3	0.3	0.3	0.3
Target/ Filter	Mo/Rh	Mo/Rh	Mo/Rh	Mo/Rh	Mo/Rh
mAs setting	30	30	30	30	30
Exposure Measurements (mR):					
No Aluminum Filtration, E_0	212.3	279.2	357.7	432	545.4
0.2 mm of added Aluminum, E_2	145.8	197.7	248.4	310.5	377.7
0.3 mm of added Aluminum, E_3	-	-	-	-	-
0.4 mm of added Aluminum, E_4	101.1	137.8	183.5	229.6	290.4
0.5 mm of added Aluminum, E_5	-	119.9	154.8	194.7	252.5
Calculation :					
$E_{0/2}$ Value, $E_{1/2}$	106.15	139.6	178.85	216	272.7
Exposure greater than $E_{1/2}$: E_a	145.8	197.7	183.5	229.6	290.4
Al thickness at E_a: t_a	0.2	0.2	0.4	0.4	0.4
Exposure less than $E_{1/2}$: E_b	101.1	137.8	154.8	194.7	252.5
Al thickness at E_b: t_b	0.4	0.4	0.5	0.5	0.5
Calculated HVL(mm Al)	0.370	0.390	0.416	0.439	0.447

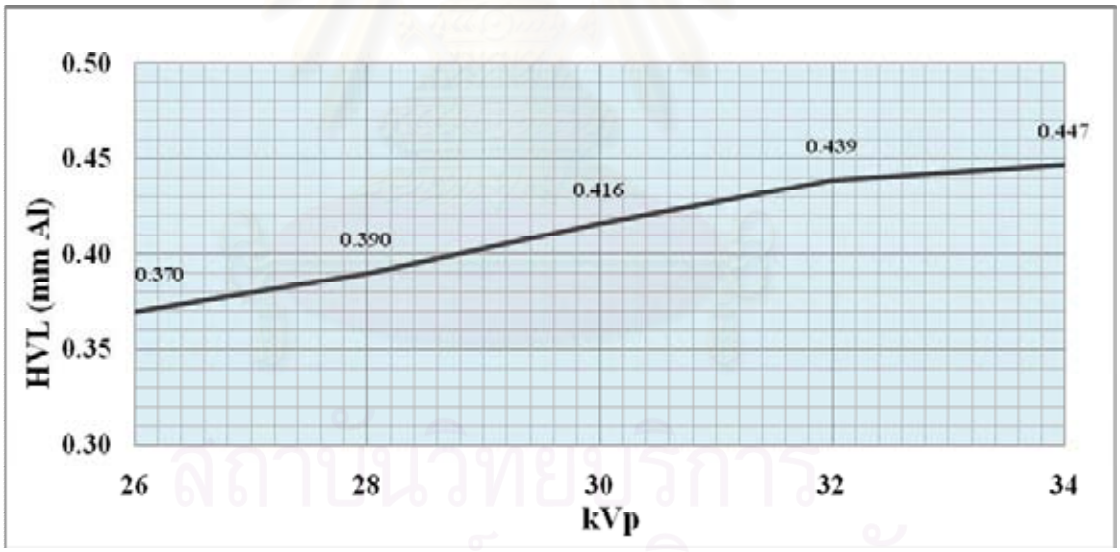

Figure IV The relationship between kVp and HVL for Mo/Rh target/filter combination

Conclusion

The test result is within the control limits for various kVp and the both Mo/Mo, Mo/Rh target/filter combination.

6. Evaluation of system resolution

Objective

To evaluate imaging performance, using the system limiting spatial resolution as a performance indicator.

Regulatory action levels and corrective action

The system limiting spatial resolution should be greater than 7 lp/mm when the bars are at 45° to the anode-cathode axis.

If these criteria are not met, a qualified service engineer must correct the problem before using the system for clinical imaging.

Result

Table XI The evaluation of system resolution in 2007

Axis	The resolution test pattern in AWS of FFDM system	Standards Limit
At 45° Anode-Cathode	14 lp/mm	>7 lp/mm
At 45° Perpendicular	14 lp/mm	>7 lp/mm

Conclusion

The test result was found within the control limits for the anode-cathode and perpendicular axis.

7. Breast entrance exposure and average glandular dose (AGD)

Objective

To measure the typical entrance exposure and calculate the corresponding glandular dose for an average patient with approximately 4.2 cm compressed breast thickness of 50% adipose, 50% glandular tissue composition.

Regulatory action levels and corrective action

The coefficient of variation for air kerma shall not exceed 0.05.The AGD delivered during a single cranio-caudal view of an FDA accepted phantom simulating a standard breast shall not exceed 3.0 mGy (0.3 rad) per exposure. The dose shall be determined with technique factor and conditions used clinically for a standard breast.

If the results fall outside the control limits, the source of the problem shall be identified and corrective actions shall be taken before any further examinations are performed.

Result

Table XII The breast entrance exposure and average glandular dose (AGD) measurements in 2007

Dosimetry System used:	Victoreen 4000 M+	
Field Restriction: Paddle	18x24 cm.	
Source-detector distance :	58 cm.	
Mode: Manual	mR/mAs : 15.81	
Nominal kVp Setting:	28	
Target/Filtration:	Mo/Mo	
mAs setting:	120	
Measured HVL (mm Al):	0.34	
Measured Entrance Exposure		R
Exposure #1	1.8940	
Exposure #2	1.8940	
Exposure #3	1.8980	
Exposure #4	1.9030	
Mean Values		1.8973
Standard Deviations (SD)		0.004
Coefficients of Variation (CV)		0.002
Energy-Corrected:		
Exposure:		1.897
Conversion factor from inverse square law		0.7722
Dose conversion factor from table (mrad/R):		174
Computed average glandular dose (mrad):		260.75

Conclusion

The test result is within the control limits, the glandular dose was 0.26 rad or 2.6 mGy. The coefficient of variation for air kerma does not exceed 0.05.

8. Radiation output rate

Objective

To measure the radiation output rate of the system.

Regulatory action levels and corrective action

The radiation output of the Lorad Selenia FFDM System should not be less than 7.0 mGy air kerma per second, equal to or greater than 800mR/sec for at least 3 second when operating at 28 kVp in the standard Mo/Mo target/filter combination.

If the results fall outside the control limits, the source of the problem shall be identified and corrective actions shall be taken within thirty days of the test date.

Result

Table XIII The radiation output rate measurements in 2007.

Dosimetry System used:		Victoreen 4000 M+		
Mode:		Manual		
Nominal kVp Setting:		28		
mAs setting:		30		
Target/Filtration:		Mo/Mo		
Source-detector distance(cm)	Time (sec)	Exposure (mR)	Rate (mR/sec)	Air Kerma /sec (mGy/sec)
58	0.503	594.9	1182.7	10.3
58	0.503	594.1	1181.1	10.3
58	0.503	594.7	1182.3	10.3

Conclusion

The test result is within the control limits, the radiation output rate is 1182 mR/sec and air kerma per second is 10.3 mGy. Which meet the criteria for acceptance.

9. Phantom Image Quality Evaluation

Objective

To assess the quality and consistency of the mammographic image.

Regulatory action levels and corrective action

The phantom image background density should never be less than 1.20, and the control limits should be ±0.20. This means that the operating level should not be less than 1.40.

The operating level for the density difference over the acrylic disk should be at least 0.40, with control limits of ±0.05.

The phantom image quality shall meet the minimum passing score shown below.

ACR Mammography Accreditation Phantom	Fiber	Speck Groups	Mass
Minimum Passing Score	5.0	4.0	4.0

If the phantom score fails to meet the recommended criteria on both printed film and Selenia Softcopy workstation (SCW) interpretation, a qualified service engineer shall correct the problem before using the system for clinical imaging.

If the phantom score fails to meet the recommended criteria on one of multiple diagnostic devices (printer or SCW) while meets the criteria on at least one diagnostic device, clinical imaging can be continued and only devices that passed the phantom score shall be used for mammographic image interpretation. Devices that failed the phantom score shall not be used for mammographic image interpretation until a qualified service engineer resolves the problem.

Any film density issue shall be addressed prior to printing clinical images. Images can still be acquired while any printer issue are being resolves providing that the phantom score meet recommended scoring criteria on another diagnostic devices used for mammographic image interpretation. Printers that did not pass the film density criteria shall not be used until a qualified service engineer resolves the problem.

Result

Table XIV The phantom score on printed film in 2006, with background density of 1.95 and density difference of 0.72

Date	Fibers	Speck Groups	Masses
5 June 2006	4.5	3.5	4.5
14 June 2006	5.5	3.5	4.5
19 June 2006	6	3.5	4.5
22 June 2006	6	4	4.5
26 June 2006	6	4	4.5
29 June 2006	6	3.5	4.5
3 July 2006	6	3.5	4.5
6 July 2006	6	3.5	4.5
20 July 2006	6	3.5	4.5
Mean	5.8	3.6	4.5

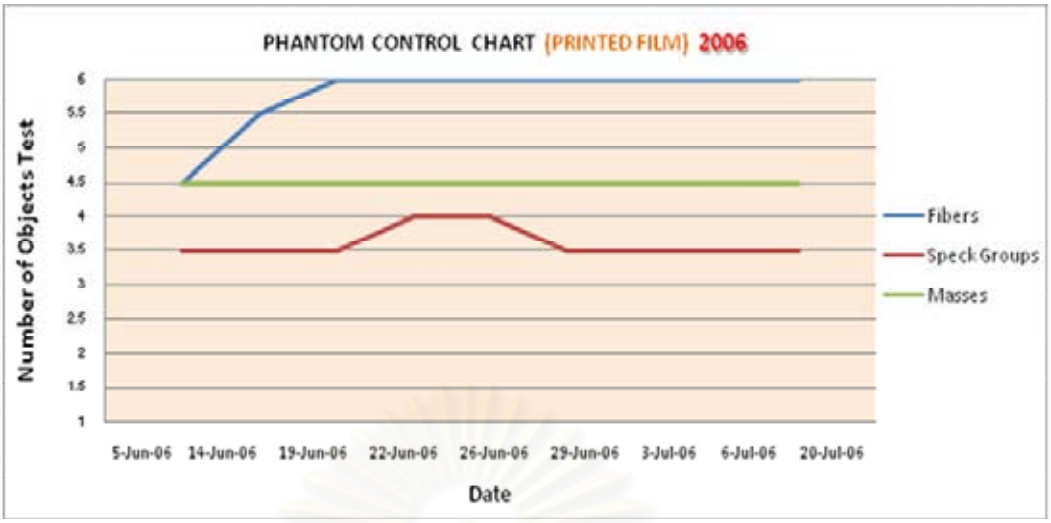

Figure V The phantom score on printed film in 2006

Table XV The phantom score on printed film in 2007, with background density of 2.01 and density difference of 0.74.

Date	Fibers	Speck Groups	Masses
24 May2007	5.5	3.5	4.5
28 May2007	5.5	3.5	4.5
30 May2007	5.5	3.5	4.5
6 June 2007	5.5	3.5	4.5
13 June 2007	5.5	3.5	4.5
19 June 2007	5.5	3.5	4.5
4 July 2007	5.5	3.5	4.5
11 July 2007	5.5	3.5	4.5
18 July 2007	5.5	3.5	4.5
Mean	5.5	3.5	4.5

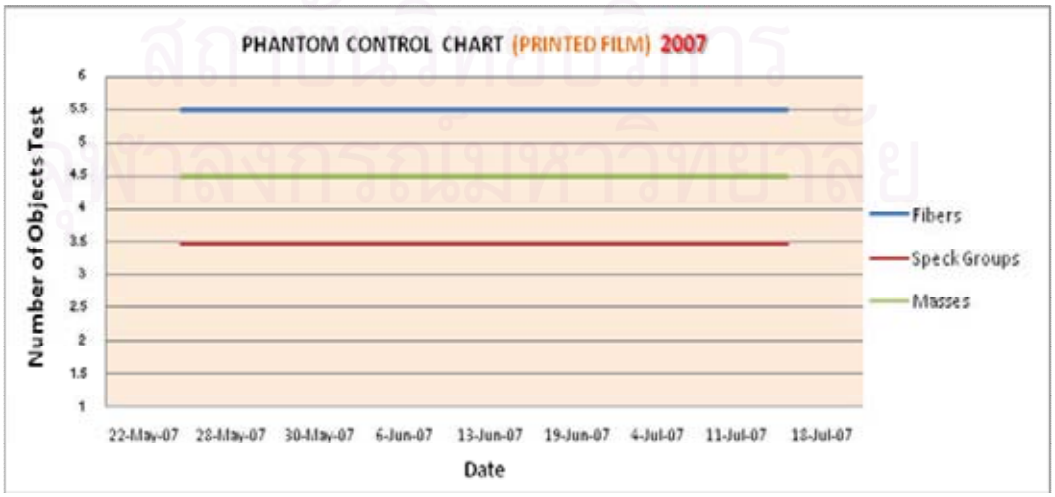

Figure VI The phantom score on printed film in 2007

Table XVI The phantom score on SCW in 2006

Date	Fibers	Speck Groups	Masses
5 June 2006	5.5	3.5	4.5
14 June 2006	5	3.5	4.5
19 June 2006	6	3.5	4.5
22 June 2006	6	4	4.5
26 June 2006	6	4	4.5
29 June 2006	6	4	5
3 July 2006	6	4	5
6 July 2006	6	4	5
13 July 2006	6	3.5	4.0
Mean	5.8	3.8	4.6

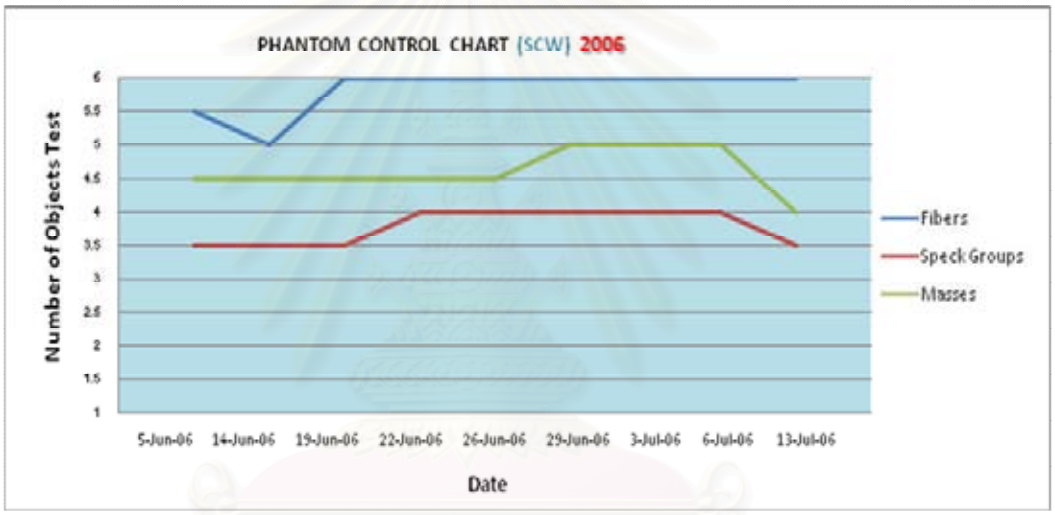

Figure VII The phantom score on SCW in 2006

Table XVII The phantom score on SCW in 2007

Date	Fibers	Speck Groups	Masses
24 May 2007	6	3.5	4.5
28 May 2007	6	3.5	4.5
30 May 2007	6	4	4.5
6 June 2007	6	4	4
13 June 2007	6	4	4.5
19 June 2007	6	4	4.5
4 July 2007	6	3.5	4.5
11 July2007	6	4	4.5
18 July2007	6	4	4.5
Mean	6	3.8	4.4

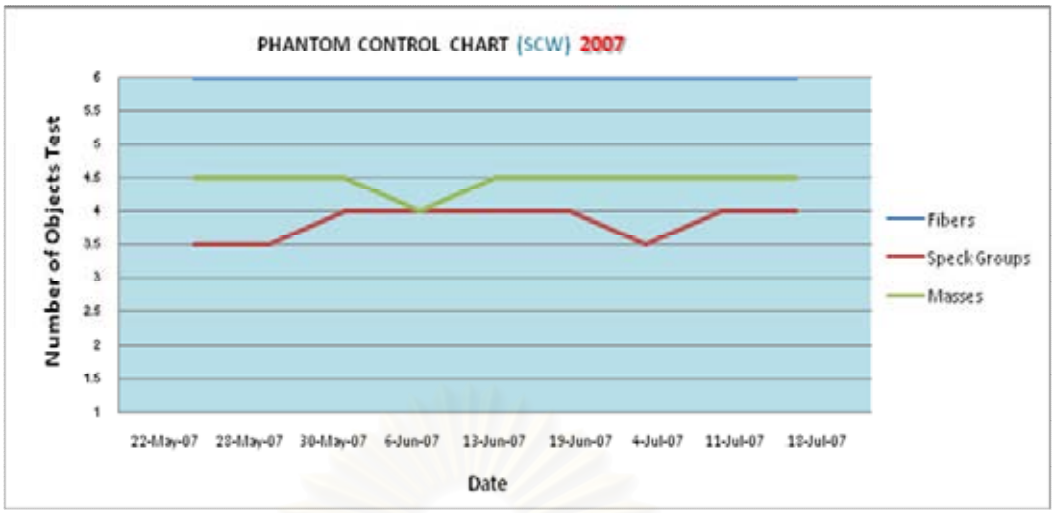

Figure VIII The phantom score on SCW in 2007

Table XVIII The phantom score on acquisition workstation (AWS) in 2006

Date	Fibers	Speck Groups	Masses
5 June 2006	4.5	3.5	4.5
14 June 2006	5.5	3.5	4.5
19 June 2006	6	3.5	4.5
22 June 2006	5.5	3.5	4.5
26 June 2006	6	3.5	5.0
29 June 2006	6	3.5	4.5
3 July 2006	5	3.5	4.5
6 July 2006	6	3.5	4.5
13 July 2006	5	3.5	4
Mean	5.5	3.5	4.5

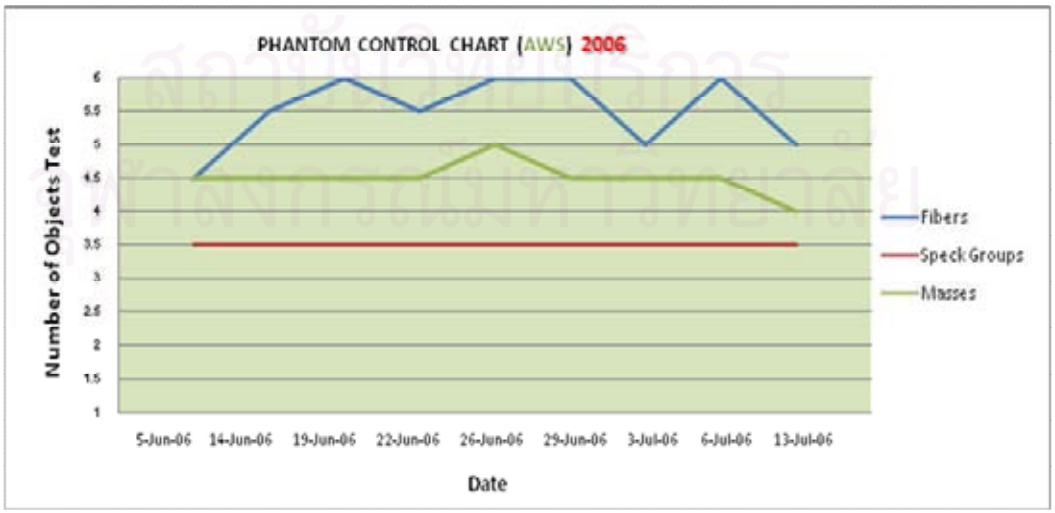

Figure IX The phantom score on AWS in 2006

Table XIX The phantom score on AWS in 2007

Date	Fibers	Speck Groups	Masses
24 May 2007	5.5	3.5	4.5
28 May 2007	5.5	3.5	4.5
30 May 2007	5.5	3.5	4.5
6 June 2007	5.5	3.5	4.5
13 June 2007	5.5	3.5	4.5
19 June 2007	5.5	3.5	4.5
4 July 2007	5.5	3.5	4.5
11 July2007	5.5	3.5	4.5
18 July2007	5.5	3.5	4.5
Mean	5.5	3.5	4.5

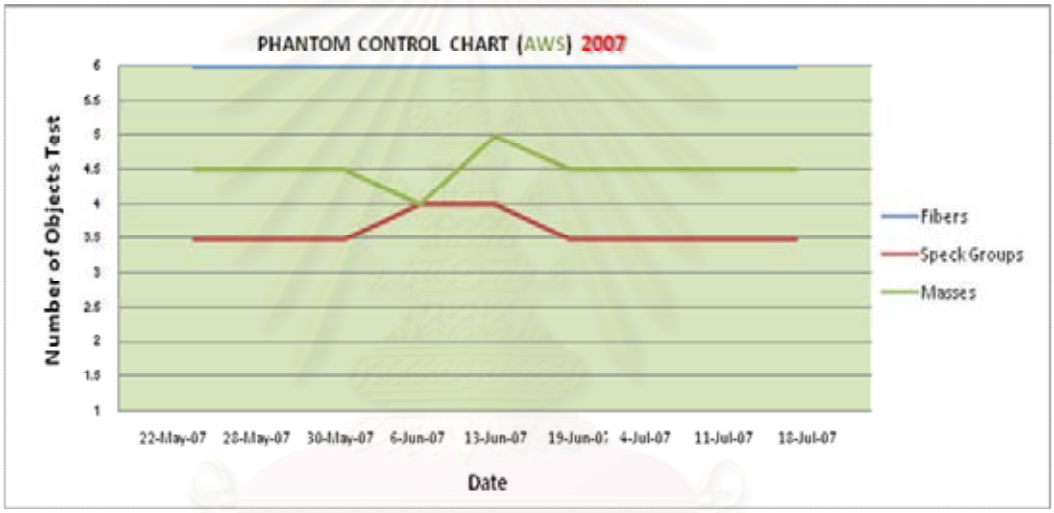

Figure X The phantom score on AWS in 2007

Conclusion

All result recorded from phantom score on printed film, SCW and AWS as shown in above table. The numbers of fibers and masses were found within the recommended criteria of the phantom score on diagnostic devices (printer, SCW, AWS) in 2006 and 2007. While the phantom score fails was found on diagnostic devices for the numbers of speck groups.

10. Signal - to - noise and contrast-to-noise measurements

Objective

To assure consistency of the digital image receptor by evaluating the signal-to-noise ratio (SNR) and contrast-to-noise ratio (CNR) of the image receptor.

Data analysis and interpretation

The SNR shall be computed using the mean and standard deviation obtained from the ROI next to the acrylic disk.

1. Compute the SNR of the detector according to

$$SNR = \frac{Mean_{background} - DC_{offset}}{STD_{background}}$$

Where $Mean_{background}$ and $STD_{background}$ are the mean and standard deviation obtained from the ROI Statistics dialog for the ROI next to the acrylic disk and DC_{offset} is a DC offset added to the detector signal and is equal to 50.

2. Compute the CNR of the detector according to

$$CNR = \frac{Mean_{background} - Mean_{disk}}{STD_{background}}$$

Where $Mean_{disk}$ is the mean value obtained from the ROI Statistics dialog for the ROI on the acrylic disk.

3. Compute the deviation from the original CNR measurement according to

$$Diff = \frac{CNR\ base - CNR\ measured}{CNR\ base} \times 100$$

Where CNR base is the CNR base value established by the medical physicist during acceptance testing of digital image detector; CNR measured is the new CNR computer in step 2.

Recommended performance criteria and corrective action

The measured SNR must be equal to or greater than 40. If it is less than 40, repeat the test.

The computed CNR must be within ±15% of the value determined by the medical physicist during the equipment evaluation when the image receptor was installed.

If these criteria are not met, a qualified service engineer must correct the problem before using the system for clinical imaging.

Result

Table XX The signal-to-noise measurements in 2006

Date	Mean Value Inside disk	Mean Value Beside disk	Standard Dev. Beside disk	SNR
5 June 2006	350.3	433.8	8.4	45.7
14 June 2006	360.7	440.6	8.7	44.9
19 June 2006	351.0	431.3	8.6	44.3
22 June 2006	357.4	445.5	8.6	46.0
26 June 2006	354.5	439.5	8.6	45.3
29 June 2006	365.8	452.3	8.6	46.8
3 July 2006	361.3	444.9	8.7	45.4
6 July 2006	367.4	454.9	8.6	47.8
13 July 2006	365.4	454.6	8.9	45.5

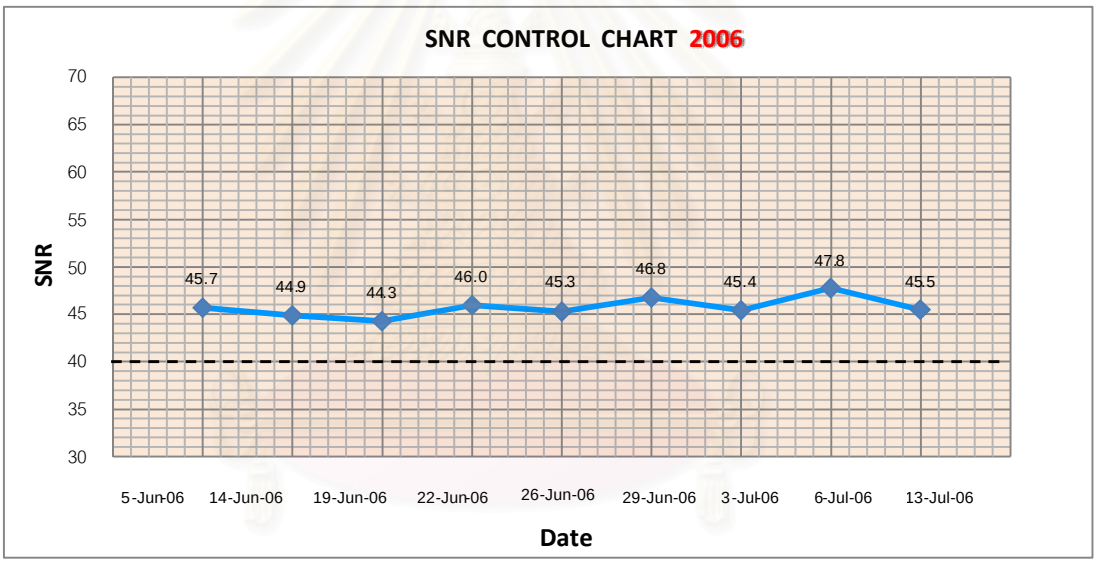

Figure XI Graph showing the signal-to-noise measurements in June-July 2006

Table XXI The signal-to-noise measurements in 2007

Date	Mean Value Inside disk	Mean Value Beside disk	Standard Dev. Beside disk	SNR
23 May 2007	472.47	582.37	10	53.24
28 May 2007	447.13	562.93	10.97	46.77
30 May 2007	447.3	550.97	9.8	51.12
6 June 2007	445.33	551.7	10.03	50.02
13 June 2007	448.66	556.83	10.13	50.03
19 June 2007	449.87	555.17	10	50.52
4 July 2007	436.63	553.13	10.3	48.85
11 July 2007	465.37	593.5	10.9	49.86
18 July 2007	482.53	613.86	11.07	50.94

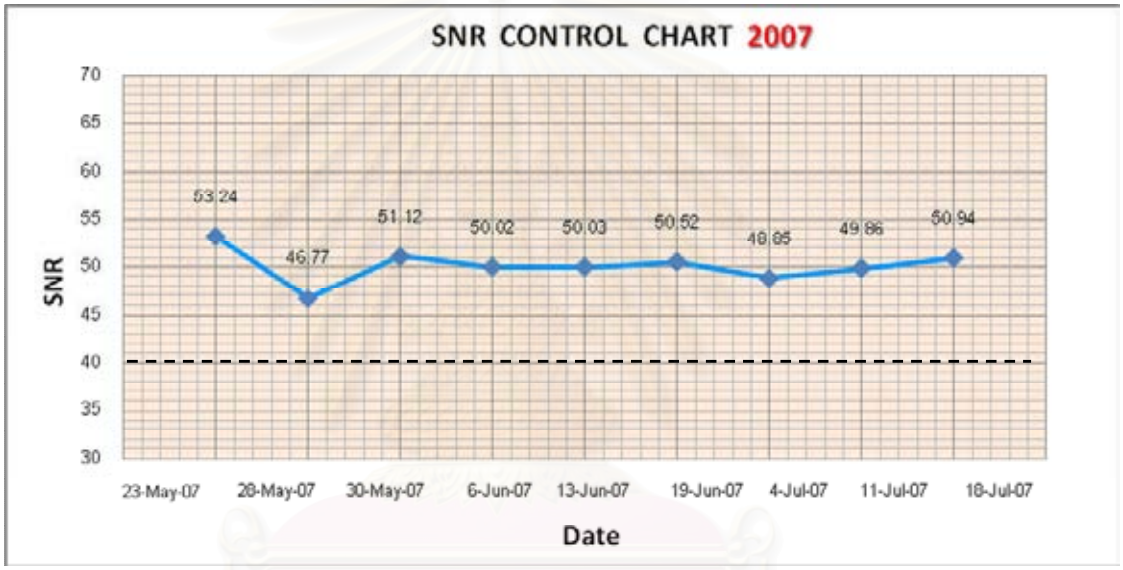

Figure XII Graph showing the signal-to-noise measurements in May-July 2007

Table XXII The contrast-to-noise measurements in 2006

Date	Mean Value Inside Disk	Mean Value Beside Disk	Standard Dev. Beside disk	CNR	%Diff
5 June 2006	350.3	433.8	8.4	9.94	-
14 June 2006	360.7	440.6	8.7	9.18	+7.1
19 June 2006	351.0	431.3	8.6	9.3	+5.96
22 June 2006	357.4	445.5	8.6	10.24	-3.53
26 June 2006	354.5	439.5	8.6	9.88	+0.10
29 June 2006	365.8	452.3	8.6	10.05	-1.61
3 July 2006	361.3	444.9	8.7	9.60	+2.93
6 July 2006	367.4	454.9	8.6	10.17	-2.83
13 July 2006	365.4	454.6	8.9	10.02	-1.31
20 July 2006	360.8	449.2	8.8	10.05	-1.62

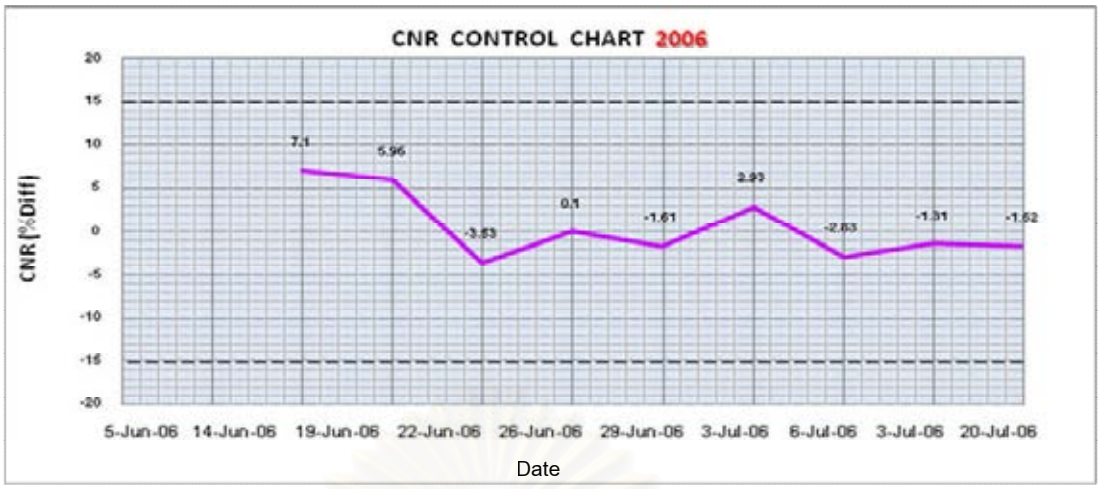

Figure XIII Graph showing the contrast-to-noise measurements in June-July 2006

Table XXIII The contrast-to-noise measurements in 2007

Date	Mean Value Inside Disk	Mean Value Beside Disk	Standard Dev. Beside disk	CNR	%Diff
23 May 2007	472.47	582.37	10	10.99	-2.62
28 May 2007	447.13	562.93	10.97	10.56	1.40
30 May 2007	447.3	550.97	9.8	10.58	1.22
6 June 2007	445.33	551.7	10.03	10.33	3.57
13 June 2007	448.66	556.83	10.13	10.68	0.29
19 June 2007	449.87	555.17	10	10.53	1.67
4 July 2007	436.63	553.13	10.3	11.31	-5.61
11 July 2007	465.37	593.5	10.9	11.76	-9.81
18 July 2007	482.53	613.86	11.07	11.86	-3.37

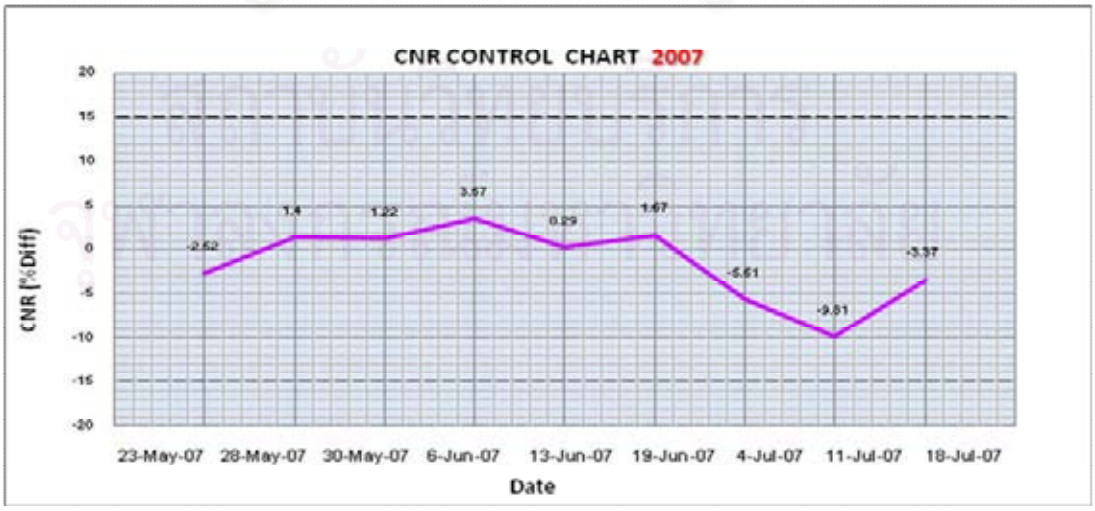

Figure XIV Graph showing the contrast-to-noise measurements in May-July 2007

Conclusion

All result recorded from signal-to-noise and contrast-to-noise measurements as shown in above table, signal-to-noise and contrast-to-noise values are within the recommended performance criteria. The signal-to-noise and contrast-to-noise values in 2007 are higher than 2006.

11. Softcopy workstation QC

Objective

To assure consistency of the brightness, contest and image presentation of the radiologist's soft-copy workstation

Recommended performance criteria and corrective action

If the test fails after the second attempt, the problem must be corrected before any clinical or phantom images are read on the softcopy workstation. The person responsible for monitor calibration (lead technologist, medical physicist, or service engineer) should perform the monitor calibration, using the appropriate software.

Images can still be acquired while any monitor issues are being resolved. Alternative diagnostic devices shall be used for mammography image interpretation until all issues are resolved and the monitors perform within recommended criteria.

Results

Table XXIV The diagnostic review workstation QC in 2006

Date: 29 June 2006 Monitor Serial Number	Left Monitor 1890024831	Right Monitor 1890033199	Comments	
White Level Performance (300 cd/m^2)	300.57 cd/m^2	297.30 cd/m^2	OK	< 6%
Black Level Performance (0 cd/m^2)	0.31 cd/m^2	0.29 cd/m^2	OK	< 1 cd/m^2
Quality Level Performance	100%	100%	Not OK	>10%
Uniformity Performance	0%	0%	OK	<15%

Table XXV The diagnostic review workstation QC in 2007

Date: 25 July 2007 Monitor Serial Number	Left Monitor 1890024831	Right Monitor 1890033199	Comments	
White Level Performance (300 cd/m^2)	302.72 cd/m^2	298.12 cd/m^2	OK	< 6%
Black Level Performance (0 cd/m^2)	0.71 cd/m^2	0.72cd/m^2	OK	< 1 cd/m^2
Quality Level Performance	100%	100%	Not OK	>10%
Uniformity Performance	0%	0%	OK	<15%

Conclusion

All result recorded from diagnostic review workstation QC are shown in above table. The white and black level performances are within control, limits of ±5, black level performance is lees than 1cd/m^2 (within recommended performance criteria).

VITAE

NAME	Miss Thunyarat Chusin
SEX	Female
NATIONALITY	Thai
DATE OF BIRTH	November 24, 1980
PLACE OF BIRTH	Kamphaengphet, Thailand
INSTITUTION ATTENDED	Naresuan University, 2003: Bachelor of Science (Radiological Technology) Chulalongkorn University, 2008: Master of Science (Medical Imaging)
HOME ADDRESS	140/1 Moo.1 Prankatai, Kamphaengphet, Thailand 62110